

A Histochemical Study on Condylar Cartilage and Glenoid Fossa during Mandibular Advancement

Payam Owtad, Author
Prof M Ali Darendeliler, Supervisor
A/Prof Gang Shen, A/Supervisor

A thesis submitted in fulfillment of the requirements for the degree of
Master of Philosophy in Dentistry



**Department of Orthodontics, Faculty of Dentistry
The University of Sydney
Australia
January 2009**

Dedication

This Thesis is dedicated to

My Lovely Family,

My Teachers, who have been my Guiding Lights

&

My Supportive Friends,

Without whom this work would not have been

possible...

Abstract

Growth modification of the lower jaw during mandibular forward positioning is a successful example for bone remodeling in response to a change in biophysical environment. This remodeling occurs by expression of cells' endogenous regulatory factors in the Mandibular Condylar Cartilage (MCC) and the Glenoid Fossa (GF) through an Endochondral Ossification (EO) and Intramembranous Ossification (IO) process. Fibroblast Growth Factor (FGF) is one factor regulating mesenchyme and chondrocyte proliferation in the MCC adaptive remodeling. FGF signaling results in a decrease in chondrocyte proliferation and acceleration in the hypertrophic differentiation in chondrocytes. Detecting Proliferating Cell Nuclear Antigen (PCNA) as a tissue marker indicates proliferative activity.

Aim: The aim of this study is to evaluate the proliferative and hypertrophic activities in the MCC and the GF during mandibular advancement in Sprague Dawley Rat's Temporomandibular Joint (TMJ), evidenced by FGF8 and PCNA.

Methods and Materials: Fifty five female 24-day old Sprague-Dawley rats were randomly divided into four experimental and control groups, with mandibular advancement appliance on the experimentals' lower jaw. The rats were euthanized on days 3, 14, 21 and 30 of the study and their TMJ was prepared for immunohistochemical staining procedure to detect FGF8 and PCNA.

Results: FGF8 expression was significantly higher in the experimentals ($p=0.002$), while PCNA expression did not increase significantly in the experimental samples ($p=0.327$). The patterns of ascension and descension of FGF8 and PCNA expressions during the experiment period was similar in experimental and control samples. However, the number of stained cells for FGF8 and PCNA differed between the MCC and the GF. The results show an overall enhanced osteogenic transition occurring in both the MCC and the GF in

experimentals in comparison with controls. The level of cellular changes in the MCC is remarkably higher than in the GF.

Conclusion: In the MCC and the GF, hypertrophic differentiations increase significantly during mandibular advancement, while cellular proliferation does not increase significantly. It could be concluded that the endochondral ossification in the MCC and intramembranous ossification in the GF occurs during adaptive remodeling.

Keywords: Mandibular condylar cartilage, Glenoid fossa, FGF8, PCNA, Adaptive bone remodeling, Mandibular advancement.

Declaration

This is to certify that the thesis comprises only my original work towards the MphilDent except where indicated. Due acknowledgement has been made in the text to all other material used; the thesis is less than 40,000 words in length, including tables, footnotes, bibliographies and appendices.

Payam Owtad

Publications

Based on the work presented in this thesis:

- A scientific paper is presented as an oral research abstract presentation at the American Association of Orthodontists (AAO) 109th Annual Session in Boston, Massachusetts - USA May 2009.

Acknowledgements

I wish to acknowledge and thank a number of people for their contribution towards the research and preparation of this thesis:

... Professor M Ali Darendeliler, chair of orthodontics, for all his support and help, and direct supervision of this work since August 2008; without his guidance this work would not have been possible.

... A/Professor Gang Shen for his mentoring and guidance as the direct supervisor of this project from the beginning until August 2008. I highly appreciate all of his efforts.

... Dr. Zoe Potres, without whose support, fantastic cooperation, positive energy and attitude, it would have been impossible for me to complete this project on time.

... Professor Eli Schwarz, the Dean of the Dental School for supporting my study and granting me the partial fee scholarship.

...Professor Neil Hunter and the other colleagues at the Institute of Dental Research (IDR - Westmead Hospital, NSW) for providing laboratory facilities and cordial support.

... Ms. Mary Simonian for her technical assistance and kind support.

... Dr. Craig Godfrey and the other staff members of the animal care facility at Westmead Hospital for all their efforts in this project.

...Professor Hans Zoellner's and the other colleagues' support at the pathology department while we used some of the laboratory facilities at Westmead Hospital.

...Ms. Maria Apostol, the administrative assistant of the Department of Orthodontics, Ms. Rebecca Granger, the postgraduate administration officer and Ms. Tracy Bowerman, the research administration support and executive assistant.

...Endeavour International Postgraduate Research Scholarship office for granting me the EIPRS scholarship.

...The helpful and supportive teachers in the School of Dentistry who have kindly supported me; especially Dr. Catherine Groenlund, A/Professor Chris Peck, Professor Greg Murray, and Dr. Tania Gerzina.

...The postgraduate students at the Department of Orthodontics; especially Dr. Vasantha Srinivasan, Dr. Gosia Kluczevska, Dr. Nour Eldin Tarraf, Dr. Lachlan Crowther, Dr. Adrian Tan, Dr. Elaine Lim and Dr. Andy Wu.

I would like to give special thanks to Dr. Rahman Showkatbakhsh, Associate Professor at the Department of Orthodontics, Shahid Beheshti Medical Science University, Tehran-Iran; a wise teacher and kind friend, who has guided me since my graduate studies to the true path of science. His cordial help and critical support on my pilot study for this project are highly appreciated.

I would also like to thank my friends in Sydney, particularly the Behrady family, Mr. Mohammad and Mrs. Parvin Behrady, Mr. Morteza Abolfathi and his family, Dr. Hossein Haghighat, Dr. Farshid Meshkani, Dr. Saeid Afshargoli and their families and Mr. Shahab Lajevardi, the graduate dental student at the University of Sydney.

List of Abbreviations

AD	Articular Disc
AE	Articular Eminence
ALP	Alkaline Phosphatase
ANOVA	Analysis of Variance
B	Bone
BMP	Bone Morphogenic Protein
BP	Binding Protein
C	Condyle
Cbfa	Core Binding Factor 1
CC	Condylar Cartilage
Cl	Class
D	Dimension
DAB	Diaminobenzidine
DNA	Deoxyribonucleic acid
E	Erosive Zone
EDTA	Ethylene-Diamine-Tetra-Acetic Acid
EO	Endochondral Ossification
FGF	Fibroblast Growth Factor
FGF8c	Fibroblast Growth Factor 8 expression in the Condyle
FGF8gf	Fibroblast Growth Factor 8 expression in the Glenoid Fossa
FGFR	Fibroblast Growth Factor Receptor
FR	Frankel functional Regulator
GF	Glenoid Fossa

H & E	Hematoxylin and Eosin
H	Hypertrophic Zone
HLGAGs	Heparan-Like Glycosaminoglycans
HRP	Horseradish Peroxidase
IDR	Institute of Dental Research
IGF	Insulin-like Growth Factor
Ihh	Indian Hedgehog
IM	Intermediate Mesoderm
IO	Intramembranous Ossification
MCC	Mandibular Condylar Cartilage
ME	Method of Error
mm	Millimeter
MMP	Matrix Metalloproteinase
MP	Mandibular Primordium
MRI	Magnetic Resonance Imaging
NM	Nephrogenic Mesoderm
NSW	New South Wales
P	Proliferative Zone
PBS	Phosphate buffered saline
PCNA	Proliferating Cell Nuclear Antigen
PCNAc	Proliferating Cell Nuclear Antigen expression in the Condyle
PCNAgf	Proliferating Cell Nuclear Antigen expression in the Glenoid Fossa
PDL	Periodontal Ligament
PTHrP	Parathyroid Hormone-related Protein
R	Resting Zone

Shh	Sonic Hedgehog
TGF	Transforming Growth Factor
TMJ	Temporomandibular Joint
VEGF	Vascular Endothelial Growth Factor
WD	Wolffian Duct
Wts	Weight at Sacrifice

Table of Contents

DEDICATION	II
ABSTRACT	III
DECLARATION	V
PUBLICATIONS	VI
ACKNOWLEDGEMENTS	VII
LIST OF ABBREVIATIONS	IX
TABLE OF CONTENTS	XII
LIST OF FIGURES	XV
LIST OF TABLES	XVII
1. INTRODUCTION	19
2. LITERATURE REVIEW	23
2.1. INTRODUCTION	23
2.2. FUNCTIONAL MANDIBULAR ADVANCEMENT	24
2.3. TMJ BONE REMODELING AND GROWTH MODIFICATION	26
2.3.1. Endochondral Ossification	32
2.3.2. Intramembranous Ossification	35
2.4. MANDIBULAR CONDYLAR CARTILAGE (MCC)	37
Histochemical Changes in Condylar Cartilage during Mandibular Advancement	43
2.5. GLENOID FOSSA (GF)	47
Histochemical Changes in Glenoid Fossa during Mandibular Advancement	47
2.6. FIBROBLAST GROWTH FACTOR (FGF)	51
2.6.1. Fibroblast Growth Factors family:	51
2.6.2. Fibroblast Growth Factor8 (FGF8):	56
2.7. PROLIFERATING CELL NUCLEAR ANTIGEN (PCNA)	61
3. METHODS AND MATERIALS	65
3.1. ANIMALS AND EXPERIMENTAL DESIGN	65
3.1.1. Anaesthesia and Appliance fitting	66

3.1.2. Weight gain recording.....	67
3.2. EUTHANASIA AND TISSUE PREPARATION.....	67
3.3. IMMUNOHISTOCHEMICAL EXAMINATIONS.....	68
3.4. QUANTITATIVE IMAGING AND STATISTICAL ANALYSIS.....	71
4. RESULTS.....	76
4.1. HISTOLOGICAL STRUCTURES.....	78
4.2. FGF8 EXPRESSIONS IN THE MANDIBULAR CONDYLAR CARTILAGE (FGF8C) AND THE GLENOID FOSSA (FGF8GF).....	79
4.3. PCNA EXPRESSIONS IN MANDIBULAR CONDYLAR CARTILAGE (PCNAC) AND GLENOID FOSSA (PCNAGF).....	84
4.4. MANDIBULAR POSITION.....	88
4.5. WEIGHT GAIN.....	92
5. DISCUSSION.....	96
5.1. FUNCTIONAL MANDIBULAR ADVANCEMENT.....	96
5.2. TMJ BONE REMODELING & GROWTH MODIFICATION.....	98
5.3. HISTOLOGICAL FEATURES.....	101
5.3.1. Cellular changes in the Mandibular Condylar Cartilage.....	101
5.3.2. Cellular changes in the GF.....	102
5.4. MOLECULAR CHANGES.....	103
5.4.1. FGF8.....	103
5.4.2. PCNA.....	104
5.5. MANDIBULAR POSITION.....	105
5.6. WEIGHT GAINING.....	106
6. CONCLUSION.....	106
FUTURE DIRECTION.....	107

APPENDICES:	110
APPENDIX 1: ELECTRO-MICROSCOPIC IMAGES OF IMMUNOSTAINED TMJ SECTIONS	110
FGF8c	110
FGF8gf.....	114
PCNAc	118
PCNAgf.....	122
APPENDIX 2: STATISTICAL ANALYSIS (SPSS OUTPUT).....	124
FGF8c	124
FGF8gf.....	134
PCNAc	144
PCNAgf.....	165
Weight.....	175
APPENDIX 3: PROGRESSIVE REPORT	183
REFERENCES	186

List of Figures

FIGURE 2-1 GROWTH RELATIVITY HYPOTHESIS ELEMENTS	29
FIGURE 2-2 CARTILAGE DIFFERENTIATE TO BONE.....	34
FIGURE 2-3 HISTOMORPHOLOGIC PICTURE OF THE CONDYLE	38
FIGURE 2-4 MCC-GF GROWTH MODIFICATION	41
FIGURE 2-5 ADVANCED CONDYLAR CARTILAGE AND GLENOID FOSSA	45
FIGURE 2-6 TMJ GROWTH MODIFICATION	49
FIGURE 2-7 THE FGF8B-FGFR2C COMPLEX AND FGF8B'S OVERALL FEATURE	53
FIGURE 2-8 FGF GENES RELATIVE EXPRESSION	60
FIGURE 2-9 PCNA	61
FIGURE 3-1 BITE JUMPING APPLIANCE	67
FIGURE 3-2 THE UNIFIED AREA FOR IMAGE TAKING.....	72
FIGURE 3-3 HRP POSITIVE IMMUNOSTAINED CELL COUNTING IN MCC AND GF	73
FIGURE 4-1 DISTINCTIVE CELLULAR LAYER IN THE MCC AND THE GF	79
FIGURE 4-2 FGF8 IN THE MCC AND THE GF	81
FIGURE 4-3 FGF8 C & GF; DIAGRAM FOR EXPERIMENTALS VS. CONTROLS	82
FIGURE 4-4 FGF8 C & GF; DIAGRAM FOR EXPERIMENTALS VS. CONTROLS IN DIFFERENT EXPERIMENT DAYS	83
FIGURE 4-5 PCNA IN CONDYLAR CARTILAGE AND GLENOID FOSSA	85
FIGURE 4-6 PCNA C & GF; DIAGRAM FOR EXPERIMENTALS VS. CONTROLS	86
FIGURE 4-7 PCNA C & GF; DIAGRAM FOR EXPERIMENTALS VS CONTROLS ON DIFFERENT EXPERIMENT DAYS	88
FIGURE 4-8 THE RAT'S MANDIBLE IN A CL II POSITION.....	90
FIGURE 4-9 A DIAGRAM FOR MANDIBULAR POSITION IN EXPERIMENTAL SAMPLES	91
FIGURE 4-10 SCHEMATIC SAGITTAL VIEW OF HUMAN AND RAT TMJ	92

FIGURE 4-11 MANDIBULAR POSITION IN EXPERIMENTAL AND CONTROL SAMPLES	92
FIGURE 4-12 THE DIAGRAM FOR RATS' WEIGHT AT SACRIFICE (WTS) (GR).....	94

List of Tables

TABLE 2-1 STOMATOGNATHIC ADAPTATION.....	27
TABLE 2-2 OSTEOGENESIS GENETIC PATTERNING	30
TABLE 2-3 TMJ ADAPTATION.....	31
TABLE 2-4 ENDOCHONDRAL AND INTRAMEMBRANOUS OSSIFICATION	32
TABLE 2-5 ENDOCHONDRAL OSSIFICATION	32
TABLE 2-6 INTRAMEMBRANOUS OSSIFICATION	36
TABLE 3-1 EXPERIMENTAL DESIGN	66
TABLE 4-1 THE WHOLE EXPERIMENT’S DETAILS AND RECORDED DATA FOR EACH SAMPLE	76
TABLE 4-2 FGF8 C & GF; EXPERIMENTALS VS. CONTROLS.....	82
TABLE 4-3 FGF8 C & GF; EXPERIMENTALS VS. CONTROLS IN DIFFERENT EXPERIMENT DAYS ..	83
TABLE 4-4 PCNA C & GF; EXPERIMENTALS VS. CONTROLS	86
TABLE 4-5 PCNAC & GF EXPERIMENTALS VS. CONTROLS ON DIFFERENT EXPERIMENT DAYS...	87
TABLE 4-6 MANDIBULAR POSITION IN EXPERIMENTAL SAMPLES.....	90
TABLE 4-7 MANDIBULAR POSITION ON THE DAY OF SACRIFICE	91
TABLE 4-8 RATS' WEIGHT ON THE DAY OF SACRIFICE (WTS) (GR)	93

INTRODUCTION

1. Introduction

Several studies have discussed mandibular advancement as a functional therapy for skeletal class II malocclusion (1-3) and have shown that a fundamental factor in regulating cellular activities during tissue morphogenesis is mechanical stress (4, 5). The forward positioning of the mandible is followed by adaptive remodeling in the MCC and the GF (6-10). Many studies with rats and monkeys have also shown that new bone formation in the condyle and the GF occurs in response to mandibular advancement (10-12).

Growth modification of the lower jaw during mandibular forward positioning is a successful example for bone remodeling in response to a change in biophysical environment (3). Vertical opening and horizontal forward positioning as components of bite-jumping mode are both important elements in this biophysical change which induce the adaptive remodeling in the CC and GF (10, 11, 13). This remodeling occurs by expression of cells' endogenous regulatory factors in the mandibular condyle through an endochondral ossification process in the MCC (2-7) and intramembranous ossification (IO) in the GF (8, 10, 11, 14-16).

Osteogenesis through an endochondral ossification (EO) in the MCC is a pathway of phenotypic and morphologic change of mesenchymal cells from initiative immature cells in the condylar superficial layer, or articular zone, downward to mature bone-making cells in the erosive zone (8, 17-21). This process creates a zone-like pattern from the superficial layer downward: 1. Articular Zone, 2. Resting Zone, 3. Proliferative Zone, 4. Hypertrophic Zone, 5. Erosive Zone (17, 22). It has been revealed that the mesenchymal cells are oriented in the CC, leading to cellular migration and condensation followed by differentiation into bone-making cells (23).

The population size of the mesenchymal cells present in the sub-periosteal connective tissues of the MCC directly impacts the number of bone-making cells available to engage in the formation of new bone during craniofacial development. The undifferentiated mesenchymal cells in the Extra-Cellular Matrices (ECM) give rise to other cell types as the need arises and they are present in the ECM of developing bones in the skull, including the temporal bone (24, 25).

Mesenchymal cells are known to proliferate and multiply until they differentiate. Differentiation of mesenchymal cells into bone-making cells curtails the population size because the proliferative activity slows down as development continues (26). Another source of mesenchymal cells is the pericytes present in the peri-vascular sites surrounding migrating blood vessels. Pericytes are primitive cells that may act as precursors to other mesenchymal cells and the proliferative mesenchymal cells (27, 28), while the intramembranous ossification is the main part of the osteogenesis pattern in GF. Thus, mesenchymal cells directly differentiate into osteoblasts (14-16) known as osteoprogenitor cells (29, 30). Fibroblast-like cells proliferate to pre-osteoblasts or early osteoblasts to ultimately form bone (31, 32).

The FGFs form a family of at least 23 growth regulatory proteins that share 35 – 50% amino acid sequence identity. Proliferation and differentiation in a wide range of cells of epithelial, mesodermal and ectodermal origin are induced by this protein family (33-41) and they regulate mesenchyme and chondrocyte proliferation in the MCC adaptive remodeling (17). FGF signaling results in a decrease in chondrocyte proliferation and an acceleration of hypertrophic differentiation and morphologic changes in chondrocytes (9).

The relative expression domains of members of the FGF and TGF β signaling pathways facilitate functional studies on endochondral ossification, which will contribute to a

better understanding of the molecular regulation of bone development. FGF8 is expressed in highly proliferating, columnar chondrocytes, in early hypertrophic and hypertrophic chondrocytes (42).

PCNA is a marker for cell proliferation (43, 44). PCNA is a highly conserved protein expressed at high levels in dividing cells. It is discovered as a stimulating factor for DNA polymerase (44, 45). PCNA detection in cells indicates proliferative activity as it functions as a DNA sliding clamp for DNA polymerase delta, and is also an important component in eukaryotic chromosomal DNA replication (43, 45). PCNA detection is an established method for studying the proliferation activity of cells in developmental processes (45-47). The PCNA is detected in the nucleus of dividing cells.

The aim of this study is to evaluate the proliferative and hypertrophic activities in the MCC and the GF during mandibular advancement in Sprague Dawley Rats, as evidenced by the FGF8 and PCNA. FGF8 is an indicator for cellular chondrogenic and morphologic differentiation and hypertrophic activity, and PCNA is a tissue marker as an indicator for cellular proliferation; these factors are used to demonstrate the histochemical nature of bone adaptive response to mandibular protrusion. Thus, this study is designed to evaluate the histochemical changes resulting in TMJ remodeling and mandibular growth modification into a forward position.

LITERATURE REVIEW

2. Literature Review

2.1. Introduction

Orthodontics is defined as a branch of dentistry concerned with facial growth, dental development, and prevention and correction of occlusal anomalies (48). Clinical orthodontics requires an understanding of both dental development and general concepts of physiological and physical growth ((49) p. 25)). It also involves the use and control of force acting on the teeth and associated structures such as sutures and TMJ ((50) p. 145)).

An orthodontic problem could be attributable to dental disorders, craniofacial skeletal anomalies or combinations of both. These problems based on the inter-arc dental and skeletal relationship are divided into different subgroups as Cl I, Cl II and Cl III malocclusions. Skeletal Cl II malocclusion is one of the most common orthodontic problems which may be caused by mandibular deficiency, excessive growth of the maxillary or a combination of these. When the mandible is small or retruded relative to the maxilla, it is called a mandibular deficiency which is the most consistent diagnostic finding in Cl II malocclusion ((50) p. 9, (51)).

Skeletal problems may be treated - based on several factors - by functional appliances, orthognathic surgeries or a combination of both ((50) p. 9, (51)). Growth modification by using headgear or functional appliances is a choice for Cl II treatment in growing patients ((52) p. 329-34) (53)). The current research is a histochemical study on the MCC and the GF during mandibular advancement, as a functional treatment for skeletal Cl II problem.

Controversy continues regarding the precise nature of the skeletal changes during growth modification of the maxilla and the mandible, although little argument remains that

orthopaedic force may modify the growth of the maxilla and the mandible (54). Histological and biochemical research in this field, such as the current study, could provide basic information about the nature of the skeletal growth modification in response to orthopaedic forces.

2.2. Functional Mandibular Advancement

Functional appliance is a term used for an orthodontic appliance which forces the mandible into an eccentric/non-eccentric relation position while it is fully seated in the mouth. Most commonly, functional appliances are used in cases of mandibular protrusion to correct the skeletal CI II relationships. The occurrence of significant additional growth from this approach is not fully verified by different studies in this field, but it has clearly been used with successful results ((52) p. 220-21, (55)).

Norman Kingsley introduced the “bite-jumping” appliance in 1879, and the history of functional appliances traces back to that year (56). Since the late 19th century many types of bite-jumping functional appliances have been endorsed to treat growing patients. The basic principle for all bite-jumping functional appliances is to keep the mandible in a protrusive position in an attempt to induce condylar and then mandibular growth. There are different removable bite-jumping functional appliances with similar basic principals; activators, bionators, Clark twin block and Frankel functional regulator II (FR II) with various modifications. Fixed bite-jumping functional appliances were well represented by Herbst appliances, which originated around 1905, and Pancherz reintroduced them in the early 1970s. A continuous mandibular protrusion is created by the telescope mechanism of the Herbst appliance (reviewed by Shen *et al* 2005 (57), (55)).

A therapeutic approach which enhances the mandibular growth is required for skeletal CI II treatment (17, 57, 58). A wide range of functional appliances are available to correct this type of skeletal and occlusal disharmony, all of which aim to stimulate mandibular growth by forward positioning or vertical bite-opening, or a combination of these two methods (3, 49, 50, 55, 59-62). Although many animal studies demonstrate skeletal mandibular changes in response to mandibular forward posturing (6-8, 63-65), the observations in human studies are more equivocal and controversial (57, 62, 66).

The effectiveness of functional treatment of mandibular growth deficiencies depends on several factors; the direction and magnitude of the force, the biological responsiveness of the MCC, the mandibular growth rate (pre-peak, peak, and post-peak growth rates with regard to the pubertal growth spurt) and treatment duration (17, 57, 62, 67-69). The effect of functional treatment with the CI II activator and the CI II activator high-pull headgear was recently studied on a 3D finite element model of the human mandible. The study demonstrated that the mandibular body is subjected to higher stress than the condylar region and the muscle attachment regions obtain the maximum stress values, such as the coronoid process (70).

The assessments show that forward positioning of the mandible by continuous bite-jumping in young adult patients with CI II malocclusion results in remodeling of the TMJ (17). In human studies the Herbst appliance is considered the highest coefficient of efficiency by 0.28 mm/month (average amount of actual extra elongation of the mandible in treated subjects), followed by the Twin-block by 0.23 mm/month (62).

Immediate alteration of the neuromuscular activity of the orofacial muscles to the functional position of the mandible is indicated by McNamara *et al* (1979). This immediate neuromuscular activity is particularly noticeable in the lateral pterygoid muscle. The

neuromuscular alterations closely follow the facial skeleton adaptive responses. The various adaptive responses depend on the maturational status of the animal. These adaptations continue until the structure of the skeletal and dentoalveolar components of the craniofacial complex are complete (65).

Several structural mechanisms could be involved in the effectiveness of functional appliances to obtain a CI II correction; (1) retardation or redirection of the mesial and vertical maxillary growth, (2) retardation of the mesial and vertical maxillary dentoalveolar growth, (3) encouragement of mandibular growth, including condylar growth, in response to anterior displacement of the condyle, (4) growth of the mesial and vertical mandibular dentoalveol, (5) combined maxillary and mandibular orthopedics effect with maxillary incisor lingual tipping and mandibular incisor labial tipping, resulting in overjet correction, and (6) TMJ remodeling (reviewed by Bishara *et al* 1989 (55)).

The current study is performed to clarify the nature of the successful effect of mandibular advancement at a biological level by using rat experiments.

2.3. TMJ Bone Remodeling and Growth Modification

Maxilla and mandible are the boney structural bases of the stomatognathic system. TMJ, periodontal ligament (PDL), alveolar process and maxillary sutures biomechanically are skeletal structures more reactive to physiologic and therapeutic biomechanical stimuli, in comparison with other parts of the jaws (Table 2-1). The jaws respond to functional and therapeutic loading via the bone modeling and remodeling mechanisms.

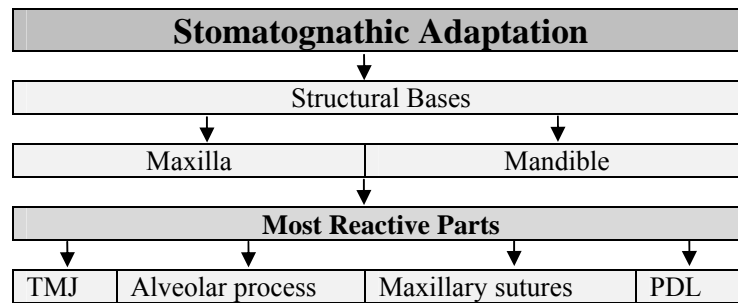


Table 2-1 Stomatognathic adaptation

Most of the responses to the orthodontics and dentofacial orthopedics are associated with the TMJ, alveolar bone, maxillary sutures and PDL (modified from Roberts *et al* 2004 (71)).

The TMJ response to functional and orthopedic appliances has been studied through clinical procedures and animal experiments. It is necessary to understand the nature of the TMJ tissues and their relations during normal growth, maturation and orthodontic treatments, for an effective consideration of the potential association between tissue response in the TMJ and orthodontic treatment. Most of the investigations of the TMJ are in various experimental animals. However, in humans, very few postnatal investigations of the TMJ development are available ((50) p.191-96) (50, 72-75)). During the postnatal period, the TMJ becomes a secondary growth site. It has two articular surfaces that can adapt to environmental changes ((summarized in Table 2-3) (72, 76)).

The MCC is a secondary, fibrous type cartilage and does not originate from a primary cartilage precursor. It is highly responsive to mechanical stimulation and grows appositionally from its peripheral. This anatomic position is altered by continuous repositioning of the mandible to its best possible functional advantage during craniofacial growth and TMJ adaptive remodeling. Mandibular posture maintenance is facilitated by both mechanisms of TMJ remodeling and continuous mandibular reposturing. The MCC has its own intrinsic growth but does not generate tissue-separating forces similar to epiphyseal plates ((52) p. 49-50, (77)).

Remodeling of the GF and the compensatory growth of the MCC adjusts with the anatomic position of the MCC in the GF. In the GF, the subarticular proliferative zone can support both anabolic and catabolic bone modeling to change the shape and position of the temporal fossa in response to environmental changes (71). The GF formation is induced by a wide range of repetitive motion and pressure against the temporal bone with cortical bone apposition (78).

Studies on monkeys and rats have shown the capability of functional adaptation in the TMJ to mandibular forward displacement. In some studies amplification in osteoblasts and prechondroblast mitotic activity is observed as the initial influence of functional mandibular advancement with acceleration in differentiation of osteoprogenitor cells to prechondroblast. This is followed by observing an increase in transformation of prechondroblast into functional chondroblasts, and more chondroblastic hypertrophy with accelerated endochondral bone growth. An increased number of dividing cells resulting in an increased thickness of the prechondroblast proliferative zone is reported ((50) p. 191-96) (79)). However, in the current research the level of proliferation in the condyle is not significantly increased during mandibular advancement.

The growth rate in rats and monkeys is faster than in human beings, and it is easier to control interfering factors such as cooperation in rats and monkeys. Therefore, the effect of mandibular anterior displacement in animal studies shows more consistent results, while observations made in clinical studies show greater discrepancies. Although it is difficult to clearly prove whether the growth of the human mandible is altered by orthopedic and functional forces, research shows orthopedic change is a combination of mandible and GF change ((50) p. 194)).

A balance of factors is at work with orthopedic appliances controlling the MCC-GF modification. At least six factors that interact and produce a positive change for each individual are identified in the growth relativity hypothesis: 1. Skeletal displacement, 2. Dental, 3. Neuromuscular, 4. Non-muscular viscoelastic tissues including synovial fluids, 5. Biodynamic intrinsic and extrinsic factors, and 6. Maturational age. These all contribute to adaptation in the TMJ complex (Figure 2-1) (80).

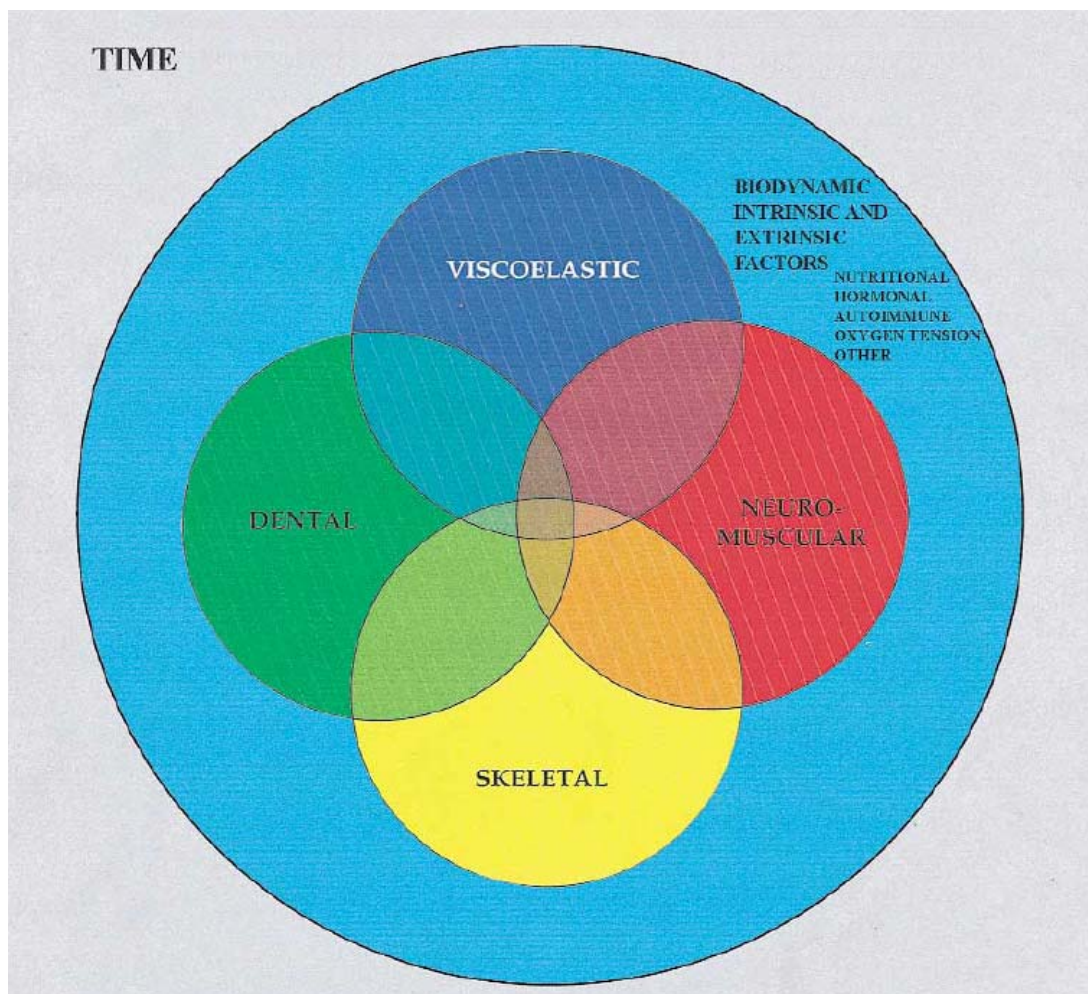


Figure 2-1 Growth Relativity Hypothesis Elements

The diagram shows the biodynamic factors involved in reactions between MCC-GF complexes to orthopedic mandibular protrusion. Extrinsic factors involved in the metabolic action of both MCC and GF are mentioned in the main circle (Biodynamic Intrinsic and Extrinsic Factors: Nutritional, Hormonal, Autoimmune, Oxygen Tension, other). The inner circles indicate the different factors of the growth relativity hypothesis and their possible overlaps during mandibular protrusion and retention (Viscoelastic, Dental, Skeletal, Neuromuscular) (modified from Voudouris *et al* 2000 (80)).

The growth relativity hypothesis is presented by Voudouris *et al* for the mechanism of MCC-GF growth modification with mandibular advancement. It involves: 1. Mandibular displacement, 2. Tissue extension forces applied to the MCC-GF through several different attachments known as viscoelastic forces, 3. Transduction of forces radiating beneath the fibrocartilage of both condyle and GF. The MCC and GF are contiguous structures, interconnected by retrodiscal tissues, and these three mechanisms result in MCC-GF growth enhancement, growth redirection and ultimately TMJ growth remodeling (80). The Functional matrix theory is the other hypothesis which describes the possible mechanism of bone remodeling in the MCC-GF complex in response to propulsive forces (81-85).

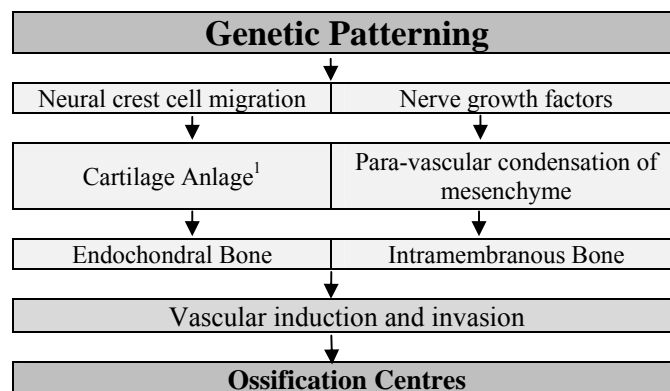


Table 2-2 Osteogenesis Genetic Patterning

Genetic patterning in craniofacial ossification centres involves neural crest cell migration along the pathways of nerve distribution. Cartilaginous or intramembranous structure formation is the result of these biologic pathways (modified from Roberts *et al* 2004 (71)).

The neurovascular distribution seems to control the patterning of ossification and subsequent response to mechanical loading of both endochondral and intramembranous bones (32).

¹ Anlage, in embryology, is the primordium which is the initial clustering of embryonic cells. It serves as a foundation from which a body part or an organ develops.

Generally, three physiologic possibilities are involved at any given site when a bone is adapting to changing loads: 1. Bone apposition, 2. Bone resorption, or 3. No change. Repetitive loading indicates the pattern of the three types of site-specific activity. The “Flexure law of bone modeling” refers to the phenomenon that “bone bending” results in patterns of surface compression and tension. These are potential sites of bone formation and resorption. Bone is generally capable of flexure up to about 2.5% without fracturing (86). The biological response to applied mechanical forces is the physiologic mechanism for skeletal adaptation to the environmental changes.

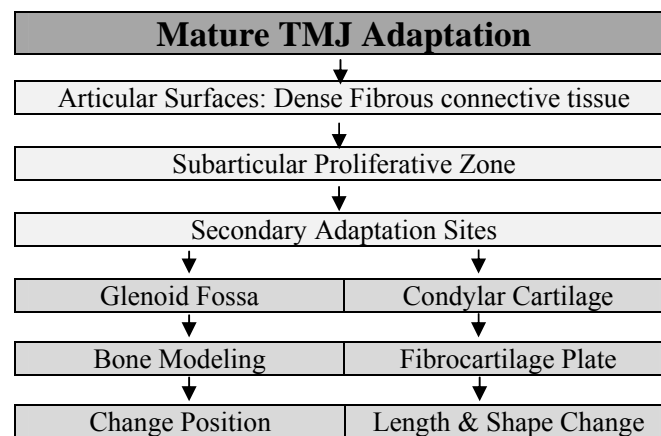


Table 2-3 TMJ Adaptation

Normal TMJ is remarkably able to heal and adapt over a lifetime. The mechanism of continuous osseous adaptation in TMJ is similar to the covering periosteum of other bones. The fibrous layer of the periosteum is a dense fibrous connective tissue covering healthy articular surfaces and the subarticular layer is a cellular proliferative zone. The mandibular condyle and the GF adaptation occur during normal growth and in response to physiologic and therapeutic forces (modified from Roberts *et al* 2004 (71)).

A five-step sequence could be used for comparing the endochondral and intramembranous ossification ((52) p. 44-45) (32));

Endochondral bone formation		Intramembranous bone formation
1	Chondrocytes hypertrophy and cartilage matrix calcification within the cartilage primordium matrix	The ectomesenchymal condensation centres differentiate to osteoblasts then produce osteoid (a fibrous bone matrix)
2	Invasion of blood vessels from the perichondrium and bringing undifferentiated connective tissue cells	Osteoblast become osteocytes and blood vessels become surrounded by bone; Cells and blood vessels are encased.
3	Osteoblasts differentiate form the connective tissue osteoprogenitor cells and deposit osteoid on the remnants of the calcified cartilage matrix	Osteoblasts in the surface periosteum adding bone to the surface of the bone (appositional bone growth)
4	Mineralization of the fibrous bone matrix	Bone matrix mineralization
5	Mature bone is covered with a membrane	Mature bone is covered with a membrane

Table 2-4 Endochondral and Intramembranous Ossification

2.3.1. Endochondral Ossification

Endochondral bone formation in the craniofacial skeleton only takes place in the bones of the cranial base and portions of the calvarium ((52) p. 44-45) (71)).

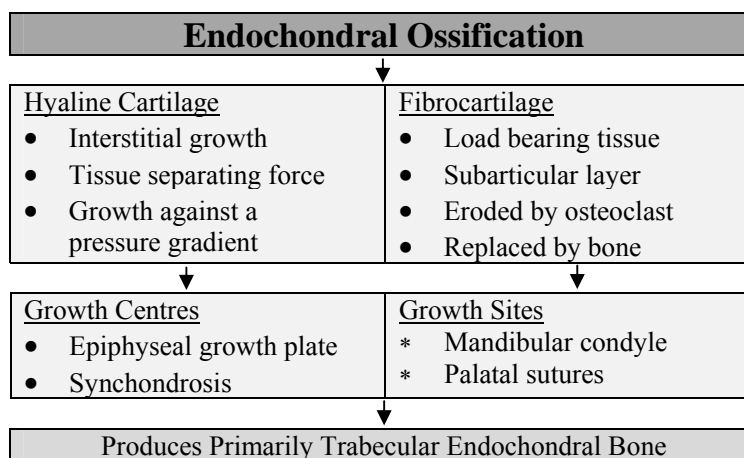


Table 2-5 Endochondral Ossification

Growth plates and synchondrosis are examples for endochondral bone formation via hyaline cartilage. These are primary growth centres. The mandibular condyle and early postnatal growth of palatal sutures are examples for endochondral bone formation via fibrocartilage structure. Fibrocartilage is the precursor for secondary growth. Characteristic patterning of trabecular endochondral bone is caused by the vascular invasion process during endochondral ossification (modified from Roberts *et al* 2004 (71)).

During the endochondral bone formation, chondrocytes initially proliferate and differentiate into hypertrophic chondrocytes. After that, many chondrocytes are dissolved and the remainders are mineralized and die. The mineralized matrix is removed by osteoclasts and the chondrocyte lacunae are eroded as the cartilage matrix calcifies. Osteoclast and mesenchymal precursors are derived by growth of vascular tissue into bone. The degraded matrix is replaced by cellular bone formed by osteoblasts. The osteoblasts act in organized units. Ultimately, bone tissue forms around the calcified cartilage, while capillaries with osteogenic cells invade the lacunae ((87) p.111-44) (88), (89)).

Previous studies indicate that hypertrophic chondrocytes can transdifferentiate or de-differentiate and re-differentiate into bone cells, osteoblasts/osteocytes, during the endochondral bone formation. They have also indicated that hypertrophic chondrocytes persist during endochondral bone formation, and it is frequently reported that at least a few chondrocytes possibly survive and enter the primary spongiosa of the MCC. This indicates that occasional survival of hypertrophic chondrocytes might be a structural feature of the condyle.

Meanwhile, in ultra-structural studies with improved fixation methods, the formation of a mainly non-collagenous matrix (presumably proteoglycans) is shown around hypertrophic chondrocytes in the peri-cellular matrix. Further investigations have also reported the formation of thick collagen fibrils in the peri-cellular matrix of hypertrophic chondrocytes in an aged rat's MCC and trachea, and in the MCC in rats with strontium rickets. Furthermore, Type I collagen have been detected in several immunohistochemical studies around the hypertrophic chondrocytes in the MCC. This indicates the importance of characterizing hypertrophic chondrocytes in various conditions by analysing the peri-cellular

matrix. Moreover, at least in part, long-term survived uneroded hypertrophic chondrocytes acquire osteocytic characteristics (reviewed in (90)).

The process of endochondral ossification is regulated at several levels by secreted signaling molecules of the FGF and transforming growth factor beta (TGF β) families. Different dwarfism syndromes in humans, such as hypochondroplasia (91), achondroplasia (92), and thanatophoric dysplasia (93) are the results of ectopic activation of FGF signaling. Evidence exists for several key molecular mechanisms that regulate these events. However, substantial gaps in understanding remain (89).

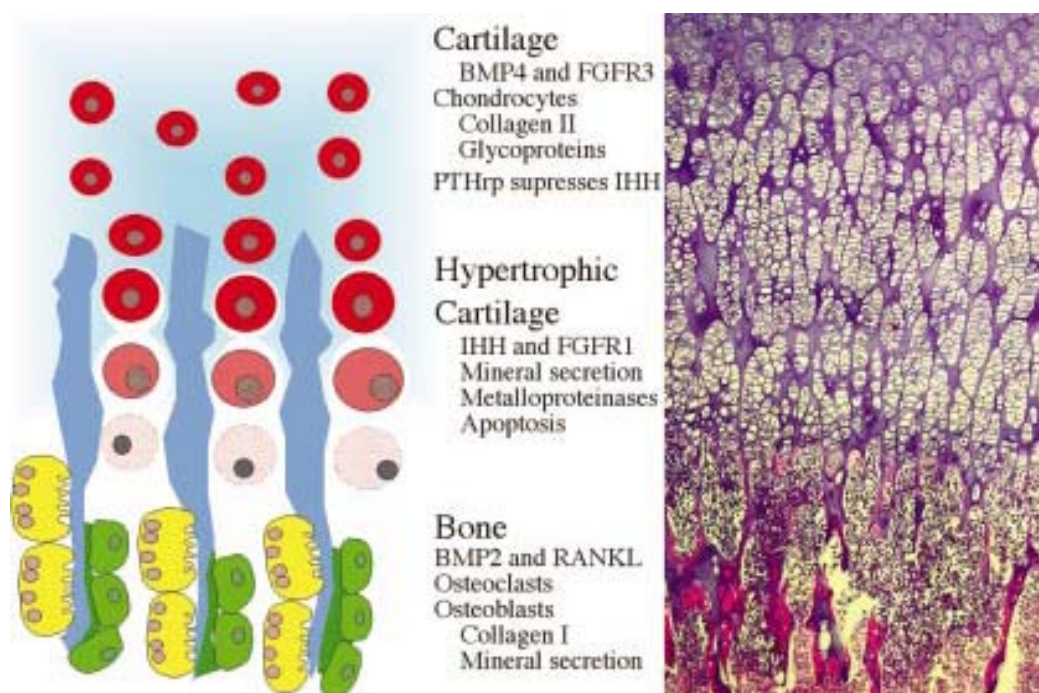


Figure 2-2 Cartilage Differentiate to Bone

The diagram is a schematic view adjacent to a section from a human growth plate (1x2 mm). The tissue section is stained by Hematoxylin and Eosin (H&E); cartilage proteoglycans (blue) and bone collagen (red). A cell cannot lineage revert once it differentiates into cartilage or bone. Mesenchymal stem cells are required for continuing differentiation in bone. They differentiate into several cell types. Feedback between Indian hedgehog (Ihh) and PTHrP and differences in FGFRs and BMP expression are critical in the cartilage transition into bone. Normal differentiation requires many other factors, such as vitamin D. The developing bone is divided into apoptotic regions, in regard to the columnar formation of hypertrophic chondrocytes. These apoptotic regions become inter-trabecular spaces. The mineralized columns are the scaffold for osteoblast bone deposition, while the remaining mineralized cartilage is degraded (modified from Blair *et al* 2002 (89)).

Complex interactions of local and systemic factors control the molecular mechanisms for developmental regulation of the growth plate. Bone morphogenetic proteins (BMPs) (94), wnts (95), FGFs (96), hedgehog proteins (97), parathyroid hormone-related protein (PTHrP) (98), insulin-like growth factors (IGF) (22), and VEGF (88) are some of the local factors. Some systemic factors are growth hormone, thyroid hormone, estrogen, androgen, vitamin D, and glucocorticoids. The systemic factors are involved in controlling the growth of long bones (reviewed by Kronenberg *et al* 2003 (99)).

Cancellous bone is the initial osseous structure resulting from endochondral bone formation. The cartilage cells die and the intercellular substance mineralizes. On the other hand, osteoclasts erode the mineralized fibrocartilage in the mandibular condyle and the fibrocartilage is replaced by lamellar bone apposition. Fibrocartilage is formed by the subarticular proliferative zone in the condyle and is a load-bearing tissue. In the metaphysis of both the mandibular condyle and long bones, lamellar trabeculae that are aligned along the line of stress are the final remodeled structure in this process (71). This progress reflects Wolff's law² in the MCC and long bone (100, 101).

2.3.2. Intramembranous Ossification

Intramembranous ossification initiates with intramembranous condensations of mesenchyme, adjacent to blood vessels. This process initiates the formation of the flat bones; facial bones, cranium, sternum and scapula. The intramembranous ossification is the origin

² **Wolff's law**, the law of bone remodeling, states that bone in a healthy person or animal will adapt to applied loads. The bone will remodel and become stronger in response to the increased load to resist that sort of loading. Furthermore, the external cortical portion will become thicker in response to the loads. Conversely, if the load decreases, the bone will become weaker due to turnover (Wolff J. "The Law of Bone Remodeling" Berlin Heidelberg New York: Springer, 1986 (translation of the German 1892 edition) (cited from Wikipedia website, 15DEC2008)).

for sub-periosteal bone formation which represents a high degree of vascularity and lack of a cartilage precursor. The areas where growth factors are secreted lateral to neurovascular bundles seem to be the initial centre of ossification. The apposition rate will finally indicate the bone type which may be of the woven or lamellar type. Woven bone has a poorly organized matrix and is formed rapidly (up to 100 $\mu\text{m}/\text{day}$) and Lamellar bone has a highly organized matrix and is formed slowly (less than 1 $\mu\text{m}/\text{day}$) (71).

Intramembranous bone formation is dependent on patent blood vessels along the bone surface. Therefore it cannot grow against a pressure gradient. This osteogenic mechanism occurs in some secondary growth sites such as the PDL, sutures and the TMJ (Table 2-6). Intramembranous bone formation at secondary growth sites is cortical bone which is formed of circumferential lamellae or primary osteons. It is in contrast to production of initial trabecular bone formation at endochondral growth centres (71).

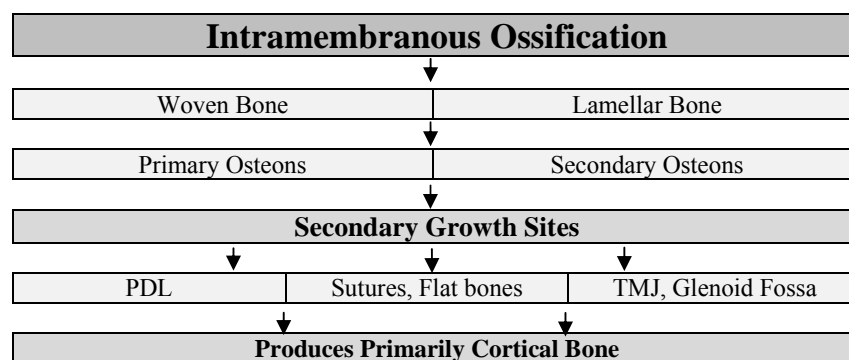


Table 2-6 Intramembranous Ossification

Intramembranous ossification produces a woven or lamellar bone, depending on the rate of apposition. All intramembranous bone formation is associated with secondary growth sites, such as the PDL, sutures of flat bones and some parts of the TMJ. Primarily cortical bone is the final production of the intramembranous ossification (modified from Roberts *et al* 2004 (71)).

From a molecular point of view, it is demonstrated that for the elongation of Meckel's cartilage FGF Receptor 3 (FGFR3), signaling is required and during intramembranous ossification of mandibular bones, FGFR2 and FGFR3 are involved (30).

2.4. Mandibular Condylar Cartilage (MCC)

The MCC is an active growth site for the mandible (102), and it has been studied as the primary focus of functional orthopedic therapy for mandibular disorders (58). Animal experimentations, contrary to human experimentations, are performed for more than just linear measurement of condylar growth and provide an insight into the MCC. Condylar growth could be monitored by histological observation, which has been conducted to identify cellular response during chondrogenesis of the MCC (9). Examination of the expression of growth factors in the MCC in response to mandibular repositioning as a biochemical approach makes it possible to reveal intrinsic aspects of condylar growth at molecular or genetic level with animal models (7).

The postnatal growth of the condyle proceeds through the biological process of endochondral ossification. This process is regulated and orchestrated by different growth factors which are mainly synthesized by chondrocytes (103). Several growth factors are studied in this field, such as transcription factor Sox9 (a critical transcription factor for differentiation of the mesenchymal cells into chondrocytes) (104, 105) parathyroid hormone-related protein (PTHrP) (106) and matrix metalloproteinase 13 (MMP- 13) (107), etc. These growth factors control condylar bone formation by facilitating and mediating the biomolecular pathway of endochondral ossification. The correlation between synthesis of some growth factors and progression of condylar bone formation have been discovered by Rabie *et al* with a series of biochemical examinations on animal experimentations (108). The biochemical examination of growth markers, such as type X collagen, is also suggested as a new approach to accurately represent the temporal pattern of condylar growth (109).

Even though the histomorphologic picture of the condyle varies in different stages of life, the following layers can usually be seen:

1. Surface Articular Zone, fibrous connective tissue.
2. Resting Zone.
3. Transitional or Proliferative Zone, containing proliferative cells and a transitional stage between undifferentiated cells and cartilage cells.
4. Hypertrophic zone, chondrocytes but not in a columnar order like epiphyseal bone.
5. Erosive Zone.
6. Bone formative zone, endochondral bone ossification ((50) p. 191-96) (17, 109)).

1. Articular Zone
.....
2. Resting Zone
.....
3. Proliferative Zone
.....
4. Hypertrophic Zone
.....
5. Erosive Zone
.....
6. Bone

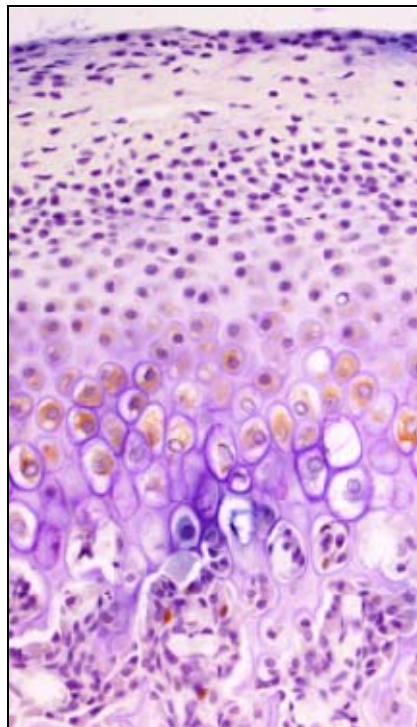


Figure 2-3 Histomorphologic picture of the Condyle

The image is a sagittal section of a 44 day-old Sprague Dawley rat's condyle after 21 days of mandibular advancement, immunohistochemically stained for FGF8. Six different cellular layers can typically be seen, which are named in the image as the histomorphologic picture of the condyle.

The MCC has several differences from growth plate cartilage and the limb bud. For example, in development it shows delayed appearance relative to the limb bud cartilage and originates from the periosteum (98, 110, 111). There are also differences in its mode of proliferation and differentiation (112, 113), cell alignment, invading capillary pattern, and extracellular matrix composition (110, 114, 115). The MCC's response to hormonal factors and mechanical loading is also different from growth plate cartilage and the limb bud's response. The MCC is covered by a thin layer of undifferentiated cells directly overlying the cartilage of the condyle (articular layer). This is in contrast to epiphyseal growth of long bones which takes place through cleavage of previously differentiated mature cartilage cells (116).

The MCC is unlike most other cartilages of the body. Embryologically, it is not derived from the primary cartilaginous skeleton and is secondary in origin; like the articular cartilage of the clavicle, the cartilages of the coronoid process and the mental region of the mandible. It is biochemically distinct from the other growth cartilages of the craniofacial region and the appendicular skeleton. Morphologically, the condyle's different cellular layers appear to be continuous with the two major layers; the periosteum along the neck of the condyle with the articular layer corresponding to the outer fibrous periosteum, and the prechondroblastic-chondroblastic layer corresponding with the inner osteogenic layer of the periosteum.

Therefore, the cells of the prechondroblastic zone and the pre-osteoblasts of the rest of the periosteum of the mandible are homologous. Thus, it is expected that alterations in mandibular function result in an altered biomechanical or biophysical environment in the TMJ region and ultimately lead to an adaptive response in the cells of the MCC (discussed by McNamara *et al* 1979 (65)).

During natural growth, the migration of mesenchymal cells from the covering membrane towards the center of the condyle results from mitosis of undifferentiated cells. Then the mesenchymal cells differentiate to immature cartilage cells. Mitosis of undifferentiated mesenchymal cells is the source of new members of the MCC family. Subsequently, the immature chondrocytes progressively mature into the hypertrophic phenotype. During chondrocytes' maturation, the calcification of the degraded cartilage, a preliminary stage of endochondral ossification, is facilitated by type X collagen. The extracellular matrix plays an important role in the differentiation of mesenchymal cells to chondrogenic cells. The cells within the articular layer are undifferentiated mesenchymal cells. They become pre-chondroblasts and later mature to chondrocytes (8).

Proliferative activity maintains in many of the condylar chondrocytes during hypertrophic differentiation in the late embryonic stage (98). Proliferating chondrocytes in CC could originate from the fibrous tissue layer covering the condyle. The fibroblasts and mesenchymal cells within the articular layer are found to be oriented in the direction of mandibular advancement. However, in mandibular natural posture the cells in this layer are packed parallel to the articular surface, showing no signs of strain. Functional appliances result in the stretch of the posterior fibres of the disc, and might also increase cellular density due to transverse compression; followed by an increase in cell-cell interaction (8).

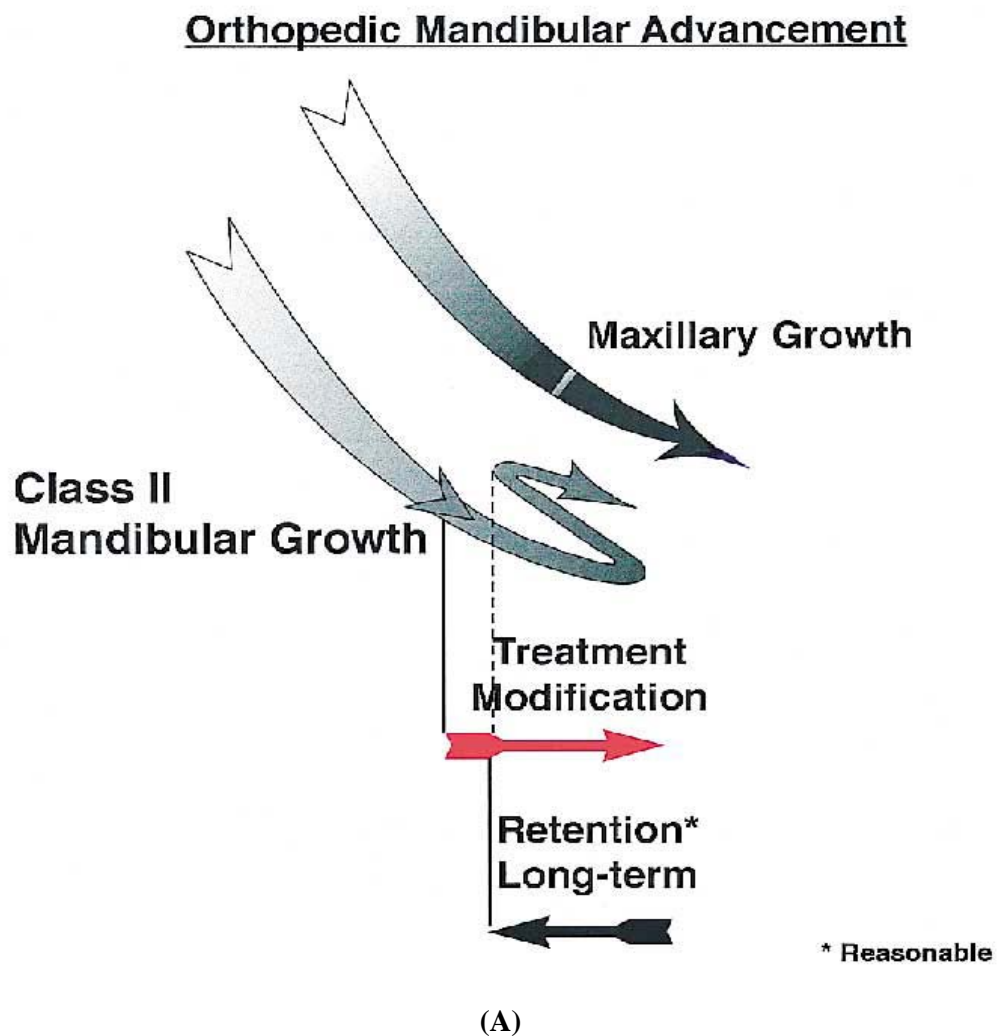
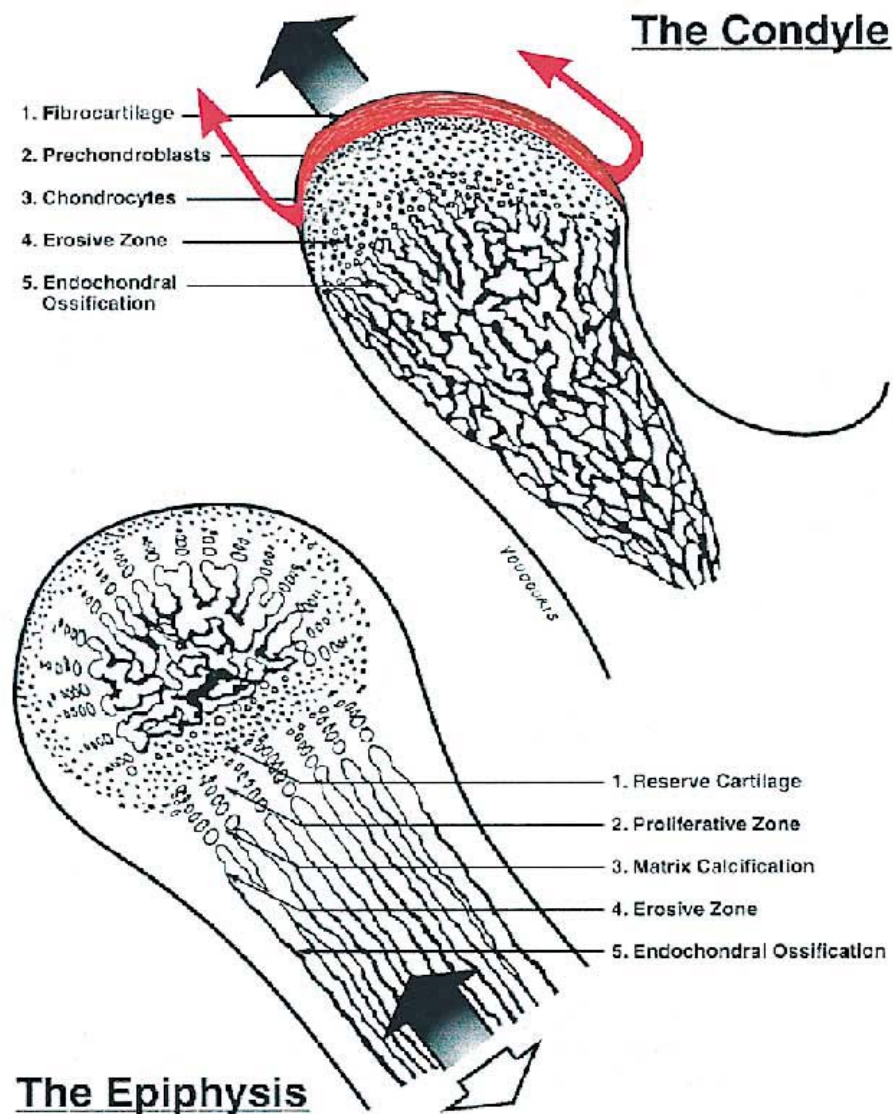


Figure 2-4 MCC-GF Growth Modification

The diagram shows an overall clinical concept MCC-GF growth modification in response to mandibular advancement. Orthopedic advancement enhances the jaw's growth (Treatment Modification *arrow*). However, relapses are reported in long term evaluations (Retention Long term *arrow*).



(B)

Figure 2-4 MCC-GF Growth Modification

The Condyle, numbered from top to bottom: 1. Fibrocartilage, 2. Prechondroblasts, 3. Chondrocytes, 4. Erosive zone, 5. Endochondral ossification. The Epiphysis, numbered from top to bottom: 1. Reserve cartilage, 2. Proliferative zone, 3. Matrix calcification, 4. Erosive zone, 5. Endochondral ossification. The condyle of the mandible and the epiphysis of long bones have significant differences. The condyle has greater potential for modification. The epiphysis does not have a fibrocartilage covering layer, but the condyle does. In comparison with epiphyseal chondrocytes, condylar prechondroblasts are not surrounded by an intercellular matrix. Therefore they are not isolated from local factors. The chondrocytes are in a columnar arrangement in the epiphyseal, but they are further oriented in a multidirectional fashion. This arrangement is more suitable for changes in growth direction in comparison with epiphysis (modified form Voudouris *et al* 2000 (80)).

Histochemical Changes in Condylar Cartilage during Mandibular Advancement

Forward mandibular positioning produces biomechanical forces which solicit cellular and molecular changes in the mandibular condyles (6, 7, 23, 117). However, several studies have reported a positive response of the condyle to mandibular advancement. Controversial issues remain in this regard and the triggering mechanisms are not completely understood (7, 8, 65, 103, 118). Although the effect of bite-jumping appliances on the growth of the mandibular condyle remains controversial in the orthodontic literature (57), with a better understanding of condylar adaptive responses to condylar repositioning, improved treatment approaches to functional appliances could be developed, based on scientific principles.

Some researchers believe that the actual growth of the mandible is the positive response to mandibular advancement (119, 120) while later studies indicate that functional treatments help the mandible to reach its final size by growth acceleration without producing a larger size overall (6, 121). The reason for this controversy is an apparent lack of tissue markers to distinguish between the two processes of actual growth and growth acceleration (6). It is reported by Rabie *et al* 2003, that forward mandibular positioning accelerates and enhances the expression of Sox 9 and type II collagen leading to acceleration and enhancement of the chondrocyte differentiation and cartilage matrix formation in the mandibular condyle. However, for most of the growth period, this enhancement of growth did not result in a subsequent pattern of subnormal growth. Therefore, functional appliance therapy could induce true enhancement of condylar growth (6).

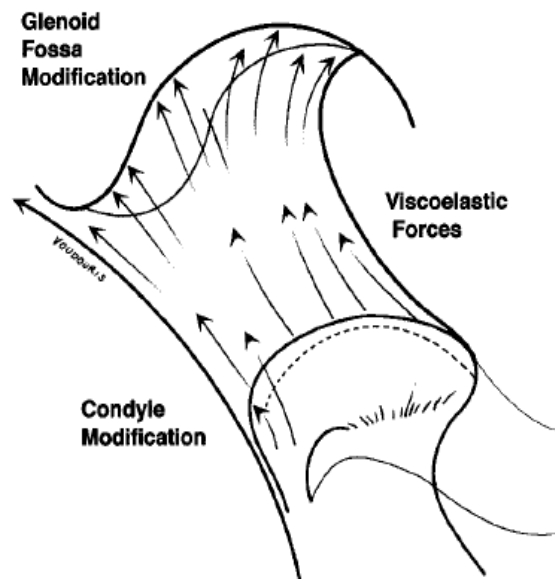
A close correlation exists between mandibular condylar repositioning and the modification of condylar growth, which results in thickening of the posterior part of the MCC. An increase in the total amount of DNA without a significant increase in proliferation

of the cells in the mandibular condyle is reported in response to mandibular advancement (122). Condylar adaptation to forward positioning has invariably been reported by a series of experimentations in rats, indicated by increased synthesis of growth regulatory factors such as Indian hedgehog (Ihh) (123) and parathyroid hormone-related peptide (PTHrP) (106). A considerable increase in endochondral ossification of the condyles is reported by Shen *et al*, in response to mandibular forward positioning by detecting the expression of type X collagen in rat samples (8). Significant increase in the rate and extent of condylar growth in response to forward condylar advancement is also reported in young Rhesus monkeys (63, 64, 124).

The maturation of the chondrogenic cells is triggered by mandibular condylar advancement, followed by an increase in endochondral ossification in the condyle. An increase in the proliferating cells in the mandibular condyles in addition to enhancing their differentiation could result in increased bone formation. This indicates that the MCC will adapt and remodel in response to the biophysical environment of the TMJ, regardless of the presence or absence of growth potential (8). There is a close correlation between the increase in the cartilage matrix and the increase in the amount of bone formed in response to mandibular advancement (6). It is also shown that longitudinal bone growth primarily depends on chondrogenesis (125).

The physical stretching and reorientation of mesenchymal cells in the articular layer might trigger the enhanced differentiation and maturation of chondrocytes. A source of mesenchymal cells could be the blood supply in the posterior connective tissue of the condyle. The blood vessels supplying the condyle are mainly localized in this particular area. Mandibular protrusion causes the posterior fibres of the disc to stretch, subsequently leading to an increased emergence of new blood vessels, or neovascularization, in this area. More mesenchymal cells are brought to the area by the increased neovascularization and induce an

enhanced differentiation and maturation of chondrocytes (126). Subsequently an increased bone formation replaces the terminally hypertrophic cartilage, followed by an increased synthesis of type X collagen and increased bone formation (8).



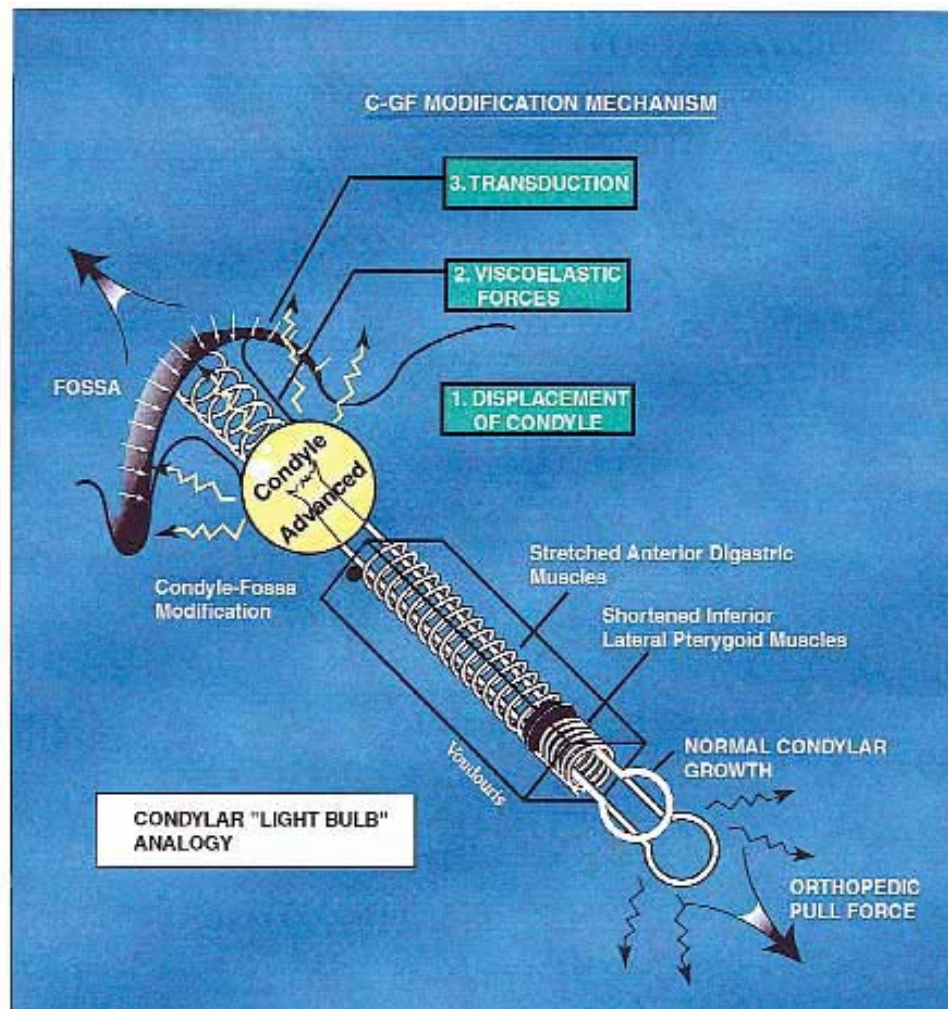
(A)

Figure 2-5 Advanced Condylar Cartilage and Glenoid Fossa

The diagram shows the advanced MCC and GF through their respective soft tissue attachments that change their growth directions.

Changes in the biophysical environment of the TMJ by forward mandibular positioning leads to the release of regulatory factors and enhancing condylar growth (6, 7). They also lead to a change in the condyle's morphology and angular relocation of the condylar head and new bone apposition, mainly located in the posterior part of the condyle (7, 65). An experiment on monkeys shows that the prechondroblastic-chondroblastic cartilage are significantly hypertrophic in the posterior condylar region, with a thickness three times that seen in normal monkeys (65). It is also demonstrated in adult rats, that by 30-day continuous mandibular advancement, adaptive morphological changes could be achieved in the MCC (127). The remodeling of the condyle ultimately results in a mandibular length

increase. The opinion that the length of the mandible is not entirely predetermined by genetic factors is consistent with this report (79, 128).



(B)

Figure 2-5 Advanced Condylar Cartilage and Glenoid Fossa

The diagram is a schematic illustration about the light bulb analogy of condylar growth and retention. The fact that a dimmer switch lights up the light bulb is schematically compared with continued advancement which lights up the growing condyle. The other elements are compared with different elements of the MCC-GF complex; muscles, retrodiscal tissues, etc. This is to describe the MCC-GF modification mechanisms and growth relativity hypothesis (modified from Voudouris *et al* 2000 (80)).

It should be considered that the changes in the MCC in response to mandibular advancement are highly related to the duration of functional therapy (65, 109), direction, amount and types of the force (57, 66, 129).

2.5. Glenoid Fossa (GF)

The temporal component of the TMJ is the S-shape curve of the temporal bone, the mandibular fossa and articular eminence, facing the articular zone of the condyle. It is lined with connective tissue and remodeling is observed in humans from early childhood in this articular fossa. The GF normally grows in a posterior and inferior direction. ((50) p. 194)(76)).

Growth and development in the GF is regulated by endogenous factors and molecular markers expressed by cells as well as in the condyle (12). A significant appositional or periosteal bone formation is seen in the fossa in response to propulsive mechanical stimuli of the condyle. The growth and remodeling process is mediated by several intrinsic and extrinsic biofeedback factors (12, 79, 130).

Histochemical Changes in Glenoid Fossa during Mandibular Advancement

The mandibular GF is rarely studied as a primary objective when investigating the effect of functional appliances (12, 130-133). Forward mandibular positioning significantly increases bone formation in the GF. Continuous bite-jumping in young rats results in enhanced mandibular growth and remodeling of the GF (12).

The remodeling of the GF due to mandibular advancement is also investigated in experiments on monkeys (64, 128, 134). MRI's for patients who received Herbst appliance therapy also shows that a combination of condylar growth and remodeling of the GF occurs during the TMJ's adaptive response to mandibular advancement in humans (3, 135). Changes in the GF are demonstrated in some human studies after treatment by an activator (2) or Herbst appliance (10, 136). It is suggested that the GF relocation contributed to the correction

of skeletal Class II Division 1 malocclusion in combinations of mesial movement of mandibular teeth (137). Its adaptive capacity has also been demonstrated in human studies of condylar fractures (138). The GF changes are also observed in several animal studies by radiographic and/or morphologic and histological investigations (12, 80, 134, 139, 140). However, there are few reports documenting how much new bone formation takes place in the GF in response to mandibular advancement, and by which mechanism this newly formed bone is induced in response to such advancement.

New bone formation is directly correlated with the amount of blood vessel invasion in the GF during natural growth and in response to mandibular advancement. A significant increase in vascular endothelial growth factor (VEGF) expression and new bone formation occurs mainly in the posterior region of the GF (69, 133). Neovascularization is enhanced by VEGF which increases the number of mesenchymal cells in the perivascular connective tissue and stimulates the vascular endothelial cells to secrete growth factors and cytokines (130, 141).

The actual mechanism of bone formation in the GF is not completely understood and the regulatory factors governing its growth have not been fully identified. However, some researchers have proposed that the formation of this kind of intermediate type of tissue is transdifferentiation of chondroid cells into either chondrocytes or osteoblasts, depending on the biochemical environment (12); however, this has yet to be precisely evaluated since bone formation in the GF is reportedly intramembranous (74).

The articular fibrous tissue from the osteoid tissue is separated by the undifferentiated reserve cells which are densely packed together toward the articular side of the GF. Osteoblasts and lacunae with osteocytes are observed in the cancellous bone layer, and the abundant dense collagenous osteoid substance surrounds the lacunae. The arrangement of the

bundle of collagen fibers is parallel to the articular surface of the GF and marrow spaces are evident in the bone. Fewer lacunae are present in the deeper down cancellous bone (12).

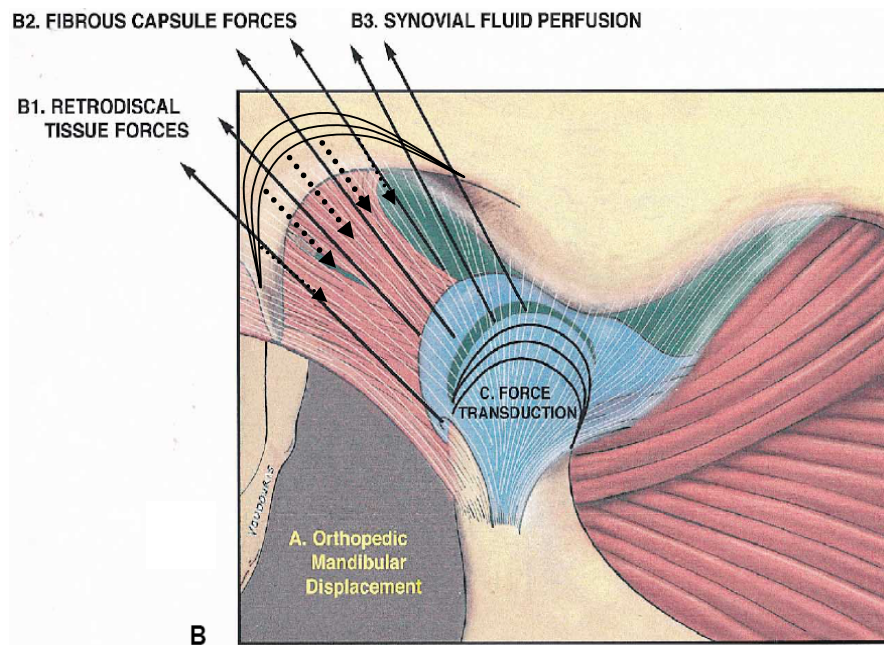


Figure 2-6 TMJ Growth Modification

Growth modification in the MCC and GF is influenced by three factors: A. Displacement, B. Viscoelastic tissue pulls (arrows), C. Transduction with fibrocartilage. Viscoelastic tissue includes three parts: superior and inferior bands of the retro-discal fibers (B1); fibrous capsule (B2, fine white lines); and synovial fluid perfusion in a posterior direction (B3). The articular disc's (blue region) posterior, anterior, lateral and medial (collateral) attachments translate the forces to the condyle in a posterior-superior direction and to the GF in an inferior-anterior direction (modified from Voudouris and Kuftinec 2000 (80)).

Furthermore, in Rabie *et al* 2001 experiment on rat samples, no obvious cellular changes were observed in the GF. However, some cellular changes were observed in the posterior aspect of the GF. In the fibrous layer, the fibroblasts were round at the beginning of the experiment but stretched, flattened and increasingly oriented in the direction of the pull by disc fibres during mandibular protrusion.

The mesenchymal cells beneath the fibrous layer were arranged in line with the articular surface on 38 day-old rats after 3 days of mandibular advancement. However, the axis of the mesenchymal cells and other cells in the extracellular matrix (ECM) are oriented

in the direction of the pull and became increasingly aligned with the presumed direction of the pull (12). Mechanical strains can bring such “strain alignment”, which may influence migration or condensation of the mesenchymal cells. When mandibular advancement results in the stretch of the sub-periosteal ECM, its matrix density will increase because of the transverse compression caused by the Poisson effect ^{3(142, 143)}. This may attract more cells from the adjacent ECM as a source of mesenchymal cells (144-147). The perivascular connective tissue that surrounds the new blood vessels could be known as the other source of mesenchymal cells. These blood vessels are recruited in response to the stretching effect. The growth potential of the condyle and the GF is influenced by the number of replicating mesenchymal cells (148). In the cancellous bone layer, at the beginning of mandibular protrusion, the osteoblasts and osteocytes were randomly packed (12).

It has been hypothesized that bone formation in the condyle and the GF due to mandibular advancement is induced by viscoelastic force, generated in the synovial fluid of the joint capsule through the connective tissue attachments of the articular disc complex and retrodiscal tissue. This bone formation takes place especially in the posterior region (80). The biomechanical mandibular forward positioning changes the ECM and the undifferentiated mesenchymal cells in the sub-periosteal connective tissue in the GF (12). Furthermore, the changes in cell-cell and/or cell-ECM interactions activate the mechanical signal transduction cascade, through a transduction molecule (149).

MRI assessment in clinical studies with the use of the Herbst appliance shows that the GF remodeling and temporal adaptive responses occur later than the condylar adaptive

³ “When a tensile stress is applied to a material, the material elongates in the direction of the applied stress, and contracts perpendicular to the direction of the applied stress. This relationship, called the Poisson effect, is a natural response to applied stress that occurs with all materials, but is particularly apparent with ductile materials”.

response. The difference between the periosteal ossification of the temporal bone and the endochondral ossification of the condyle could be the reason of this nonparallel adaptive response. However, it should be considered that periosteal ossification does not result in a marked change in MRI signal intensity, because it is not associated with a large increase in water content of the tissue. Therefore, the mentioned delayed ossification in the GF and new bone apposition along the post-glenoid spine might be due to its later visualization in the MRI, at the time when the newly formed bone has consolidated (150-152).

Bone formation and the number of replicating cells in the posterior region of the GF is significantly higher than in the anterior and middle regions, which could be due to the primary attachment of the posterior fibrous tissue of the articular disc to this particular zone (10, 16, 148).

2.6. Fibroblast Growth Factor (FGF)

2.6.1. Fibroblast Growth Factors family:

FGFs are small polypeptide growth factors, and they share certain structural characteristics in common. Many FGFs are secreted into the extracellular environment and they contain signal peptides for secretion. There they can bind to the Heparan-like Glycosaminoglycans (HLGAGs) of the Extracellular Matrix (ECM). From this reservoir, they can act in different ways. They can act directly on target cells or be released through digestion of the ECM or the activity of a secreted FGF binding protein as a carrier protein.

In the context of HLGAGs, FGFs bind specific receptor tyrosine kinases. These bindings induce receptor dimerization and activation. The activation of various signal transduction cascades is the ultimate result in this process. Some FGFs are effective

angiogenic factors and most of the FGFs play important roles in embryonic development and wound healing. Basic cellular activities are governed by cell signaling as a part of a complex system of communication and this signaling progress also coordinates cell actions (153). FGF signaling seems to play a role in tumor growth and angiogenesis, and autocrine FGF signaling may be particularly important in the development of steroid hormone-dependent cancers to a hormone-independent state (Abstracted by Powers et. al. 2000 (40)).

Twenty distinct FGFs have been discovered and numbered from 1 to 20. FGFs in cells of mesodermal and neuroectodermal origin induce mitogenic, chemotactic and angiogenic activities on diverse target cells (33). FGFs' family members are present in the extracellular matrix, most noticeably in FGF2, and their activity is through high affinity extracellular receptors; therefore, most FGFs act extracellularly (154). However, they are not only stored in the extracellular matrix itself, but also in endothelial cells (155) and fibroblasts (156). The Crystal Structure of FGF 8 isotype b (FGF8b) in complex with FGF Receptor (FGFR) 2c is shown in Figure 2-7.

FGFs, upon release to the ECM, quickly become associated with the HLGAGs. FGF protection from proteolysis and the creation of a local reservoir of growth factors may be afforded by this association. The protection of the FGFs from degradation and the creation of a local reservoir of growth factors are the two physiologically relevant goals of the FGFs. These goals may be served by the binding of the FGFs to heparin or HLGAGs. The role of FGFs in development is a clear example of the FGFs goal as a local reservoir of growth factors.

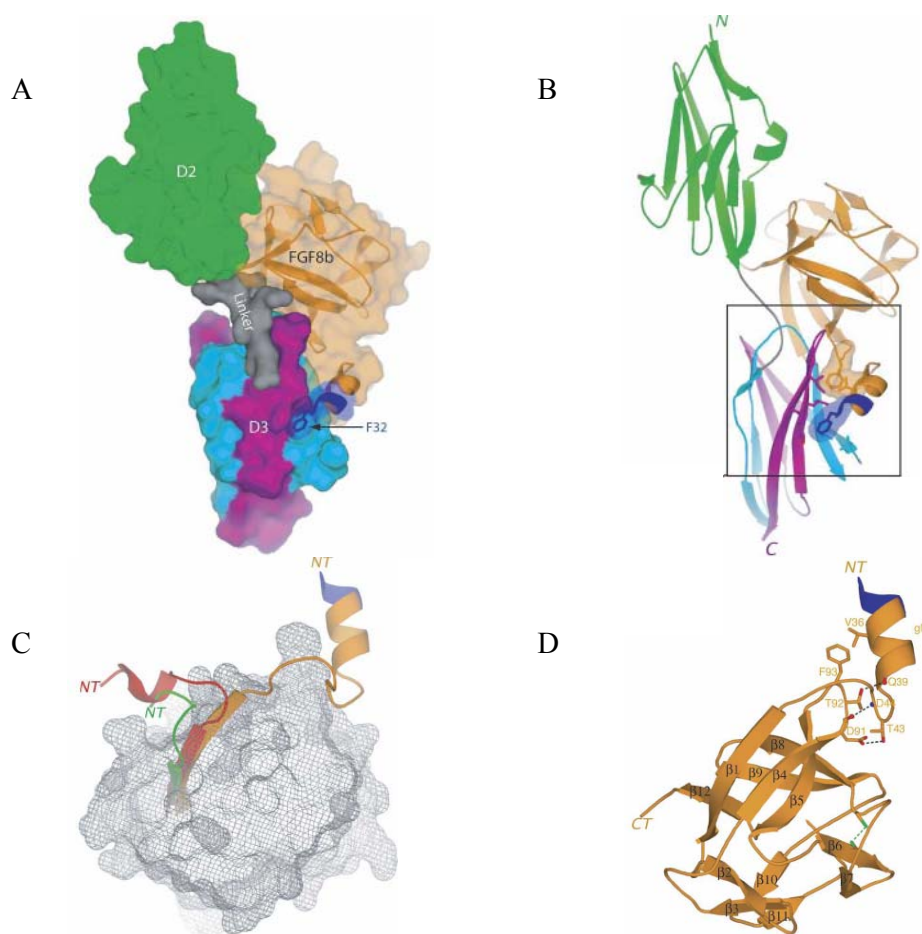


Figure 2-7 The FGF8b-FGFR2c complex and FGF8b's overall feature

The Crystal Structure of the FGF8 isotype b (FGF8b) in complex with FGF Receptor (FGFR) 2c; FGF8b is one of the four human FGF8 splice isoforms, which is expressed in the mid-hindbrain region during development.

- (A) The figure represents the molecular surface of the FGF8b–FGFR2c structure. FGF8b is represented as a ribbon diagram and is colored orange. Alternative splicing modulates the biological activity of FGF8, therefore, phenylalanine 32 (F32, shown as sticks) is a key player in the FGF8's molecular mechanism. D2 and D3 are receptors with a gray color linker. The constant N-terminal and the spliced C-terminal half of the D3 receptor are colored cyan and purple. The only three residues from the spliced N-terminal region of FGF8b are colored blue.
- (B) The diagram shows the contact between the N-terminal helix and beta4–beta5 loop of FGF8b with the D3 hydrophobic groove of FGFR2c, which dictate FGF8–FGFR-binding specificity. Interactions in stereo and coloring are the same as in A. F32 is the only residue from the alternatively spliced region of FGF8b that interacts with FGFR.
- (C) The spatial positioning of the FGF8b N terminus relative to the beta-trefoil core. The view of FGF8b is the same as in D. The surface of the FGF8b beta-trefoil core is shown as gray mesh. The beta1 strands and N termini of FGF8 is colored orange. The green and red ribbons are FGF1 and FGF10. The blue is the ordered residue from the alternatively spliced region of FGF8b. The N termini of FGF8, FGF1, and FGF10 are labeled NT.
- (D) Ribbon representation of FGF8b from the FGF8b–FGFR2c structure. The beta-strands of FGF8b are marked based on the conventional strand nomenclature for FGF1 and FGF2.

(NT) N terminus of FGF8b; (CT) C terminus of FGF8b; (gN) N-terminal helix of FGF8b. The diagram, shown as ribbon, indicates intramolecular interactions that stabilize the unique conformation of the FGF8b N terminus and tether the N-terminal helix to the core. Dashed black lines show hydrogen bonds. Dashed green lines show the disulfide bridge between cysteines 109 (in beta6) and 127 (in beta8), which stabilize the conformation of the beta7–beta8 loop. This loop is one residue longer in FGF8 subfamily members with regards to other FGFs (modified from reference (157)).

FGFs play their mitogenic and angiogenic roles in target cells by signaling through cell-surface, tyrosine kinase receptors. Different cell responses to FGFs indicate that the different cells express altered forms of the FGF receptor. FGF is produced by cells, enters the ECM and eventually binds to cell surface receptors on target cells and activates them. Afterward, protein phosphorylation mediates a signal transduction cascade which is triggered by receptor binding. Small changes in gene expression are the ultimate result of this process. However, the biologic interaction between FGF secretion and receptor activation is not yet precisely clear.

Still, two mutually compatible mechanisms are reported on how the FGF may activate the FGFR from its association with the ECM. First, the FGF bound to the ECM may be available to cell surface receptors and may not actually be sequestered. The signaling pathway can be activated when a cell comes in contact with this FGF-primed ECM. This allows a strict spatial regulation of FGF signaling. The FGF may signal from the ECM to promote chemotaxis and cell migration during development with this mechanism. Second, proteolysis can rapidly mobilize this store of FGFs. This could be the activity of heparinases, or the activity of a secreted binding protein, the FGF binding protein (FGF-BP). This may explain FGF signaling during wound repair and tumor angiogenesis. Numerous proteolytic enzymes and heparinases are activated during these processes.

FGF receptors are similar to other receptor tyrosine kinases. Extracellular signals to various cytoplasmic signal transduction pathways through tyrosine phosphorylation are

transmitted by FGF receptors. Ligand binding and dimerization make the receptors capable of phosphorylating specific tyrosine residues on their own and each other's cytoplasmic tails. Therefore, receptor dimerization is the key step from the extracellular to the intracellular signaling pathways. In craniofacial skeletogenesis, mutations of FGF receptors relate to syndromic and non-syndromic craniosynostosis (158). During long bone development, FGF receptors are expressed in different zones of the epiphyseal growth plates; FGFR3 in the proliferating chondrocytes; FGFR1 in the hypertrophic chondrocytes; FGFR1 and FGFR2 in the perichondrium (159, 160); FGFR2 is also expressed in early mesenchymal condensates and in the periosteal collar around the cartilage models (161).

Chondrocyte differentiation is critically controlled by FGF Receptors (FGFR3) signaling. For example, missense mutations in the FGFR3 gene cause three inherited human syndromes, hypochondroplasia, achondroplasia, and thanatophoric dysplasia (91-93, 162). The FGF signaling pathway in evolution is highly conserved and plays important and necessary roles in development. It is involved in almost all structural development in the craniofacial region, from early patterning to growth regulation. It is present in both the epithelia and mesenchyme and mediates the epithelial-mesenchymal interaction in advancing development. The FGF signal pathway plays crucial roles in suture and synchondrosis regulation during craniofacial skeletogenesis (158).

Some other functions are reported for FGF signaling: regulating chondrocyte proliferation and differentiation, acting upstream of Indian Hedgehog (IHH) in regulating the onset of chondrocytes' hypertrophic differentiation (e.g. in FGF2 treatment) and accelerating the hypertrophic differentiation, acting as an antagonist of Bone Morphogenic Protein (BMP) signaling during cartilage development. Chondrocyte proliferation and hypertrophic differentiation is integrated by interaction of FGF, Ihh / PTHrP (Parathyroid Hormone-like

Peptide), and BMP signaling. Crystal Structure of FGF8 isotope b (FGF8b) in complex with FGF Receptor (FGFR) 2c is shown in Figure 2-7.

FGFs are involved in different biologic functions; angiogenesis and wound healing, inflammation (FGF1), repair (FGF2), regeneration (FGF7-FGFR2 (IIIb)), limb development (FGF5, 8 and 10). The most fully characterized role for FGFs is induction of limb buds (FGF3 and 4) and proliferation of developing limbs (FGF2 and 4) and cancer. FGFs have been reported to be relevant in organogenesis, especially in the nervous system, the lung and limbs (reviewed by Powers *et al.* 2000 (40)).

2.6.2. Fibroblast Growth Factor8 (FGF8):

FGF8 was initially identified as an Androgen Induced Growth Factor (AIGF) found in the conditioned medium of the androgen-dependent mouse mammary carcinoma cell line SC-3 (35). FGF8 has 7 isoforms, all with signal sequences. The amino-termini of these isoforms are different, but the signal sequence is not altered. FGF8 signalling is through FGF receptors 1, 2-IIIc, 3-IIIc and 4 (FGFR1; FGFR2, IIIc; FGFR3, IIIc; FGFR4). In response to treatment with androgens in both the human breast cancer cell line MDA-MB-231 and the SC-3 cell lines, FGF8 was found to be expressed and secreted (163). Androgen induced growth of SC-3 cells is blocked by a blockade of FGF8 activity by antisense oligo-nucleotides (164). This suggests that FGF8 plays a key role in mediating the effect of androgens on this cell line. It is reported that FGF8 is expressed by a great proportion of malignant breast and prostate tumors, and may be involved in the formation of osteosclerotic bone metastases (165).

FGF8 and its functions in some organs of chicks, fish, mice, rabbits, rats and humans in different life stages are widely studied (166-188). For example, some recent studies concern its role in inducing in vitro odontoblast-like cell differentiation of cranial neural crest

cells (169); its instructive role in limb proximal-distal patterning (189) and regulating mesenchymal differentiation and skeletal patterning along the limb bud proximodistal axis (96); its role in early human kidney development (172); its role in human prostate cancer (170, 171); its role in controlling regional identity in the developing thalamus (177) and the effect of decreased FGF8 signaling on gonadotropin-releasing hormone in humans and mice (178). However, there are few studies on FGF8 in TMJ during growth, development and bone remodeling.

FGF8 is required for cells that have undergone an epithelial-mesenchymal transition to move away from the primitive streak in mouse embryos (190). In FGF8 knockout mice the absence of embryonic mesoderm- and endoderm- derived tissues occurs due to the failure in cell migration. A disturbance in the patterning of the prospective neuroectoderm is also reported in FGF8 knockout mice. Furthermore, FGF8 has an important role in midbrain development (188) and cell patterning of the neural plate (191). FGF8 expression in the Nephrogenic Mesoderm (NM) is triggered by limb bud induction which seems to occur as a result of a signal from the Wolffian Duct (WD)⁴⁽¹⁹²⁾. In this position FGF8 is capable of inducing limb bud formation by acting on the lateral plate mesoderm (reviewed by Powers *et al.* 2000 (40)).

FGF8 is also widely expressed in the developing skeleton but its function has remained unclear. Adding the FGF8 to mouse bone marrow cultures effectively increases initial cell proliferation. In the cultures at an early stage of osteoblastic differentiation it also eases bone formation *in vitro*, which is also possible *in vivo*. In mouse bone marrow culture FGF8 regulates different stages of mesenchymal stem cell differentiation in the direction of

⁴ Wolffian Duct (WD) and the Nephrogenic Mesoderm (NM) are the components of the Intermediate Mesoderm (IM) which lies between the lateral plate mesoderm and the somites; IM is the normal source of the limb induction signal (Geduspan & Solursh 1992).

osteogenic lineage. It also increases the osteogenic capacity of bone marrow cells at the early stage of their differentiation; therefore, it may be involved in bone formation (165).

Several functions are reported for FGF8; regulation of cartilage formation in the vertebrate skull (193), involvement in cartilage and bone formation (concluded from its wide expression in the developing skeleton), influencing rib development (194), stimulating the avian chondrocytes (195) and cultured dental mesenchyme (196). The expression of core binding factor 1 (cbfa; an osteoblast-specific transcription factor) in fibroblasts is induced by FGF8 and FGF2 (165, 197).

It is shown that FGF8 induces osteoblast differentiation. It is also able to efficiently stimulate the proliferation of cultured mouse bone marrow cells and to induce their early stage differentiation as a precondition for subsequent bone nodule formation and osteoblast-specific alkaline phosphatase (ALP) production. FGF8 stimulates the proliferation of hypothetical osteogenic stem cells in bone marrow and tumours. It is conducive to their osteogenic potential, leading to osteoblastic differentiation and bone formation. However, continued exposure of osteoblastic cultures to FGF8 inhibits bone formation. (165).

During the development of chick limbs, FGF8 has effects on distal cartilage formation, synergistic with Indian Hedgehog (Ihh). It has a strong synergistic effect on promoting cartilage outgrowth with Sonic Hedgehog (Shh) during chick cranial development (198, 199), as well as a strong synergistic effect with Shh on chondrogenesis in vitro and promoting chondrogenesis in vivo, during early facial primordia development (198, 200). FGF8 is expressed in the beak primordial through much of the early to mid-development in the chick embryo and regulates the development of the beak in chick embryos, along with Shh. Rostral-ventral epithelium of the mandibular primordium (MP) is one of the distinct

domains in the developing head, where FGF8 is expressed during early to mid-stages of chick development.

Therefore, to localize the extent of chondrogenic skeletogenesis in the developing head, the limited expression domain of FGF8 could be important. FGF8 is able to induce chondrogenesis from the cranial neural crest. This is important since FGF8 could be a precise control key of localization and patterning of many cartilage and endochondral bone elements in the head (198). It is suggested that FGF8 signaling is required for the development of the distal cartilage element although it is indicated that FGF8 plays a role in the differentiation of mesenchymal cells (169).

FGF8 is a critical FGF ligand with FGFR1 and 2 as critical receptors in facial primordia. In this regard, common developmental disorders in human beings are facial clefts and insufficiency of craniofacial development (summarized by Nie *et al* 2006 (158)). However, the mechanism of mesenchymal cell proliferation and differentiation into chondrocytes is still unclear (169). In this field, FGF8 has also been studied in rabbit embryos (201) . Overall, FGF8 is an essential component in early craniofacial patterning and growth (158, 202).

On a molecular level, FGF signaling results in a chondrocyte proliferation decrease and an acceleration of chondrocyte hypertrophic differentiation (162).

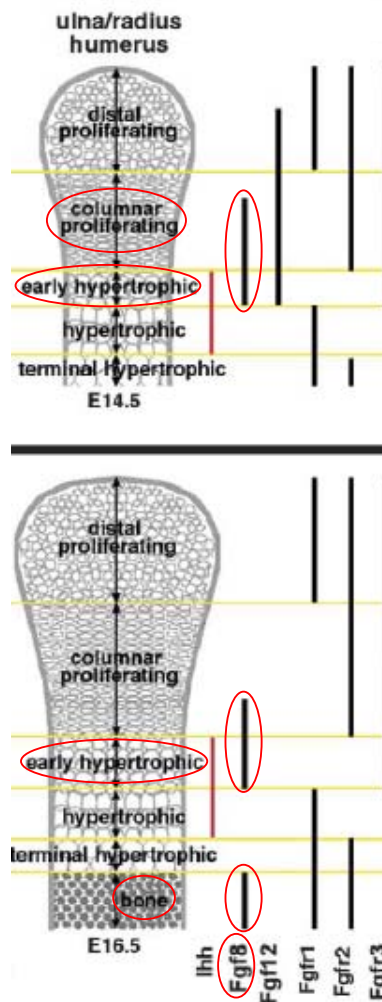


Figure 2-8 FGF Genes Relative Expression

FGF genes relative expression pattern in forelimbs of mouse embryo (Modified from Minina et.al. 2005 (42))

FGF8 subfamily members have higher relative activity on FGFR3c cells and less activity toward FGFR1c. The FGF8 subfamily is expressed in epithelial tissues and c splice forms of FGFRs are activated by FGF8. Therefore, FGF and FGFRs binding specificity is critical for the spatial regulation of FGF signaling. The below diagram shows relative activity of FGF8 with other FGF subgroups and FGF receptors(203).



In mouse embryos, FGF8 is detected in tissues surrounding the developing bones such as the muscles and skin. Weak expression of FGF8 is also found at embryonic day 14.5 (E14.5) in proliferating and early hypertrophic chondrocytes. It is weakly expressed in proliferating chondrocytes and in the bone (E16.5) (Figure 2-8).

2.7. Proliferating Cell Nuclear Antigen (PCNA)

PCNA is a sliding clamp protein (a protein ring), found in all organisms in eukaryotes. The sliding clamp proteins are called the beta clamp in prokaryotes. These proteins form a ring around DNA. The sliding clamp, the DNA polymerases and a clamp-loading complex are the components of the ring type polymerases and their primary role is to replicate the genome, so they are also called replicases. Identical promoters form the sliding clamp that oligomerize to form a ring that encircles DNA (Figure 2-9) (44).

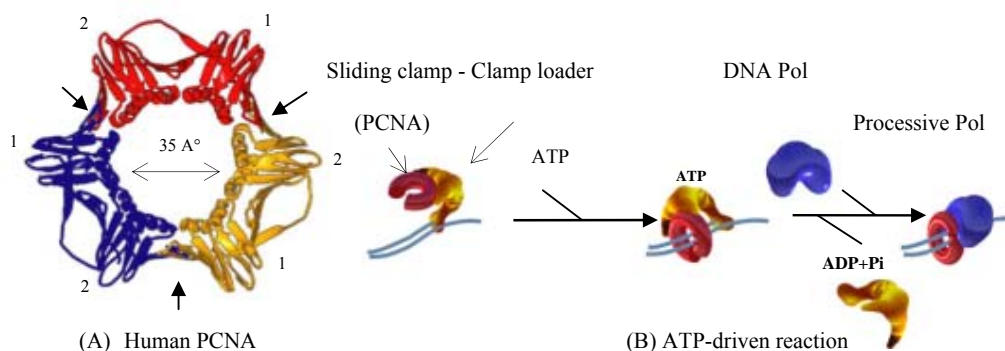


Figure 2-9 PCNA

- (A) The sliding clamp ring in humans is constructed from two monomers to yield a ring composed of six domains. The inside diameter of the ring is about 35 Angstrom, allowing ample room to encircle the DNA.
- (B) In an ATP-driven reaction, a clamp-loader complex assembles the sliding clamp protein ring onto a primed template junction. The ring on the DNA then assembles with the DNA polymerase (Pol) to form a highly processive polymerase. The ring is pulled along behind the processive Pol while remaining tethered to DNA by the ring during chain extension (Modified from Bruck and O'Donnell, 2001; Genome Biology Vol 2 No 1 (44)).

PCNA is originally characterized as a DNA polymerase accessory protein. It functions as a DNA sliding clamp for DNA polymerase delta. Furthermore, it is an essential component for eukaryotic chromosomal DNA replication. A striking feature of PCNA revealed in recent studies is its ability to interact with multiple partners; for example, PCNA's roles in DNA repair, Okazaki fragment joining, DNA methylation and chromatin assembly. PCNA has applications as a marker for DNA synthesis, since these reactions mainly take place while replicating DNA (Abstracted by Tsurimoto *et al* 1999 (43)).

PCNA, a well-known cell cycle marker protein, was originally identified as an antigen for autoimmune disease in systemic lupus erythematosus patients (204). Its involvement in DNA replication is suggested due to periodic appearances in S phase nuclei, co-localized with incorporated bromodeoxyuridine (205, 206). Indeed, PCNA as an essential factor for SV40 (Simian Virus 40) DNA replication was later identified in vitro (207). Additionally, it is demonstrated that PCNA is essential for chromosomal DNA replication in biochemical and genetic studies with budding yeast (208-210). It is also analogous to the Pol III beta-subunit and the T4 gene45 protein (encircles DNA and freely slides along DNA with its closed ring structure), functioning as a DNA sliding clamp (211). PCNA gene expression is associated with cell proliferation and the promoter sequence contains binding sites for many transcription factors (44).

There are specific interactions between PCNA and several DNA repair-related gene products (212). PCNA is involved in both mismatch repair and excision in eukaryotes (44). It is required for DNA synthesis during replication, for DNA repair, DNA recombination-driven synthesis and post-replicative DNA processing (213).

PCNA is not only a clamp to a master molecule for chromosome processing but is also a necessity for all organisms as the existence of a DNA sliding clamp. However, during

evolution, clamp molecules gained an increasing number of functions. Indeed, PCNA binding proteins have only been identified in mammals and they are active in cell cycle regulation or replicated chromosome reorganization (43).

PCNA is immunocytochemically detectable during the late G1- and S-phases (214). It is an established method to study the proliferation activity of cells with specific antibodies in developmental processes and clinical studies (215-217). PCNA-positive cells are mainly present in the proliferative zone in the condyle (47, 98). Furthermore, detected PCNAs in the deeper layer of condyle could indicate that proliferation, to some extent, remains active in hypertrophic chondrocytes.

Therefore, PCNA is an indicator for cellular proliferative activity in tissue organs (46, 47, 198, 218-220) and in the current study it is detected in the MCC to quantitatively evaluate the proliferative activity in the condyle during mandibular advancement.

METHODS and MATERIALS

3. Methods and Materials

3.1. Animals and experimental design

Fifty five female Sprague Dawley rats at the age of 24 days were randomly divided into the experimental group (n = 35) and the control group (n = 20); the study was approved by Westmead Animal Ethical Committee (Protocol No: 4113.06-08). The animals were housed five per cage at the Westmead Hospital's animal laboratory unit. All of the rats were kept in the same well-controlled temperature and humidity environment. They were fed a soft palate diet and they had uninhibited access to water 24 hours a day throughout the entire experimental period.

According to the planned experiment, on day 3, day 14, day 21 and day 30 the animals were further divided into four experimental subgroups (10 rats each in groups 1, 2 and 3, and 5 rats in group 4) and four control subgroups with 5 rats each. The bite-jumping appliance was placed on the 24 day-old experimental rats to induce mandibular advancement at Day 0. Rats were 21 days-old at their arrival to the animal laboratory. The first three days were assigned for the initial settlement of the rats into the new environment of the animal laboratory.

Table 3-1 Experimental Design

Experiment Days	Rats Age (Days)*	Study Criteria		
Day 0	24 Days (No sacrifice)	Entry to the experiment, random grouping and laboratory initial settlements		
	Age at the day of sacrifice	Experimental Group (35 rats)	Control Group (15 rats)	Total sacrificed samples (55 rats)
Day 3	27 Days	10 rats	5 rats	15 rats
Day 14	38 Days	10 rats	5 rats	15 rats
Day 21	45 Days	10 rats	5 rats	15 rats
Day 30	54 Days	5 rats	5 rats	10 rats

* Female Sprague-Dawley rats were collected for the study; approved by Westmead Animal Ethical Committee.

3.1.1. Anaesthesia and Appliance fitting

The animals were sedated with ketamine hydrochloride (Ketavet®, Delvet, NSW Australia) and xylazine hydrochloride (Ilium Xylazil-20®, Troy Laboratories, NSW, Australia).

The lower anterior incisors were washed and dried. The teeth were coated by Transbond™ Plus Self Etching Primer (3M Unitek, Monrovia, California) evenly through the whole surfaces and pediatric crown former (3M™ ESPE™ Strip Crown Form Refills, USA) were adjusted on the lower incisors with light cure composite (3M™ ESPE™ Z100™ Restorative dispenser for capsule, USA). The crown former was positioned in such a way that it caused mandibular forward-downward positioning during the rats' rest and functional bite (Figure 3-1B). The animals in the control groups were not fitted with an appliance and were untreated (Figure 3-1A). Body weight was monitored throughout the experiment.

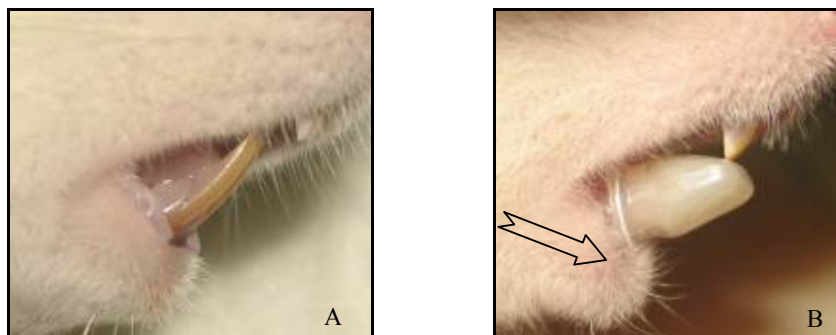


Figure 3-1 Bite Jumping Appliance

(A) Normal incisal relationship in control rats.

(B) Bite-jumping appliance is adjusted on the lower incisors of experimental rats to move their mandible into a forward position during rest and function.

3.1.2. Weight gain recording

The weight was recorded at the beginning of the experiment and the day of sacrifice. The weight was recorded to evaluate and compare the somatic growth status between experimental and control samples.

3.2. Euthanasia and Tissue Preparation

The animals in each subgroup were euthanized respectively, by Carbon Dioxide Gas (Aligal 2, Air Liquid, Australia) on days 3, 14, 21 (10 experimentals and 5 controls on each day) and Day 30 (5 experimentals and 5 controls) of the experiment which were the 27th, 38th, 45th and 54th day of the rats' age.

Immediately after death, the heads were removed and fixed in 4% paraformaldehyde for 24 hours. The method of making one liter of 4% paraformaldehyde was based on the histology laboratory manual at the Institute of Dental Research (IDR), Westmead Hospital, NSW, Australia; the fixative solution should be prepared fresh each time before use.

The aim of the fixation is the coagulation or precipitation of the substances making up the protoplasm; e.g. proteins, lipids, carbohydrates and inorganic salts. This process renders

the cells, tissues and their elements resistant to further changes prior to microscopic examination. Its effects are to penetrate tissues and kill them quickly, preserve all tissue elements, and to harden the tissues so they will not be affected by the subsequent dehydration, cleaning, impregnation, embedding, staining and other preparative processes.

The heads were then decalcified in 20% ethylene-diamine-tetra-acetic acid (EDTA), pH 7-7.4, at 4-8°C for 4–6 weeks. It is made of 100mg EDTA powder, 50ml PBS and 400ml distilled water plus 100-130 NaCl tablets for 500ml 20% EDTA, PH 7-7.4.

The TMJ was dissected and the surrounding soft tissues were removed until the TMJ was exposed. Excess tissues were removed and the specimens with the buccal surface of ramus parallel to the surface of the block were embedded in paraffin. 5 μ thick serial sections were cut through the TMJ at the parasagittal plane using a rotary microtome (Leitz 1516, Leica Microsystems, Wetzlar, Germany); sectioning was continued until approximately reaching the middle of the condyle. At that level a few sections were floated onto glass slides coated with Poly L Lysine.

Individual variations occur in the TMJ orientation in the skull. Thus, in order to make a reliable comparison, the plane of each section throughout each of these anatomic variables was adjusted as identically as possible between samples. The sections cut from each sample were assigned to the immunohistochemical staining for FGF8 and PCNA.

3.3. Immunohistochemical examinations

The specific primary antibodies used were FGF-8 goat polyclonal antibody collagen (N-19, cat#sc-6958, Lot#E300, 200 μ g/ml, Santa Cruz Biotechnology, USA) and Mouse PCNA Unconjugated Purified antibody with multiple reactivity (200 μ g, catalogue# 13-3900,

mouse anti-PCNA; Zymed®; RUO, supplied by Invitrogen). The secondary antibodies were rabbit -anti- goat IgG (HRP, Code No.P0449, Dako A/S, Denmark) for FGF-8 and for PCNA.

Immunohistochemistry was carried out using a method in which, after the sections were dewaxed and rehydrated, were treated with glycine (1 in 10 phosphate buffer solution (PBS)) and then in 3% hydrogen peroxide (1 in 10 PBS) for 5 minutes to retrieve the antigen. Non-specific bindings were blocked with horse serum (1 in 5 PBS) for 45 min. Then the samples were incubated with the primary antibody (1 in 50 fetal calf serum (FCS)) for 120 minutes. Free antibodies were removed by washing the samples in a phosphate buffer solution (PBS) thoroughly. After washing, sections were incubated with the secondary antibody (1 in 100 FCS) for 30 minutes, followed by washing.

Then the slides were dipped in 3, 3'-diaminobenzidine (DAB) in chromogen solution (Dako Liquid DAB+ Substrate Chromogen System, Code K3467, Denmark) for 6 minutes to identify the binding sites. Sections were finally counterstained with Mayer's Hematoxylin for background staining. Negative controls were included, on which the primary antibody was replaced by FGF-8 blocking peptide (N-19 P, cat#sc-6958 P, Lot# F268, 100 µg/0.5ml, Santa Cruz Biotechnology, USA) to ascertain the specificity of the immunostaining.

The slides were covered by Mounting Medium (Fisher Scientific Permount, for mounting and storage, SO-P-15, 500 ml-1.1 pt., USA) and a cover slip for long term storage of slides and further microscopic studies.

The slide preparation could be summarised as follow:

1. Heating in the dry oven for 30-45 minutes.
2. Washing in running distilled water.
3. Dewaxing; floating the slides in Histoclear for 2x5 minutes, 100% Ethanol for 2x2 minutes, 95% Ethanol for 2 minutes and 70% Ethanol for 2 minutes.

4. Washing in running distilled water.
5. Covering the tissue with Glycine (1 in 10 PBS) for 10 minutes.
6. Rinsing with PBS.
7. Covering the tissue with 3% Hydrogen Peroxide ((OH) 3%, 1 in 10 PBS) for 5 minutes.
8. Rinsing with PBS.
9. Covering the tissue with Horse Serum (1 in 5 PBS) for 45 minutes.
10. Rinsing with PBS.
11. Primary antibody and blocking peptide;
 - 11.1. Covering the tissue with primary antibody (1 in 50 FCS) for 2 hours.
 - 11.2. For preparing negative controls, instead of primary antibody, one piece of tissue section on each slide were covered by blocking peptide (1 in 10 FCS) for 2 hours while the other section was normally incubated by primary antibody; on each slide there were two pieces of tissue from two slices next to each other.
12. Rinsing with PBS and floating the slides in PBS for 3x5 minutes.
13. Covering the tissue with secondary antibody (1 in 100 FCS) for positive staining for FGF8 or PCNA for 1 hour.
14. Rinsing with PBS and floating the slides in PBS for 3x5 minutes.
15. Covering the tissue with DAB+ for 6 minutes.
16. Washing in running water.
17. Floating the slides in Hematoxylin for 3-5 seconds.
18. Floating the slides in water for few seconds, until the water becomes homogenously blue.
19. Clearing the slides by floating them in Histoclear and Ethanol in seven different dishes, 1 minute each; 70% Ethanol, 90% Ethanol, 95% Ethanol, 100% Ethanol and then in three separate dishes of Histoclear.

20. Covering the tissue by Mounting Medium and cover slip;

These slides are prepared for microscopic studies and long term storage.

3.4. Quantitative imaging and statistical analysis

Digital images were taken from stained tissues with a Leica digital imaging microscope and its software (Leica application suit software) by 10 times, 20 times and 60 times magnification. The unified area for microscopic image-taking is shown in figure 3-2.

The expressions of FGF8 and PCNA were quantified by manually counting the cells of positive reacted immunostaining signals on the computer screen from the 20 times magnified images. The cells were counted from the middle quarter of the MCC and distal third of the GF, where the most prominent cellular responses to mandibular repositioning occur (6, 11, 148). The cells which were stained with certain intensity were counted and those which were weakly stained were excluded.

The repeatable counting method used in this study is summarised as follows:

1. Cropping the middle quarter of the MCC and distal third of the GF from the 20 times magnified microscopic images with the software, Microsoft Office Picture Manager 2007.
2. Transferring the cropped piece of the image to the Adobe Photoshop CS software and putting dots on typically stained cells.
3. Then counting the cells in a directed order.

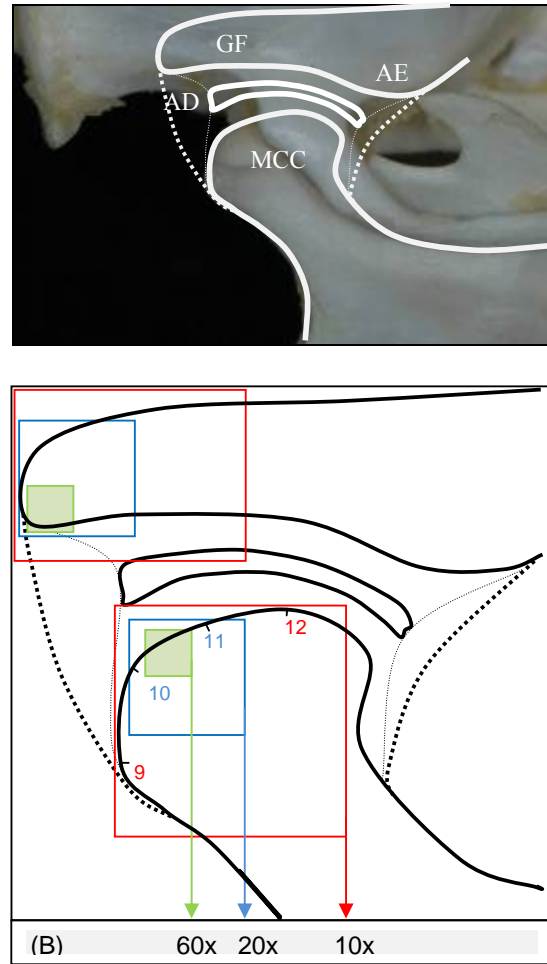


Figure 3-2 the unified area for image taking

- (A) The schematic view of the rat's TMJ is drawn by following the anatomic outlines of the condyle and the GF. The condyle, articular disc (AD), the glenoid fossa (GF) and the articular eminence (AE) are drawn with hard lines and the outer and inner limits of the soft tissues are approximately shown by heavy and light dashes.
- (B) The images are taken from the unified areas for all samples. The boundaries of different magnifications are shown with red (10x), blue (20x) and green (60x) squares on the most distal and superior part of the condyle and the most distal part of the GF. The unified areas on the condyle are approximately from 9-12 o'clock for 10x, from 10-11 o'clock for 20x and between 10 and 11 o'clock for 60x.

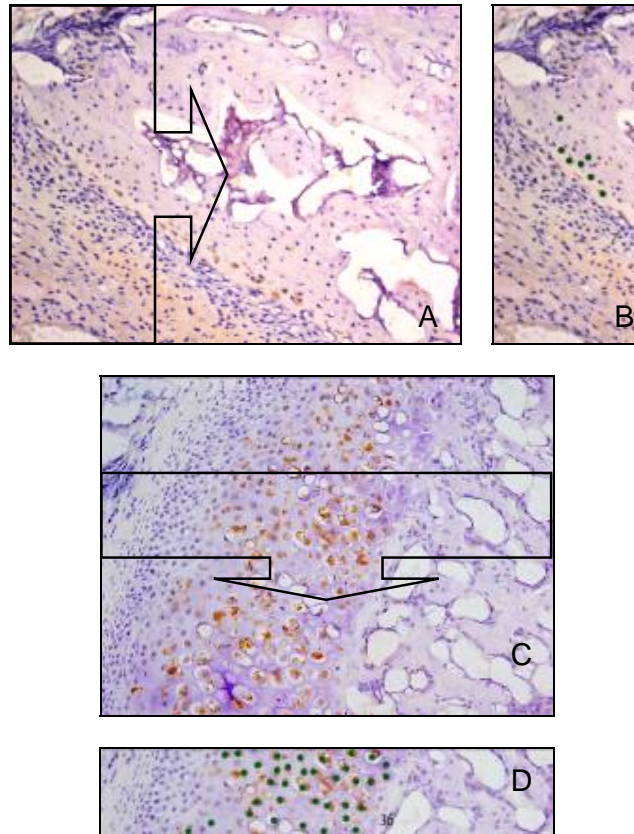


Figure 3-3 HRP positive immunostained cell counting in MCC and GF

- (A) The GF of a 38 day-old Sprague Dawley rat from group 3, experimental. Horse radish peroxidase (HRP) positive stained cells for FGF8 are brown.
- (B) The distal third of the section (A) in which the heavily stained cells are marked with dark green dots for cell counting. 7 dots are counted in this section.
- (C) The MCC of a 45 day-old Sprague Dawley rat from group 3, control. HRP positive stained cells for FGF8 are brown.
- (D) The middle quarter of the section (C) in which the heavily stained cells are marked with dark green dots for cell counting. 36 dots are counted in this section.

After the first counting, the data were collected again four weeks later by the same observer and the Method of error (ME) was tested by using the formula:

$$ME = \sqrt{\frac{\sum d^2}{2n}}$$

In this formula, “d” is the difference between the two registrations of a pair and “n” is the number of double registrations. For ME analysis ten readings were randomly drawn. Paired t tests were used to compare the two registrations. There was no statistically significant

difference among the registrations. Data were analysed using a statistical package (SPSS for Windows Version 16.0; SPSS, Chicago, IL).

The ANOVA (Analysis of Variance) statistical evaluation for each of the FGF8 and PCNA antibodies was carried out using day and appliance as factors and weight at sacrifice (wts) as a covariate, although to some extent the effect of weight at sacrifice is 'captured' by day. A day by appliance interaction was included if it was significant but dropped if otherwise. Not surprisingly, day was significant for all antibodies; weight at sacrifice was significant for only some.

RESULTS

4. Results

Table 4-1 The whole experiment's details and recorded data for each sample
Group 1

Experiment						Number of immunopositive stained cells for FGF8 and PCNA**				Weight	
Reference	Experiment Day of Sac	Age (Days)	Group	Appliance ***	Class****	FGF8c	FGF8gf	PCNAc	PCNAgf	Initial weight	Weight at Sacrifice (wts)
201*	3	27	1	1	II	20	19	20	30	79.6	84
202	3	27	1	1	II	25	13	41	31	93.5	97
203	3	27	1	1	III	28	18	37	n/a	75.3	108
204	3	27	1	1	II	27	16	63	32	92.2	102
205	3	27	1	1	III	16	15	36	21	91	97
206	3	27	1	1	III	19	19	22	12	87.5	96
207	3	27	1	1	III	22	18	54	20	92.2	104
208	3	27	1	1	III	24	n/a	n/a	13	81.2	84
209	3	27	1	1	III	18	21	55	23	95.9	102
210	3	27	1	1	III	22	19	36	20	85.7	86
111	3	27	1	0	I	15	12	20	24	91.3	100
112	3	27	1	0	I	n/a	8	68	18	90.6	100
113	3	27	1	0	I	20	10	23	n/a	81	111
114	3	27	1	0	I	14	15	24	8	89	115
115	3	27	1	0	I	17	9	33	9	85	110

Table 4-1 The whole experiment's details and recorded data for each sample
Group 2

Experiment						Number of immunopositive stained cells for FGF8 and PCNA**				Weight	
Reference	Experiment Day of Sac	Age (Days)	Group	Appliance***	Class****	FGF8c	FGF8gf	PCNAc	PCNAgf	Initial weight	Weight at Sacrifice (wts)
216	14	38	2	1	II	79	3	41	16	96.4	153
217	14	38	2	1	III	78	1	52	22	90.2	146
218	14	38	2	1	III	76	2	38	19	93.3	158
219	14	38	2	1	II	71	4	43	22	97.4	156
220	14	38	2	1	III	73	8	79	20	100.7	154
221	14	38	2	1	III	64	1	63	10	96.7	164
222	14	38	2	1	II	69	1	65	10	85.5	154
223	14	38	2	1	III	73	0	n/a	15	98.1	144
224	14	38	2	1	III deviated to the right	67	7	44	14	95.6	145
225	14	38	2	1	II	77	2	36	11	83.7	130
126	14	38	2	0	I	63	1	31	14	98.1	159
127	14	38	2	0	I	61	2	63	15	90.4	153
128	14	38	2	0	I	n/a	2	80	15	89.2	150
129	14	38	2	0	I	61	0	34	13	101.1	166
130	14	38	2	0	I	60	0	32	12	n/a	157

Table 4-1 The whole experiment's details and recorded data for each sample
Group3

Experiment						Number of immunopositive stained cells for FGF8 and PCNA**				Weight	
Reference	Experiment Day of Sac	Age (Days)	Group	Appliance***	Class****	FGF8c	FGF8gf	PCNAc	PCNAgf	Initial weight	Weight at Sacrifice (wts)
231	21	45	3	1	III	45	n/a	96	8	93.4	155
232	21	45	3	1	Appliance broke and came off	56	1	80	11	91.6	160
233	21	45	3	1	II	63	1	103	11	88.7	149
234	21	45	3	1	II	58	0	64	12	91.3	174
235	21	45	3	1	III	49	0	30	n/a	99.9	180
236	21	45	3	1	III	47	0	79	21	97.6	135
237	21	45	3	1	III	50	0	170	6	94.3	163
238	21	45	3	1	III	45	0	100	14	91.3	164
239	21	45	3	1	II	60	1	120	13	91.7	178
240	21	45	3	1	Appliance broke and came off	48	0	117	10	92.2	157
141	21	45	3	0	I	51	1	74	1	87.5	175
142	21	45	3	0	I	46	n/a	72	6	n/a	172
143	21	45	3	0	I	41	0	80	8	86.7	161
144	21	45	3	0	I	39	0	110	2	90	178
145	21	45	3	0	I	42	0	110	7	94.3	185

Table 4-1 The whole experiment's details and recorded data for each sample
Group 4

Experiment						Number of immunopositive stained cells for FGF8 and PCNA**				Weight	
Reference	Experiment Day of Sac	Age (Days)	Group	Appliance ***	Class****	FGF8c	FGF8gf	PCNAc	PCNAgf	Initial weight	Weight at Sacrifice (wts)
246	30	54	4	1	III	27	1	78	1	84.4	168
247	30	54	4	1	II	30	0	160	0	91.1	182
248	30	54	4	1	III	23	0	72	5	100	177
249	30	54	4	1	II	20	1	76	11	97.1	180
250	30	54	4	1	III	25	1	90	0	97.7	158
151	30	54	4	0	I	26	1	57	2	92.1	205
152	30	54	4	0	I	23	0	52	4	92.3	215
153	30	54	4	0	I	27	0	62	1	96	214
154	30	54	4	0	I	30	0	60	n/a	87.1	180
155	30	54	4	0	I	n/a	n/a	41	n/a	93.2	218

* In the reference column, the first digit 1 stands for control samples and 2 stands for experimentals. The next two digits are the particular number for each sample from 1 (the first experimental rat in group 1) to 55 (the fifth control rat in group 4).

** In each slide, the cells which were positively immunostained for the FGF8 or PCNA were counted. The cells with a stain that was not certainly intense were excluded.

*** In the appliance column, 1 stands for samples wearing bite-jumping appliance and 0 stands for samples without an appliance.

**** In the class column, Type of occlusion is reported due to the upper and lower incisors relationship. I stands for CI I; lower incisors were located behind the upper in contact with the lingual surface of the upper incisors (which is observed in all control samples). II stands for CI II; lower incisors were located behind the lingual surface of the upper incisors, further backward with no contact due to the bulk of the bite-jumping appliance. III stands for CI III; lower incisors were positioned in front of the upper incisors, which is comparable to the human CI III incisal relationship.

4.1. Histological Structures

The five distinctive cellular layers and the bone of the MCC and the GF are shown in figures 4-1 and 2-3. The articular layer is the most superficial layer with small, globular, densely distributed mesenchymal cells. The articular surface of the MCC and the articular surface of the GF are basically similar. They are covered by a layer of dense fibrous tissue which is the Articular Zone (A).

Underneath the fibrous layer, there is an undifferentiated mesenchymal cell zone. The undifferentiated reserve cells are dense and packed together. The underlying layer is the resting layer (R). Prechondroblasts beneath the resting layer are known as the Proliferative Zone (P).

The next layer is the Hypertrophic Zone which is accommodated with chondroblasts. Mature chondrocytes are deep in this layer (H). The Erosive layer is further down where highly hypertrophic chondrocytes are broken down and their surrounding matrices are degenerated (E). The frontier of the newly formed bone is beneath the erosive layer (B) (17).

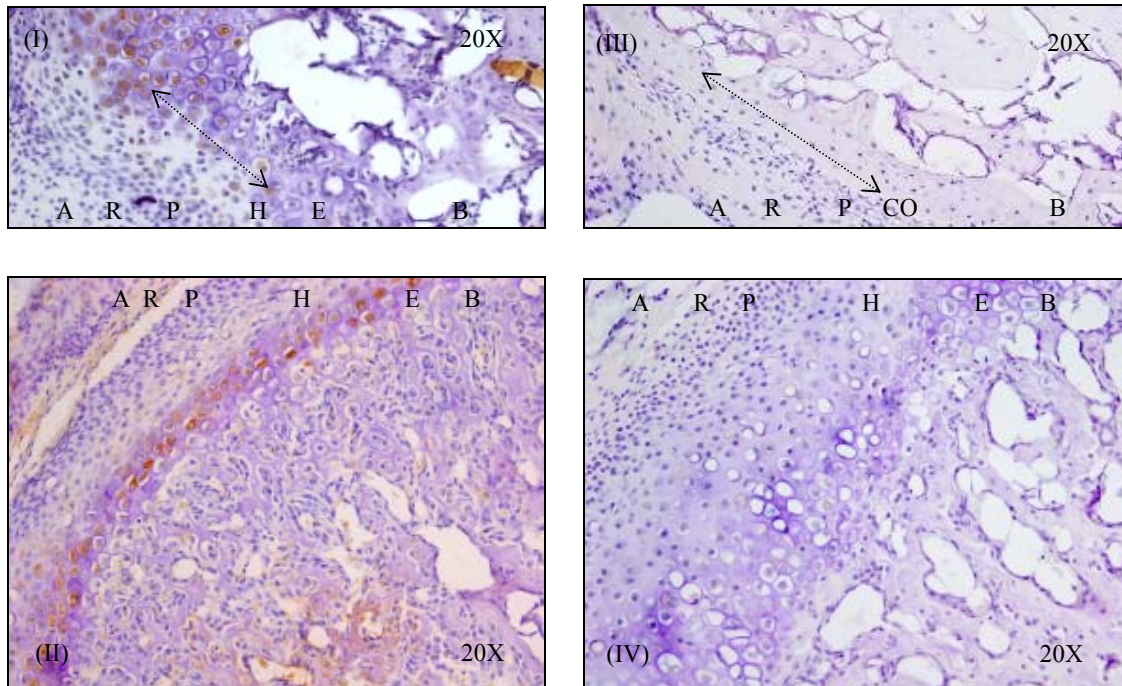


Figure 4-1 Distinctive cellular layer in the MCC and the GF

The GF (I) and the MCC (II) of an experimental sample (27-day old Sprague Dawley rat wearing bite-jumping appliance for 3 days), immunostained for FGF8; GF (III) and the MCC (IV) of a control sample (45-day old Sprague Dawley rat without orthodontic appliance), negative control slide for a FGF8 immunostained slide; Different cellular layers in the MCC and the GF named as A-Articular Zone, R-Resting Zone, P-Proliferating Zone, H-Hypertrophic Zone (arrow (I)), E-Erosive Zone and CO-Connective tissue-Osteoblasts (arrow (III)). The thickness of cartilage indicates the dominance of endochondral ossification, except in image (III)-CO, in which the Hypertrophic and Erosive zones are replaced with Connective tissue and Osteoblasts. This suggests the dominance of intramembranous ossification in female Sprague Dawley rats after 5-7 weeks of age or it implies that the active growth and development of their GF is until 5-7 weeks of age (10, 17, 22, 64, 130, 131, 148).

4.2. FGF8 Expressions in the Mandibular Condylar Cartilage (FGF8c) and the Glenoid Fossa (FGF8gf)

The FGF8 was mainly expressed in the early hypertrophic layer and hypertrophic layer of the MCC and GF in the control and experimental groups (42, 45).

The level of FGF8c progressively increased from Day 3 to Day 14 in the MCC, after which the expression declined gradually until Day 30. However, the level of FGF8gf expression in the GF progressively decreased from Day 3 to Day 14, followed by a slight decrease from Day 14 to Day 21 and a little increase on Day 30. The level of increase from

Day 21 to Day 30 was still significantly lower than the same measurement on Day 14 (Figure 4-4).

In the experimental samples generally the expression of FGF8 in response to mandibular advancement in both the MCC and the GF is significantly higher than control groups ($p=0.002$) (Table 4-2, Figure 4-3). However, there was an exception on Day 30 for the MCC which the amount of FGF8 expression in control group was non-significantly higher than experimental group (Table 4-2). Over all, the level of FGF8 expression was remarkably higher in the MCC than GF (Table 4-2, Figure 4-3, Figure 4-4).

The pattern of expression in experimental groups and Control groups for each tissue was similar, but the pattern of expression in the MCC was different from the one in the GF. The pattern of expression across the MCC led to a maximum expression on Day 14 followed by a gradual decrease, while the maximum expression in the GF was on Day 3 followed by a significant severe decrease on Day 14 followed by a light decrease toward the end of the experiment. The little increase from Day 21 to Day 30 could be omitted as it is a non significant change plus considering a very low level of FGF8 expression. The important results were that generally the effect of appliance is significant for FGF8 in the GF and the MCC (FGF8c, $p=0.002$ and FGF8gf, $p=0.002$) (Table 4-2, Figure 4-3, Figure 4-4).

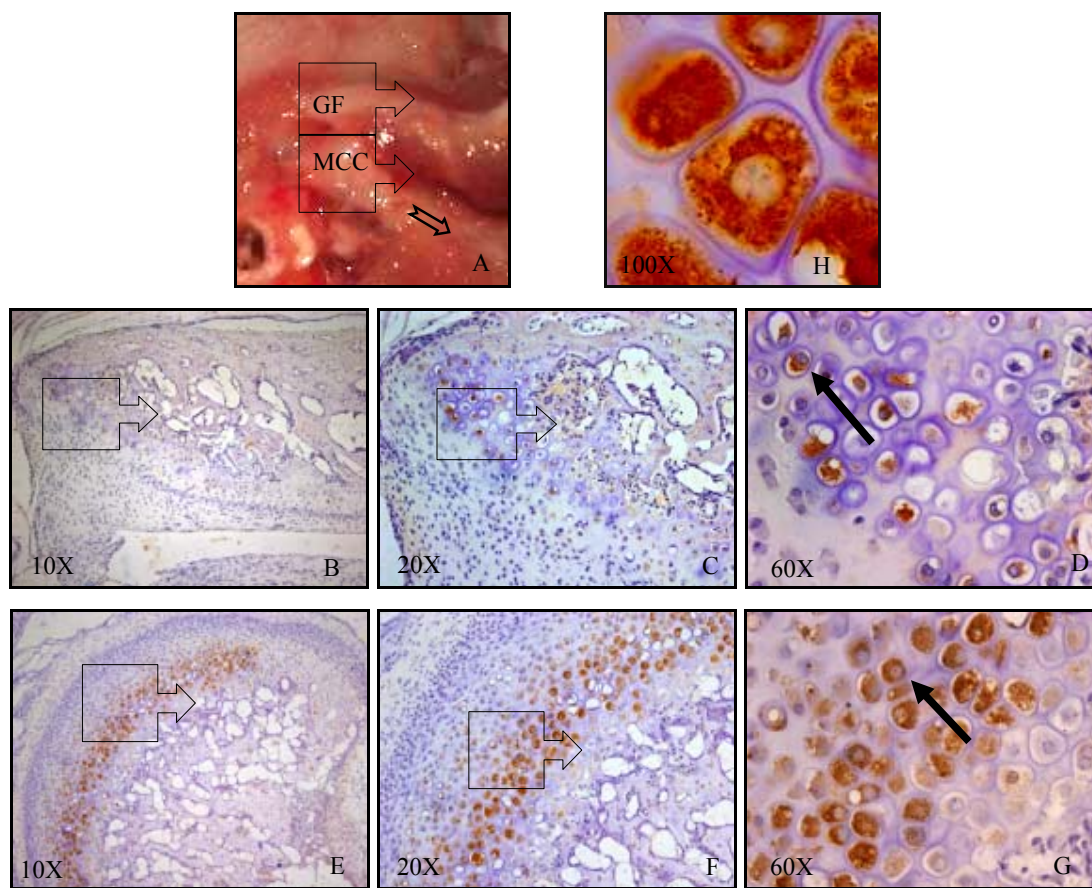


Figure 4-2 FGF8 in the MCC and the GF

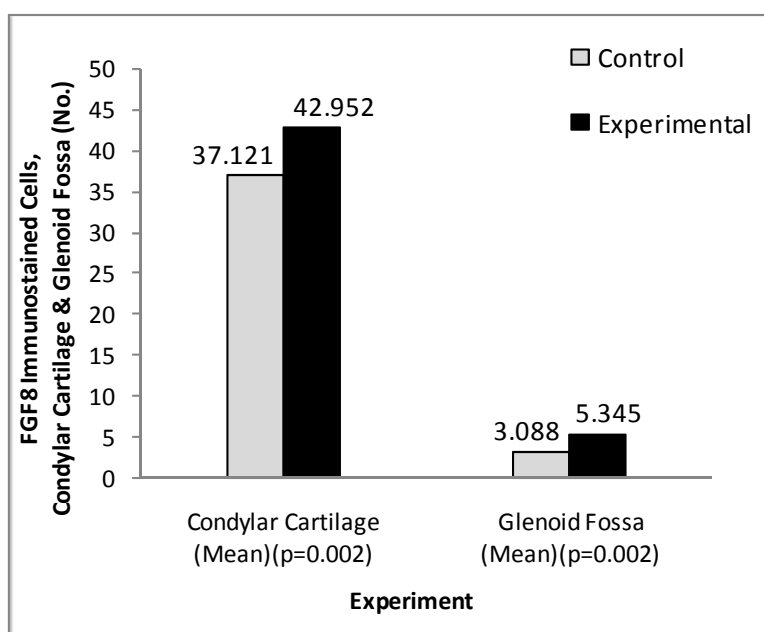
Photograph of a female Sprague Dawley rat's TMJ (A) shows the anatomic relationship of the condyle (A-MCC) and the articular fossa (A-G) and the arrow (A) shows the direction of forward-downward displacement of the condyle during mandibular advancement. Photomicrographs show immunostaining for FGF8 expressed in and the GF of another experimental sample (27-day old rat, wearing bite jumping appliance for 3 days) (B, C and D) and the MCC of an experimental sample (38-day old rat, wearing bite jumping appliance for 14 days) (E, F, and G); The cytoplasm of early hypertrophic and hypertrophic cells, beneath the layer of cell proliferation and above the erosive zone were positively stained for FGF8 (arrow (D, G)). FGF8 is mainly located in cytoplasm of osteochondroprogenitor cells, chondroblasts and chondrocytes before their degeneration, which is shown by extra magnification of a typical immunopositive-cell for FGF8 from the hypertrophic layer of the MCC of a 38-day old experimental sample (H). The location of FGF8 expression was consistent with other reports which suggest that FGF8 could be known as an indicator for osteogenesis through an endochondral ossification process by patterning and regulating the chondrocytes' proliferation and their hypertrophic morphological differentiation (42, 158, 162). For more images see appendix 1, section FGF8c and FGF8gf.

Table 4-2 FGF8 c & gf; Experimentals vs. Controls

Quantitative analysis of FGF8 expression in Condylar Cartilage (FGF8c) and Glenoid Fossa (FGF8gf). The number of FGF8 immunopositive cells is considered for calculating the values and statistical analysis of experimental samples versus controls. This indicates the overall effect of the bite jumping appliance on the level of FGF8 expression.

	Group	Mean(No.)	Std. Error	95% Confidence Interval	
				Lower Bound	Upper Bound
Condylar Cartilage (FGF8c)	Control	37.121 ^a	1.451	34.194	40.047
	Experimental ^b	42.952 ^a	.852	41.233	44.671
Glenoid Fossa (FGF8gf)	Control	3.088 ^a	.573	1.933	4.244
	Experimental ^b	5.345 ^a	.349	4.641	6.050

a. Covariates appearing in the model were evaluated at the following values: wts = 148.077(c) & 147.824 (gf)
b. P=0.002 (The effect of the appliance was statistically significant for FGF8c & FGF8gf)

**Figure 4-3 FGF8 c & gf; diagram for Experimentals vs. Controls**

In this diagram the mean of the number of FGF8 immunopositive cells in the MCC (FGF8c) and Glenoid Fossa (FGF) are compared in experimentals and controls. The level of FGF8 expression in experimentals' condyle and the GF was significantly higher than their relevant control samples ($p=0.002$). Furthermore, the diagram clearly shows that the amount of cellular activity in the MCC was greatly higher than GF in both controls and experimentals.

Table 4-3 FGF8 c & gf; Experimentals vs. Controls in different experiment days

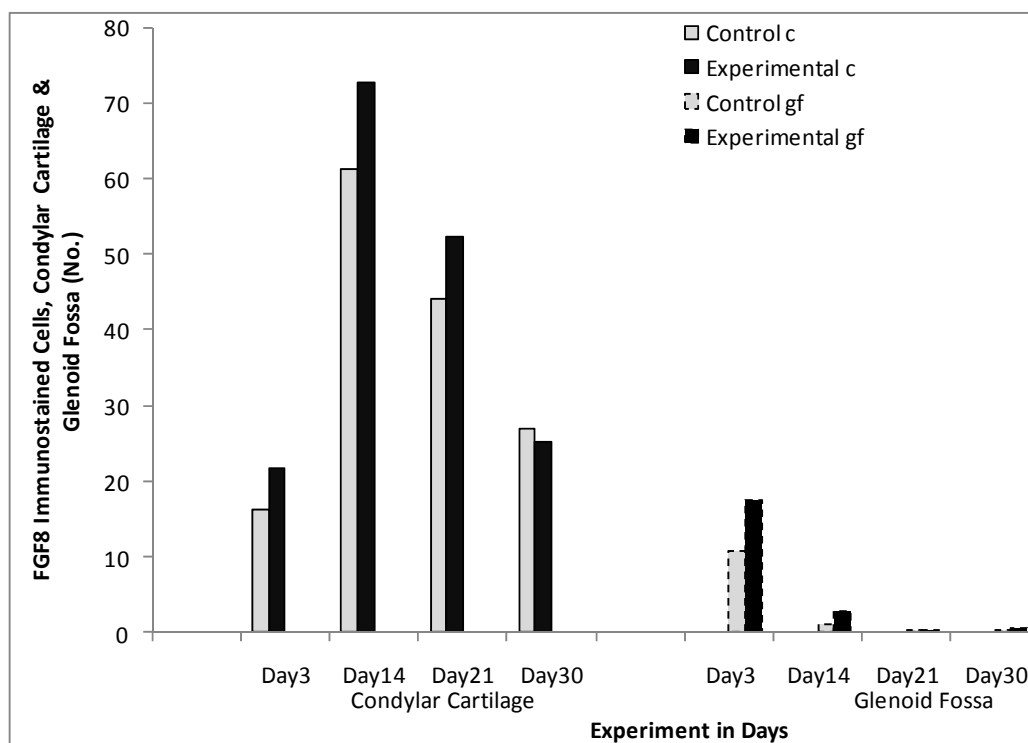
Quantitative analysis of FGF8 expression in Condylar Cartilage (FGF8c) and Glenoid Fossa (FGF8gf). The number of FGF8 immunopositive cells is considered for calculating the values and statistical analysis of experimental samples versus controls in different experiment days. This indicates the effect of the bite jumping appliance on the level of FGF8 expression in different stages of rat's growth.

	Group ^{a, b}	Day 3	Day 14	Day21	Day 30
Condylar Cartilage	Exp. ^c	21.676 ^a ±3.798	72.719 ^a ± 1.494	52.209 ^a ± 1.738	25.203 ^a ± 2.686
	95% CI	14.017, 29.336	69.706, 75.732	48.705, 55.713	19.786, 30.619
	Cont.	16.182 ^a ±3.521	61.337 ^a ±2.456	44.012 ^a ±2.737	26.951 ^a ±4.400
	95% CI	9.081, 23.283	56.384, 66.290	38.494, 49.531	18.078, 35.823
Glenoid Fossa	Exp. ^b	17.503 ^a ±1.526	2.903 ^a ± 0.607	0.348 ^a ± 0.749	0.626 ^a ±1.098
	95% CI	14.424, 20.583	1.678, 4.128	-1.162, 1.859	-1.590, 2.842
	Cont.	10.758 ^a ±1.405	1.010 ^a ±0.889	0.278 ^a ±1.207	0.308 ^a ±1.803
	95% CI	7.923, 13.592	-0.785, 2.804	-2.157, 2.713	-3.330, 3.945

a. Data were presented as M ± SE (Standard Error)(No.); CI: Confidence Interval- Lower, Upper

b. Covariates appearing in the model were evaluated at the following values: wts = 148.077(c) & 147.824 (gf)

c. p=0.002; The effect of the appliance was statistically significant for FGF8c & FGF8gf.

**Figure 4-4 FGF8 c & gf; diagram for experimentals vs. controls in different experiment days**

In this diagram the mean of the number of FGF8 immunopositive cells in the MCC (FGF8c) and the GF (FGF8gf) were compared in experimentals and controls in different experiment days. The level of FGF8 expression in experimentals' condyle and GF generally was significantly higher than their relevant control samples. Furthermore, it was clear that the amount of cellular activity in the MCC is greatly higher than the GF in both controls and experimentals in different stages of growth and development.

For more details and diagrams on statistical analysis see appendix 2, section FGF8c and FGF8gf.

4.3. PCNA Expressions in Mandibular Condylar Cartilage⁵ (PCNAc) and Glenoid Fossa (PCNAgf)

The PCNA was expressed mainly in proliferative cellular layer during normal growth and adaptive response to mandibular protrusion in the MCC and the GF (Table 4-4) (42, 45).

The level of PCNA expression gradually increases from Day 3 to a maximum expression on Day 21 in the MCC after which the expression declines on Day 30. However, the level of expression of PCNA gradually decreases from Day 3 towards the end of the experiment in the GF (Table 4-5, Figure 4-7).

In the experimental samples generally the expression of PCNA in both MCC and GF in response to mandibular advancement was higher than control groups. The level of extra PCNA expression in the MCC was not statistically significant ($p=0.327$) but it was significant in the GF (Table 4-4). Generally, the level of PCNA expression was remarkably higher in the MCC than the GF (Table 4-4, Figure 4-6).

The pattern of expression in experimental groups and control groups for both of condyle and the GF was similar, but the pattern of expression in the MCC was different from the one in the GF. The pattern of expression across the MCC led to a maximum expression on Day 21 followed by a decrease on Day 30, while the maximum expression in the GF was on Day 3 followed by a gradual drop toward the end of the experiment. The important results

⁵ The data and images of PCNA - Condylar Cartilage are transferred from Dr. Zoe Potres' study on the same samples using the same methods and materials, perusing her MPhil degree through the project. It is reported here for consistency and completeness of the current part of the text followed by a more coherent discussion and conclusion.

were that the effect of appliance in the GF and in the MCC was not significant for PCNA (PCNA_{gf}, $p=0.327$ - PCNA_{Ac}, $p=0.327$).

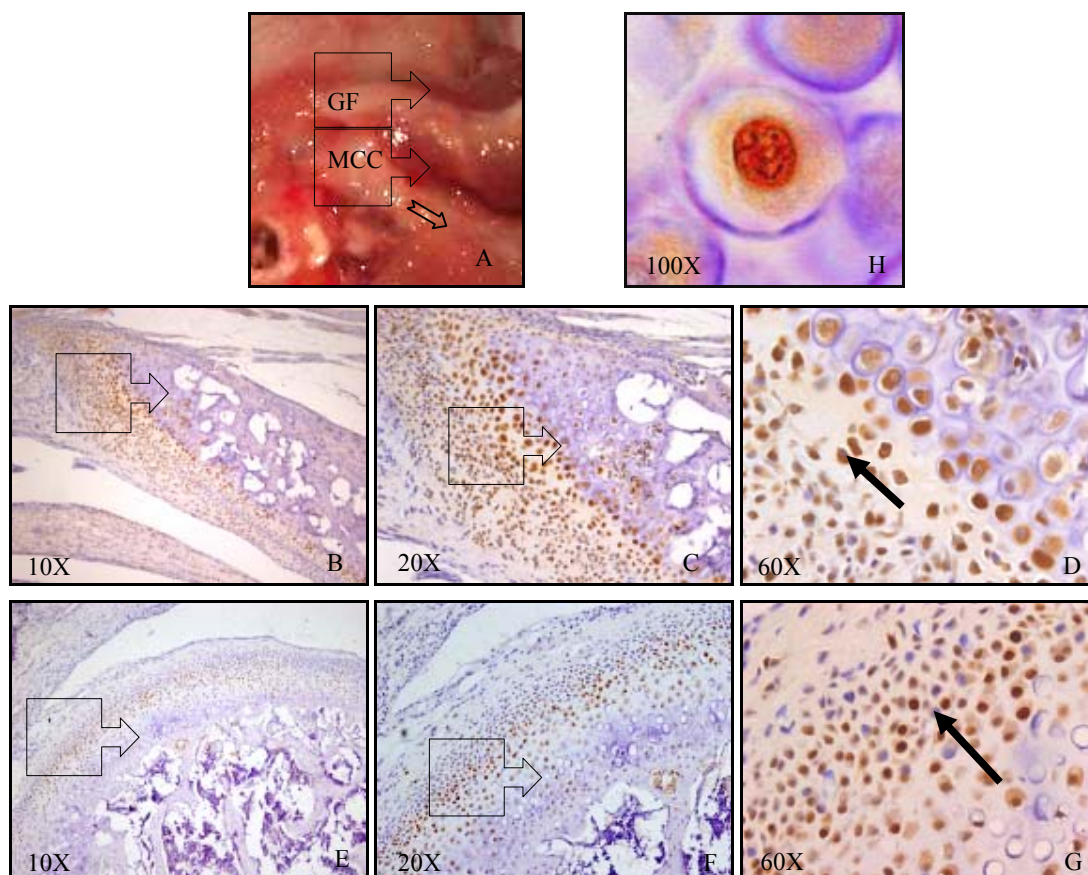


Figure 4-5 PCNA in Condylar Cartilage and Glenoid Fossa

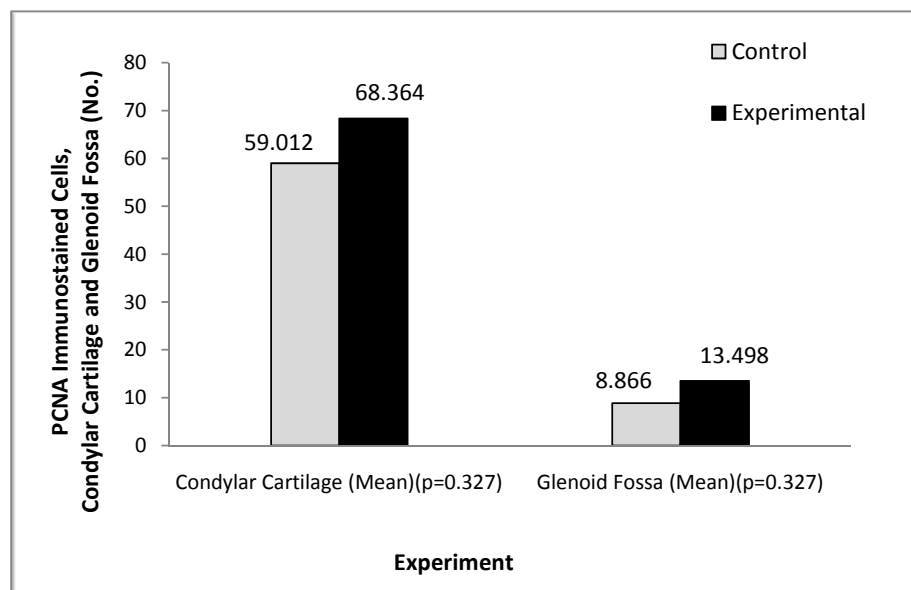
Photograph of a female Sprague Dawley rat's TMJ (A) shows the anatomic relationship of the condyle (A-MCC) and the GF (A-GF) and the arrow (A) shows the forward-downward displacement of the condyle during mandibular protrusion. Photomicrographs show immunostaining for PCNA expressed in the GF of another experimental sample (27 day-old rat, wearing bite-jumping appliance for 3 days) (B, C and D) and the MCC of an experimental sample (45 day-old rat, wearing bite-jumping appliance for 21 days) (E, F, and G); The nucleus of proliferative cells, beneath the resting zone and above the hypertrophic zone, were the majority of PCNA immunopositive cells (arrow (D, G)). PCNA was located mainly in the nucleus of the mesenchymal cells and osteochondroprogenitor cells during their active proliferation, which is shown by extra magnification of a typical immunopositive cell for PCNA from the hypertrophic layer of the MCC of a 38 day-old experimental sample (H). As expected, the location of PCNA detection was consistent with other reports introducing the PCNA as an indicator for cells' active proliferation and PCNA immunopositive nucleuses in other layers could suggest that some cells were still dividing beside morphologic and degenerative changes of the other cells in a particular cellular zone (1, 22, 43-47, 221)

Table 4-4 PCNA c & gf; Experimentals vs. Controls

Quantitative analysis of PCNA detection in Condylar Cartilage and Glenoid Fossa. The number of PCNA immunopositive cells is considered for calculating the values and statistical analysis of experimental samples versus controls. This indicates the effect of the bite-jumping appliance on the level of cellular proliferation in general.

	Group	Mean(No.)	Std. Error	95% Confidence Interval	
				Lower Bound	Upper Bound
Condylar Cartilage	Control	59.012 ^a	6.595	45.745	72.728
	Experimental ^b	68.364 ^a	4.499	59.313	77.414
Glenoid Fossa	Control	8.866 ^a	1.604	5.632	12.099
	Experimental ^c	13.498 ^a	.935	11.614	15.382

- a. Covariates appearing in the model were evaluated at the following values: wts = 149.811(c), 147.420(gf)
- b. P=0.327; The effect of the appliance was not statistically significant for PCNA in the Condyle (PCNAc)
- c. P=0.327; The effect of the appliance was not statistically significant for PCNA in the GF (PCNAgf)

**Figure 4-6 PCNA c & gf; diagram for Experimentals vs. Controls**

In this diagram the mean of the number of PCNA immunopositive cells in the MCC and in the GF were compared in experimentals and controls. The level of PCNA expression in the experimentals' GF was not significantly higher than their relevant control samples. It was also not statistically significantly higher in the experimentals' MCC. Furthermore, the diagram clearly shows that the amount of cellular proliferation in the MCC was greatly higher than in the GF in both controls and experimentals.

Table 4-5 PCNAc & gf experimentals vs. controls on different experiment days

Quantitative analysis of PCNA expression in Condylar Cartilage and Glenoid Fossa. The number of PCNA immunopositive cells is considered for calculating the values and statistical analysis of experimental samples versus controls on different experiment days. This indicates the effect of the bite-jumping appliance on the level of cellular proliferation expression in different stages of rat's growth.

	Group ^{a, b}	Day 3	Day 14	Day21	Day 30
Condylar Cartilage	Exp. ^c	42.941 ^a ±20.049	51.160 ^a ±8.219	95.344 ^a ±8.787	94.097 ^a ±13.658
	95% CI	2.536,83.347	34.597,67.724	77.635,113.052	66.570 , 121.623
	Cont.	35.628 ^a ±18.489	47.658 ^a ±11.291	88.040 ^a ±13.910	51.707 ^a ±22.590
	95% CI	-1.634, 72.889	24.902,70.414	60.006,116.073	6.181,97.234
Glenoid Fossa	Exp. ^b	20.433 ^a ±4.763	16.014 ^a ±1.646	12.236 ^a ±1.992	4.375 ^a ±3.153
	95% CI	10.813, 30.053	12.689, 19.339	8.214, 16.259	-1.991, 10.742
	Cont.	13.180 ^a ±4.318	14.165 ^a ±2.438	5.821 ^a ±3.222	4.770 ^a ±6.149
	95% CI	4.459, 21.901	9.241, 19.090	-0.687, 12.329	-7.648, 17.189

- a. Data were presented as M ± SE (Standard Error) (No.); CI: Confidence Interval-Lower, Upper
- b. Covariates appearing in the model were evaluated at the following values: wts = 149.811(c) & 147.420 (gf)
- c. P=0.327; The effect of the appliance was not statistically significant for PCNA in the Condyle (PCNAc)
- d. P=0.327; The effect of the appliance was not statistically significant for PCNA in the GF (PCNAgf)

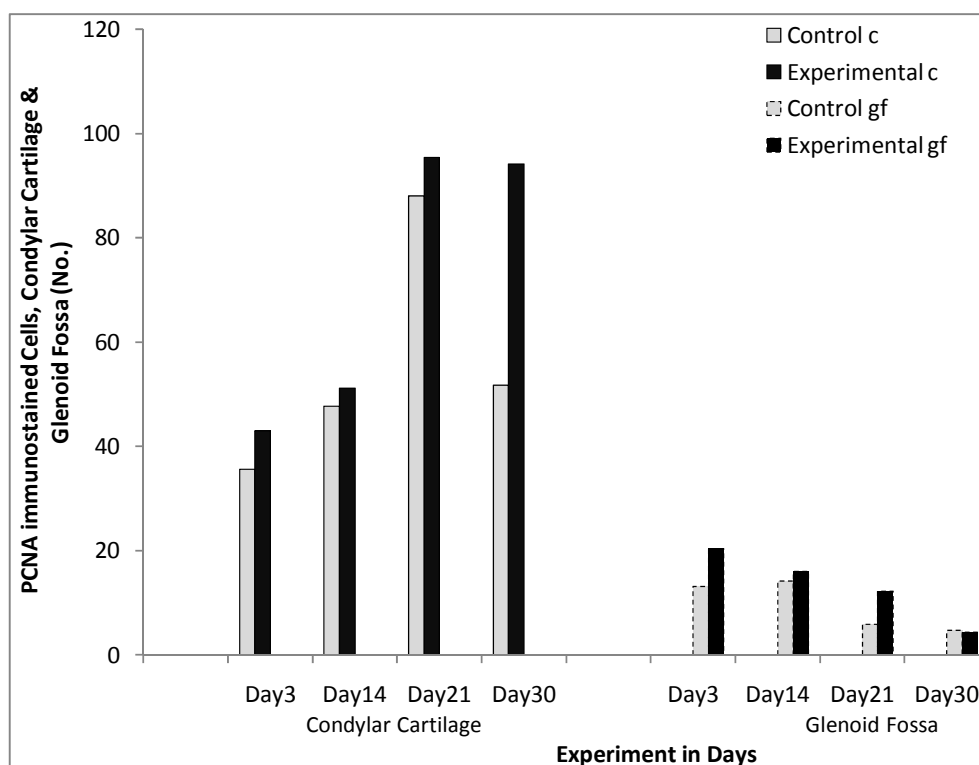


Figure 4-7 PCNA c & gf; diagram for experimentals vs controls on different experiment days

In this diagram the mean of the number of PCNA immunopositive cells in the MCC and the GF were compared on different experiment days. The level of detected PCNAs in the samples' MCC and GF indicates that the amount of cellular proliferation in the MCC was greatly higher than in the GF during different stages of the rats' growth and development. Additionally, the pick of proliferative activity in the MCC and GF shows that the progenitor cells' dividing slowed down after 45 days of rats' age in the condyle and after 27 days of age in the GF with different patterns of expression. The changes were significant on different days of experiment.

For more details and diagrams on statistical analysis see appendix 2, section PCNAc and PCNAgf.

4.4. Mandibular Position

The control groups had normal CI I relationship without any appliances. The bite-jumping appliances were adjusted on the lower incisors of experimental rats to move their mandible into a forward position, to a CI III skeletal relationship. The experimental samples

were able to function and chew during the experimental period with their appliance in place. Most of the samples' mandible remained in a forward position (CI III relationship) until the end of the experiment (Figure 3-1B), while two samples in group 3 (Day 21) had broken appliances at the day of sacrifice with their jaws in a CI I relationship and the rest (around 35%) had a CI II relationship (Figure 4-8), because of their mandibular backward movement during the experiment (Table 4-6, Figure 4-9).

The ANOVA replaces appliance by class shows that the effect of class II and III on the level of PCNA and FGF8 expression were not significantly different (Bonferroni adjusted $p = 0.61$). Therefore, it was not necessary to investigate different classes further on most of the data. However, there were a few exceptions.

For PCNA_{gf}, the mean difference between CI I and II was significant ($p=0.023$), while it was neither significant between CI I and III ($p=1.000$) nor between CI II and III ($p=0.110$) (appendix 2, pairwise comparisons, dependent variable: PCNA_{gf}).

For FGF8_c, it was significant between CI I and II ($p=0.000$) and between CI II and III ($p=0.009$) but not between CI I and CI III ($p=0.118$). However, the overall statistical analysis shows significant changes for FGF8 during the experiment between controls and experimentals, considering the day and class at the same time ($p=0.002$) (appendix 2, tests of between-subjects effects, dependent variable: FGF8_c, source: day*class). The significant difference between CI II and III was not considered for further discussion as the current study was aimed at revealing the nature of the histochemical changes in response to environmental changes and not specifically about the differences of CI II and III treatments.

For FGF8_{gf}, it was only significant between CI I and III ($p=0.020$) but not between CI I and II ($p=0.139$) or between CI II and III ($p=1.000$) (appendix 2, pairwise comparisons, dependent variable: FGF8_{gf}).

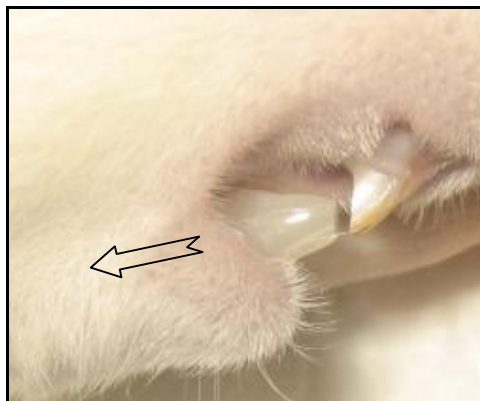


Figure 4-8 the rat's Mandible in a CI II position

The Mandible in about 35% of experimental samples was in a CI II position on the day of sacrifice (Table 4-6). In these samples, lower incisors were positioned behind the upper incisors with extra mandibular backward movement due to the bulk of the bite-jumping appliance (arrow direction). The GF in Sprague Dawley rats is shallow and there is not a hard tissue stop at the distal of the condyle, which differs in humans (Figure 4-10). Therefore, due to this particular anatomic form, their condyle can easily move backward within the range of soft tissue limits. The ANOVA replaces appliance by class shows that CI II and III were not significantly different (Bonferroni adjusted $p = 0.61$) with the intention of their effect on the level of cellular and molecular activity in the condyle and GF.

Table 4-6 Mandibular Position in experimental samples

The number of the experimental rats with different Mandibular Position on the day of sacrifice.

Day	Class I ^a	Class II	Class III
3	0	3	7
14	0	4	6
21	2 ^b	3	5
30	0	2	3
Total	2	12	21
* Mandibular position in all 15 Control samples was normal; known as CI I.			
* The appliance broke in 2 rats of group "Day 21" experimental samples.			

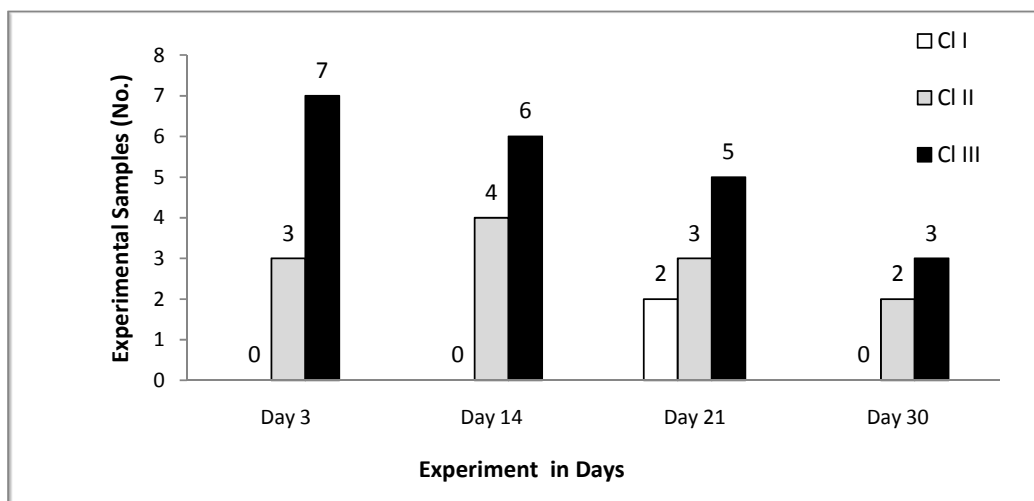


Figure 4-9 A Diagram for Mandibular Position in experimental samples

The diagram shows the number of rats in each experimental group with different mandibular positions. The number of CI IIIs was reduced during the experiment. This could be due to the special anatomy of the rats' TMJ which allows the condyle to move backward as the GF is shallow (A). During function, chewing cycle and rest, it was possible that instead of a CI III position, rats move their lower incisors behind the upper incisors while they wear the appliance (Figure 3-1). Therefore, the bulk of the appliance causes a CI II effect and the anatomy of their TMJ provides room for this backward movement. However, the ANOVA replaces appliance by class shows that CI II and III were not significantly different (Bonferroni adjusted $p = 0.61$) with the intention of histochemical changes in the experimentals' condyle and GF.

The anatomic structure of the rat TMJ does not restrict the condylar head from backward movement. Therefore, some experimental rats in the current study had CI II occlusion at the day of sacrifice. The anatomic structure of the rat TMJ is compared with the human TMJ in Figure 4-10.

Table 4-7 Mandibular Position on the day of sacrifice

Group	Class I (No.)	Class II (No.)	Class III (No.)
Control *	20/20	0/20	0/20
Experimental	2/35	12/35	21/35

* Mandible was in normal CI I position in all control samples.

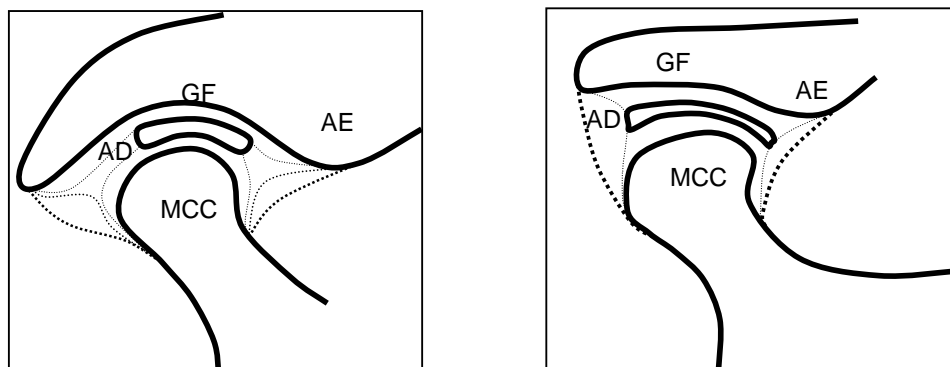


Figure 4-10 Schematic sagittal view of human and rat TMJ

The diagram shows a schematic view of a sagittal section of the human TMJ (A) and the rat TMJ (B); The mandibular condylar cartilage (MCC), the articular disc (AD), the glenoid fossa (GF) and the articular eminence (AE) is drawn with hard lines and the outer and inner limits of soft tissues were approximately shown by heavy and light dashes. Regardless of the actual diameter there were differences in the anatomic structure of the rat TMJ in comparison with the human TMJ. In rats the GF is shallower, the AE is less eminent and the distal part of the temporal bone facing the condyle is less extended downward. Therefore, the rat condyle could move forward and backward within the soft tissue limits, while in the human condyle the movement is much more restricted.

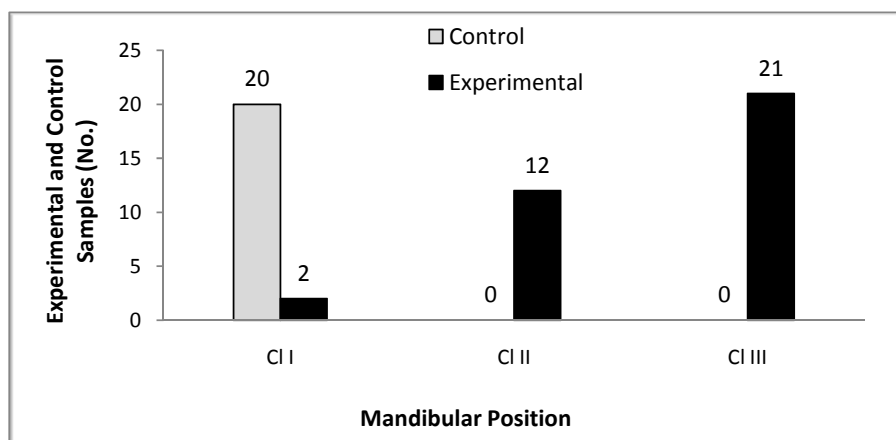


Figure 4-11 mandibular position in experimental and control samples

For more details and diagrams on statistical analysis see appendix 2.

4.5. Weight Gain

The pattern of weight gain in the experimental and control groups is shown in Figure 4-12. Not surprisingly, the samples' weight increased over time and animals with the

appliance generally had a lower weight on sacrifice day, coupled with less weight gain during the experiment. The ANOVA backs this up, showing that days were significantly different ($p < 0.001$) and that the appliance had a significant effect ($p < 0.001$) on weight gain. Also, the change over time was significantly different in those animals with the appliance ($p = 0.017$).

Table 4-8 Rats' Weight on the day of Sacrifice (wts) (gr)

The Dependent Variable was rats' Weight at Sacrifice (wts)/day-class, and was compared within experimentals vs. controls.

Day	Group	Class	Mean	Std. Error	95% Confidence Interval	
					Lower Bound	Upper Bound
3	Control	Cl I	110.09 ^a	4.905	100.164	120.023
	Experimental	Cl II	96.48 ^a	6.180	83.971	108.993
		Cl III	99.90 ^a	4.246	91.301	108.492
14	Control	Cl I	154.72 ^a	5.385	143.816	165.620
	Experimental	Cl II	148.76 ^a	5.291	138.050	159.472
		Cl III	148.80 ^a	4.528	139.631	157.964
21	Control	Cl I	176.06 ^a	5.319	165.289	186.824
	Experimental	Cl II	167.64 ^a	6.111	155.270	180.011
		Cl III	156.69 ^a	4.883	146.809	166.579
30	Control	Cl I	205.93 ^a	4.733	196.347	215.509
	Experimental	Cl II	179.14 ^a	7.522	163.914	194.371
		Cl III	165.86 ^a	6.158	153.390	178.323

- Covariates appearing in the model were evaluated at the following values: Weight at four weeks of age (wt4) = 91.489.
- Weight gain was not significantly different between Cl II and Cl III experimentals; $p = 0.614$.
- Between controls and experimentals the difference was significant; $p = 0.005$ for Cl I and II, $p = 0.000$ for Cl I and III.

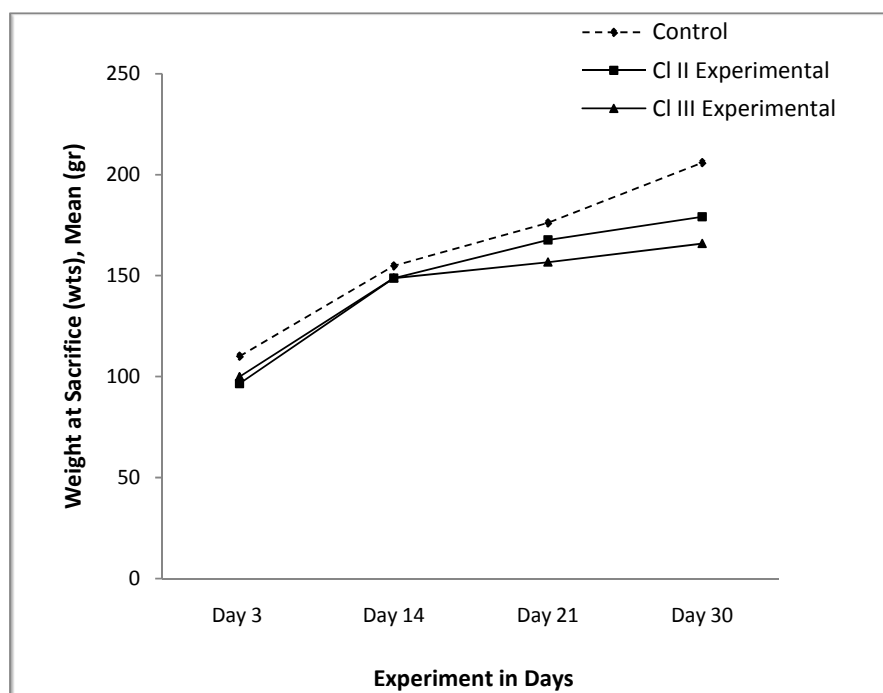


Figure 4-12 the diagram for rats' Weight at Sacrifice (wts) (gr)

The pattern of weight gain in the experimentals and controls was similar. However, the bite-jumping appliance significantly affected the weight gain process by reducing the level of weight gain ($p=0.005$ for CI II and $p=0.000$ for CI III). This could be due to functional restrictions during eating in experimental samples, with regard to the bulk and position of the bite-jumping appliance. CI III experimental weight gain was lesser than CI II samples, but it was not statistically significant ($p=0.614$).

For more details and diagrams on statistical analysis see appendix 2, section weight.

DISCUSSION and CONCLUSION

5. Discussion

The histological structures of the rats' TMJ are similar to that of humans, with some differences in morphology (19, 222). Due to this similarity and the possibility of a histochemical study on rats, based on previous studies (108, 109), fifty-five Sprague Dawley rats were used in this experiment, as used in other histological and biochemical investigations (6-9, 12, 19, 23, 28, 109, 123, 126, 130, 131, 133, 148, 223-231).

The rats continuously gain weight during their life. It is mentioned by Shen *et al* 2006 that the maximum rate of rats' growth is between 5 to 9 weeks of their age and resembles the adolescent growth spurt in humans (8). The accurate growth curve for the human condyle by approaches of gross measurement, such as cephalometric analysis, is difficult to obtain. In this situation it is of particular significance to investigate the temporal pattern of the condylar growth through biochemical studies in a rat experimental model, which could help to infer upon that of a human (109, 232)

5.1. Functional Mandibular Advancement

This experiment, based on previous similar studies, is performed to clarify the mechanism of condylar and GF adaptation in response to the mandibular advancement (2, 10, 15, 20). In growing patients with retrusive mandibles, growth modification of the mandible is the main goal of orthodontic treatments and most of these remodeling activities occur in the TMJ area, which is the target of several studies in this field (2, 6-8, 10, 19, 61, 233).

Even though some studies on monkeys indicate that such adaptive responses are non-existent, and negligible (63, 124, 234, 235), several other findings indicate positive

significant TMJ adaptation in response to mandibular advancement (6, 7, 23, 64, 118, 128, 129, 132, 236).

The bite-jumping appliance in this study is used to move the mandible to a forward position while slightly opening the bite. This functional appliance will activate different parts of the TMJ (13, 62, 128, 237). The effect of the bite-jumping appliance is affected by different factors, such as the duration of the treatment, the rate of the mandibular growth, the direction and the magnitude of the force (17, 57, 62, 67-69). These factors, which affect the results of the study, were kept as consistent as possible for all samples.

The translation of the condyle toward the articular eminence with a posterior-inferior rotation of the entire mandible causes space reduction in superior joint spaces in the condyle whilst posterior joint space increases. This function applies stretching forces to the distal and distal-superior part of the condyle and the areas of the GF facing these areas of the condyle. On the other site, compressive forces are applied on the anterior and anterior-superior parts of the condyle and their transactional sites on the GF (8, 19, 61, 131, 238).

A CI II functional correction occurs through different structural mechanisms by affecting maxillary and mandibular structures, such as TMJ remodeling and encouragement of mandibular growth, retardation or redirection of the maxillary growth in the mesial or vertical direction, and furthermore by inducing dentoalveolar changes in the maxillary and the mandibular anterior segment (55). The current study is to evaluate the nature of histochemical changes occurring in the MCC and the GF. The results of these changes are TMJ remodeling and mandibular growth modification. The Mandible is ultimately replaced to a more forward position.

5.2. TMJ Bone Remodeling & Growth Modification

Structural bases of the stomatognathic system are the maxillary and the mandibular skeletal structures. The boney parts of the TMJ are the condyle of the mandible and the GF of the temporal bone.

The MCC is the most posterior-superior part of the mandible and the mandibular GF is part of the temporal bone. The temporal bone in the rat consists of the squamosal, petrosal, tympanic, and mastoid bones. The only relevant part to the joint is the squamosal bone, which is a shallow bowl-like bone. The retrotympanic and the zygomatic are two strong processes of the squamosal bone. The mandibular GF is located ventral to the base of the zygomatic process, narrow and sagittally oriented. This fossa in the rat's TMJ is shallow with an anteroposterior long axis. It has a lateral flange and no posterior or anterior flanges and the articular eminence is much less distinct in comparison with the human's articular eminence (reported by Rabie *et al* 2001(12)).

The posterior, middle, and anterior parts of the GF are compared by Rabie *et al* 2001 during mandibular advancement. A substantial increase in bone formation in all of these three main regions of the GF on mandibular protrusion is shown when compared with untreated matched control rats. The highest level of bone formation was recorded in the posterior regions (12).

The aim of this study was evaluating the patterns of hypertrophic and proliferative activities in the posterior-superior part of the MCC and the posterior part of the GF during their adaptive remodeling response to the mandibular protrusion.

The evidence confirms that the MCC and the GF have the capability of functional adaptation in response to the environmental changes and responsive to mechanical

stimulation. This is consistent with many other investigations (71, 72, 76-78). The pattern of this adaptive response is different in the MCC and the GF, but the MCC and the GF growth modification are in harmony with each other.

This harmony could be described by the growth relativity hypothesis and the functional matrix theory. The mandible is displaced to a forward position, viscoelastic forces are applied on the MCC-GF complex at the same time in reverse directions, and the forces are transduced by being radiated beneath the articular layers of both the MCC and the GF (see pages 23-25) (80-85). This force transduction results in an overall significant difference between the experimental and control animals on cellular and molecular activities in the MCC and the GF during the experiment.

The role of the MCC in the process of the TMJ's growth and development and its adaptive response to mandibular advancement is remarkably higher, particularly during the period of the present study. The rate of cellular proliferative and hypertrophic activities and morphological changes in the GF is much lower than in the MCC, even at the 3rd day of the experiment. This level of activity drops down towards the end of the study, to the extent that in a few samples no PCNA or FGF8 expression is detected in the GF. It could be inferred from this finding that during the 27-54 days of rats' age, only a little amount of bone formation and adaptive remodeling occurs in the GF.

During mandibular forward positioning, the TMJ adaptation occurs mostly in the MCC and less in the GF, because the level of cellular and molecular activity in the GF is remarkably lower than in the MCC. The level of cellular and molecular activities during the current study showed a significant decrease in the GF after the 3rd day of the experiment.

This lower amount of activity in the GF might show that the whole TMJ's adaptation occurs mainly by ossification and relocation of the MCC and relocation of the GF, as a

harmonised biologic response to mandibular protrusion. Otherwise, it is possible that the GF is not significantly relocated from its initial position, which could be a reason for future relapses of a successful functional mandibular treatment. If the GF does not remarkably remodel or relocate, then the soft tissue attachments pull the condyle back to its initial relationship with the GF. For clearer and more detailed information in this regard, these possibilities should be precisely studied and evaluated by a combination of histochemical, cephalometric and electromyographic methods for a longer period of time.

Signaling molecules of the FGF and Tgfb families regulate the endochondral ossification at several levels (89), therefore the results of the current study might be consistent with the fact that the mandibular condyle is a growth site and is ossified through endochondral ossification (71) (see pages 26-29).

However, endochondral ossification in the GF is only observed during the initial stages of rats' growth (27 days of rats age), indicated by detecting FGF8 at that age and not after that. This might indicate that osteogenesis generally slows down in the rats' GF at this age, or that the intramembranous ossification is the dominant ossification process in the GF afterward and there is no cartilage tissue in the GF during later growth and development. Intramembranous ossification in the GF is similarly reported in other studies (74).

The evidence and results suggest the endochondral ossification in the MCC and more likely intramembranous ossification in the GF take place during normal growth, development and adaptive remodeling in response to functional therapy.

On the whole, FGF8 and PCNA findings indicates that extra bone formation in response to mandibular forward positioning is due to extra molecular activity and cellular morphologic differentiations, and not due to extra cellular proliferation.

5.3. Histological Features

The chondrocytes in the early hypertrophic zone have proliferative activity in the late embryonic stage (98) and the first sign of cartilage calcification is present in this zone (17). Immunopositive cells for FGF8 molecules are detected in the cytoplasm of the chondrogenic cells in the early hypertrophic and hypertrophic zones, which is consistent with earlier research (42, 89).

The cells in the proliferative layer are in their active dividing mitotic stage and PCNA molecules are mainly localized in this layer, which is similarly observed by other observers (43-45, 47). However, some cells are positively stained for PCNA in more superficial and deeper layers as well. This could indicate that cells in the other layers have a dividing capability but a lesser amount of activity, in both the MCC and the GF (see pages 75-80).

5.3.1. Cellular changes in the Mandibular Condylar Cartilage

Even though in this study particular methods are not applied for a clear distinction between different cellular layers in the MCC, the six different layers could be determined in the MCC—as reported by other researchers—as five distinctive cellular zones plus the bone area (17, 19, 22, 89) (see pages 32, 70).

It is reported that longitudinal bone growth during endochondral bone formation depends on chondrogenesis and the increase in the cartilage matrix is closely correlated to the bone formation in response to mandibular advancement (6, 8, 125). Mesenchymal cells in the articular layer and the proliferative zone are re-oriented by physical stretching of the posterior fibers of the disc which might trigger the enhanced differentiation and maturation of the chondrocytes in the hypertrophic layer. This could indicate more chondrogenesis and therefore more endochondral ossification (126).

The results show that in the MCC the hypertrophic activities significantly increased while the proliferative activity did not differ significantly between the experimental samples and the controls. This indicates that thickening of the posterior part of the condyle as an adaptive response to the condyle's forward positioning (122) is due to cellular morphologic changes and not due to an increase in the number of cells. Other methods of investigation are required for individually counting the cells distinctively and accurately in different layers and comparing the layers with each other.

5.3.2. Cellular changes in the GF

The cellular features in the GF are similar to those in the Rabie *et al* 2001 study (12); however there is no particular method for pure cellular investigation in the present study. The fibroblasts in the superficial fibrous layer were observed as round cells during the first stage of the experiment in the 27 day-old rats. Subsequently, they were stretched, flattened and more oriented towards the direction of the mandibular forward positioning (see pages 38-43, 70 Figure 4-1).

The cellular layers are narrower in the GF and barely distinguishable in comparison with the MCC, and some layers are also different from the MCC (239) (Figure 4-1). Only six different layers are observed in 27 day-old rats and in older samples beneath the layer of proliferation, hypertrophic cells and chondrocytes do not exist and connective tissue and osteoblasts with different morphology replace the proliferative zone and the erosive zone. This could indicate the nature of intramembranous ossification in the GF, which is also reported by Wright *et al* 1974 (74).

5.4. Molecular Changes

Several growth factors regulate the chondrogenesis process which is regarded as the initial stage of condyle and GF remodeling, such as Sox9 (6), PTHrP (106), Cbfa1 (108), type X collagen (230) type II collagen (6, 7, 19), VEGF(140, 240), IGF I and II (22), FGF (17, 42).

The higher amount of FGF8 and PCNA expression in experimental samples, in comparison with control samples, generally shows an enhanced osteogenic transition occurring in both the MCC and the GF, with the exception of FGF8c and PCNA_{gf} on experiment day 30, during which the level of expression in the control animals was slightly, though not significantly, higher than in the experimentals. Further long-term studies are required to find out the reason for the lower molecular and cellular activities in the MCC and the GF.

5.4.1. FGF8

The results show that FGF8 expression is significantly affected by mandibular advancement. This indicates that the change in biophysical environment of the TMJ leads to the MCC-GF adaptation and enhances molecular activity in both the MCC and the GF (7, 19, 239, 241).

The zone of FGF8 expression is mainly located within the deep columnar proliferative layer and early hypertrophic layer. By considering the level of PCNA expression as an indicator for proliferative activity (42, 43), which did not significantly increase in this study in the experimental samples, the zone of FGF8 expression indicates that FGF8 is more involved in hypertrophic activities than in chondrocytes proliferation. FGF8 plays a role in cellular chondrogenic differentiation and creating morphologic changes from mesenchymal

cells to chondroblasts and chondroblasts to bone-making cells. This is also reported by Minina *et al*: on the molecular level, FGF signaling reduces chondrocyte proliferation and induces hypertrophic differentiation of chondrocytes (162).

Evaluating the expression of FGF8 in experimentals versus controls suggests that mandibular advancement does not change the pattern of molecular activity but just increases the level of activity. The pattern of FGF8 expression follows the pattern of the TMJ's normal growth and development, in reference to the controls, which reached the maximum level of expression on the 38th day of the rats' age in the MCC (23) and on the 27th day in the GF (Figure 4-4). This indicates endochondral ossification in the MCC and non-chondrogenic ossification in the GF (130).

The role of FGF8 in regulating the cartilage formation in the skull (193) and its involvement in cartilage and bone formation (194) and stimulating the chondrocytes (evidenced in the avian) (195) is considered in the current study. This is important because FGF8 is reported as a precise control key of localization and patterning of cartilage and endochondral bone elements in the head (42, 169, 198) (see pages 48-53).

The FGF8 pick of expression is approximately at the same level in experimentals and controls. Considering this evidence, and the fact that FGF8c is slightly higher in controls on Day 30, it is possible that stepwise advancement may generate more changes in the MCC-GF complex than one-step advancement. This is similarly suggested by other researchers (23, 130).

5.4.2. PCNA

PCNA is a marker for cell proliferation; thus, detecting PCNA in cells indicates proliferative activity (44-47, 198, 214-220). The zone of PCNA expression in the current

study is clearly immunolocalized in the proliferative layer, which is consistent with other reports on PCNA (43, 47) (see pages 53-55).

It is reported that the growth potential of the MCC and the GF is influenced by the number of replicating mesenchymal cells and this replication is increased by functional orthopedics, such as the effect of bite-jumping appliances on the the MCC in young rats (22, 148).

However, the results in the current experiment do not show a significant difference between PCNA expression in the MCC and the GF of experimentals and controls. This finding indicates that more bone formation during the MCC-GF complex adaptation is not due to more cellular proliferation. By considering this, along with the level of FGF8 expression, it can be inferred that more bone formation occurs as a result of more cellular activity, because FGF8 could be known as an indicator for cellular morphologic changes and hypertrophic activities (42, 158, 162).

Even though overall results note no significant difference in PCNA-values between the control and the experimental groups, the level of PCNA expression in the experimentals is higher than in the controls, while in the GF it is still remarkably lower than the MCC in both controls and experimentals (Table 4-4, Figure 4-6). This suggests that most of the growth, developmental procedures and adaptive responses which finally result in mandibular growth, are taking place in the condyle and much less in the GF (Table 4-2Table 4-4, Figure 4-3Figure 4-6).

5.5. Mandibular position

The bite-jumping appliance was designed to reposition the rats' mandible to a more forward position in a CI III relationship with the maxilla. But, twelve experimental rats out of

thirty experimentals end up in a CI II position. This is due to the anatomic structure of the rats' TMJ and its surrounding soft tissues, which make the condyle capable of functionally moving backward (see pages 80-84).

Overall, based on the statistical analysis, the TMJ's histochemical differences between CI II and III animals related to the level of PCNA and FGF8 expression are non-significant (Bonferroni adjusted $p = 0.61$). However, there are few exceptions. Additionally, this study aims to investigate the nature of the TMJ's biologic response to the environmental changes. Therefore, the mandibular CI II and CI III positions are not separately evaluated and discussed. For detailed statistical analysis see appendix 2.

5.6. Weight gaining

The bulk of the bite-jumping appliance and its interference with the rats' normal chewing function could be the reason for less weight gain in the experimental samples. The effect of weight as a covariate on all dependent variables of the study is non-significant; FGF8c ($p=0.431$), FGF8gf ($p=0.782$), PCNAc ($p=0.817$) and PCNAgf ($p=0.439$).

6. Conclusion

1. The results of this study indicate that structural and molecular adaptations occurred in the MCC and the GF of the experimental animals;

The results of this study indicate that structural and molecular adaptations occurred in the MCC and the GF of the experimental animals. Increased proliferation was noted in the MCC and the GF, but not significantly. However, hypertrophic differentiations were significantly increased in both parts, which could cause more bone formation during the

adaptive response. Therefore, mandibular growth modification takes place as an end result of extra cellular morphologic differentiations and hypertrophic changes in the TMJ.

2. Mandibular growth modification takes place as an end result of cellular morphologic differentiation and hypertrophic changes in both the MCC and the GF;
3. Endochondral bone formation is involved in the MCC's bone formation and more intramembranous ossification in the GF;

The level and the pattern of FGF8 expression suggests that bone formation and remodeling in the MCC is mainly achieved through an endochondral ossification process, while endochondral ossification in the GF might not be the prominent procedure in the GF's growth, development and adaptive response. Therefore, more intramembranous ossification is involved in the GF.

4. The relapse of CI II functional treatment might be due to remarkably lesser adaptation in the GF in comparison with the MCC.

Future direction

The future direction would be to design and perform studies covering longer periods of the rats' lives and comparing the condyle and the GF with other growth centres and growth sites on each sample; such as Epiphyseal plates, Synchondrosis (e.g. Spheno-occipital Synchondrosis), Maxillary sutures (e.g. Intermaxillary suture), Cranial sutures and Mandibular Symphyses at earlier stages of growth. This could be completed with cephalometric evaluations during the period of the experiment to measure the level and directions of growth and development beside the histochemical evaluations.

This wide range of evaluations and comparison within different structures could be helpful for better investigations on the correlations and possible interactions between different tissues during natural growth and development, and under the effect of different orthodontic appliances.

This information is essential for better diagnoses and treatment plans for orthodontic problems, since orthodontics, and particularly orthopedic treatments deal with growth modifications, redirections or retardations through histochemical changes. Therefore, better understanding of the relevant mechanisms at the level of histochemistry will guide practitioners to better approaches on the clinical level.

APPENDIX

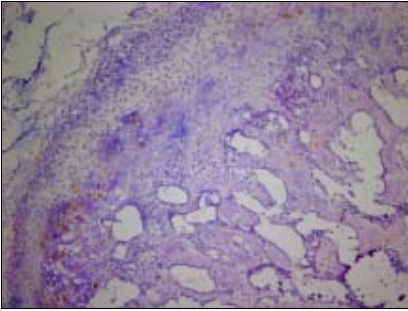
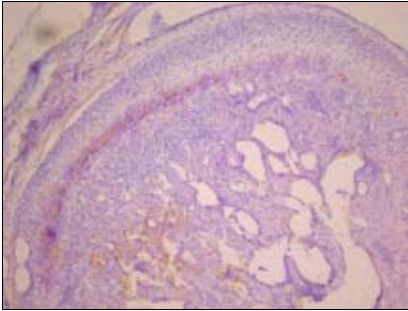
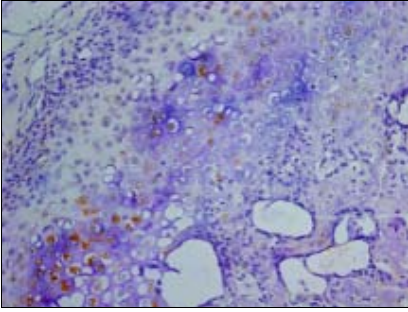
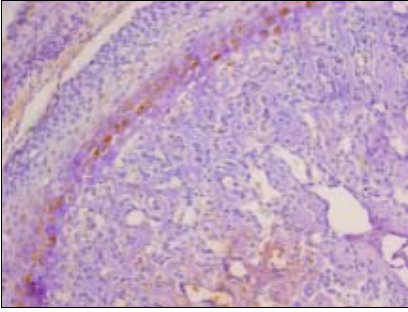
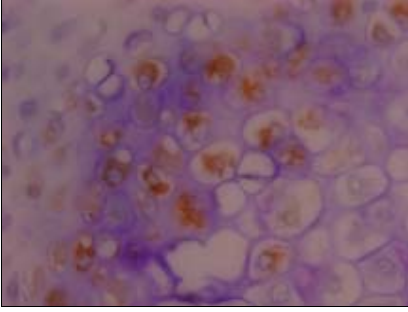
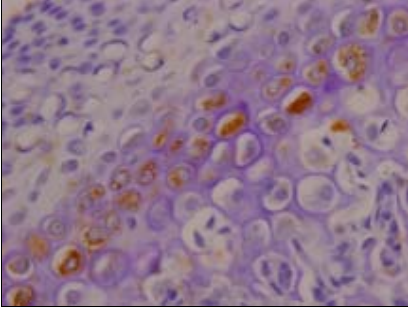
Appendices:

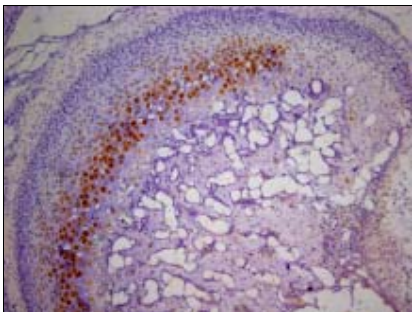
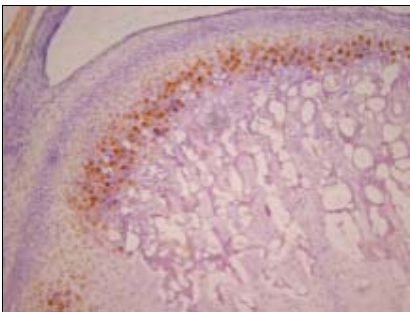
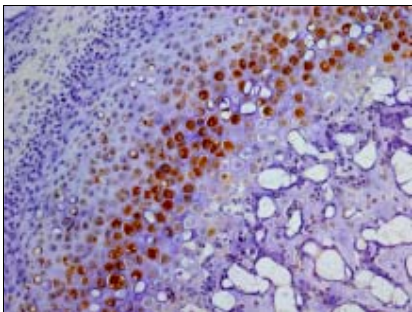
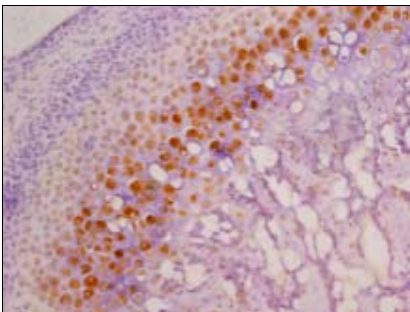
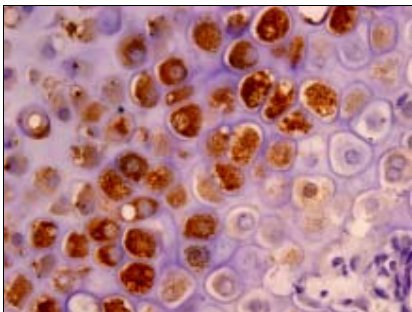
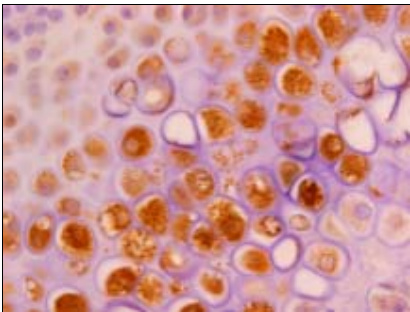
Appendix 1: Electro-microscopic images of Immunostained TMJ sections

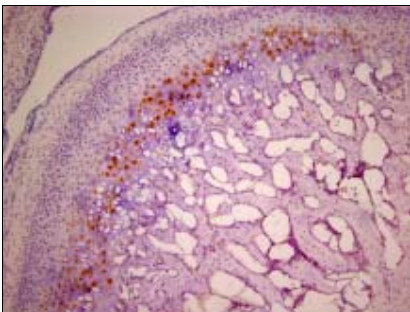
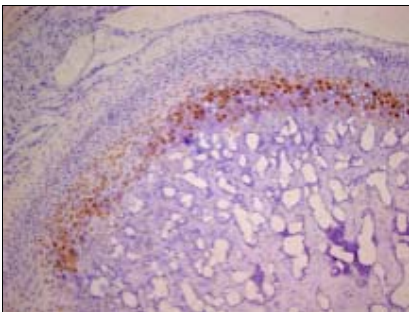
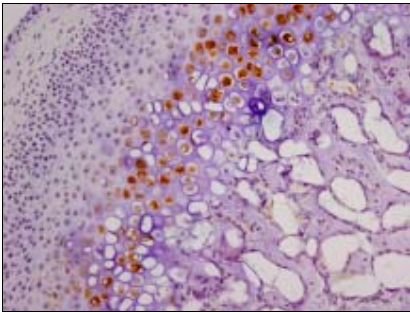
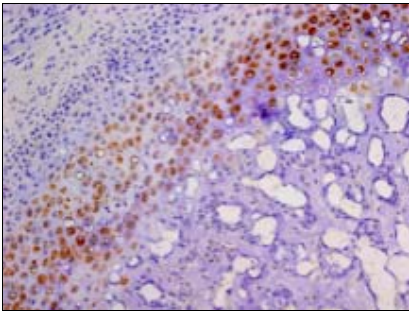
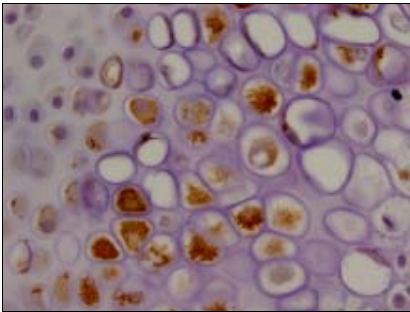
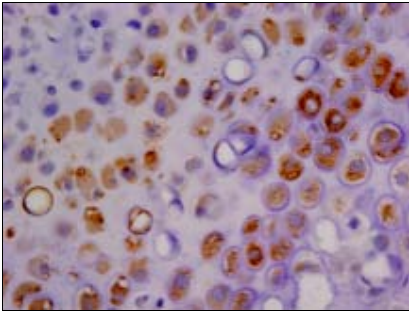
Slides are randomly collected, and different magnifications in each column of each table are related to the same section.

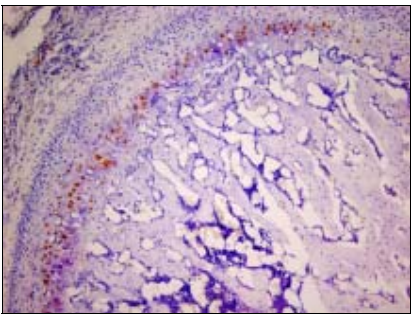
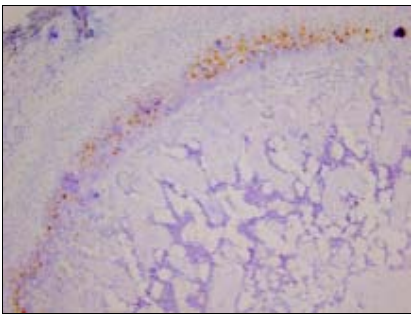
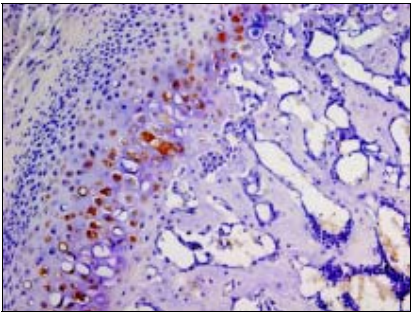
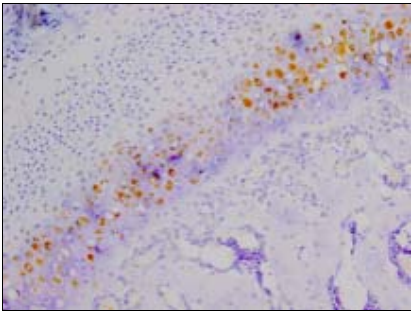
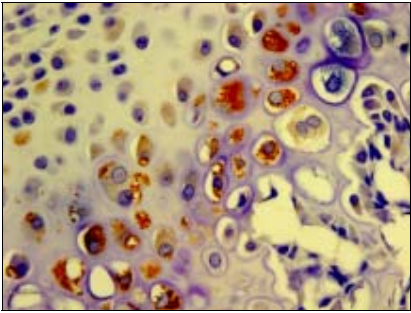
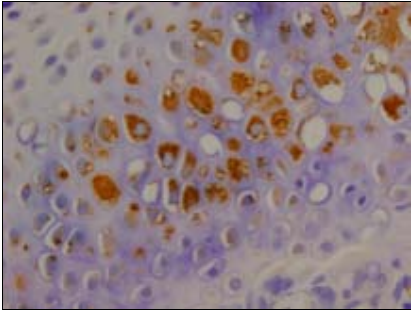
FGF8c

- Electro-microscope images from immunohistochemically stained sections for Fibroblast Growth Factor 8 in the mandibular condylar cartilage

Group 1; Day 3; 27-day old rats		
Condyle		
Magnification	FGF8 Control	FGF8 Experimental
10X		
20X		
60X		

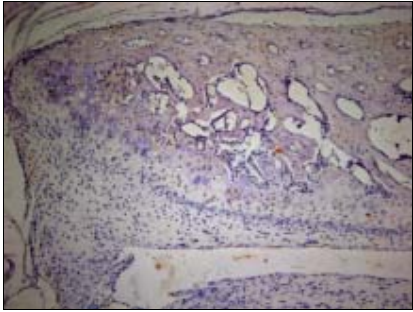
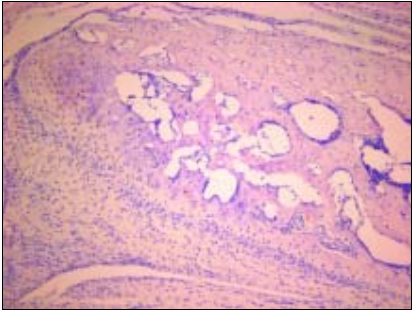
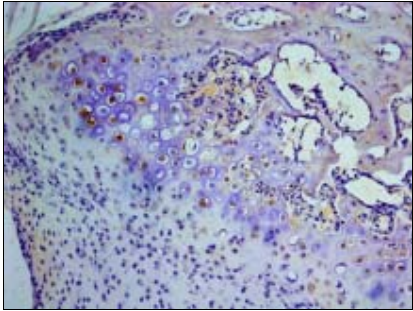
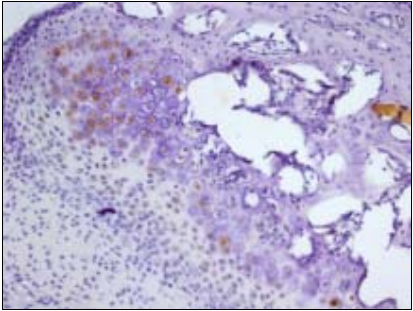
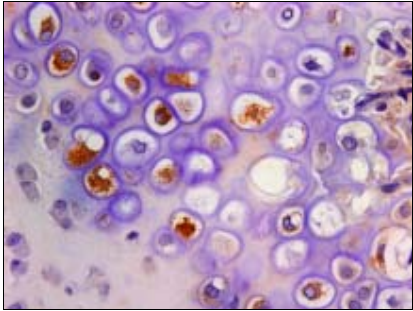
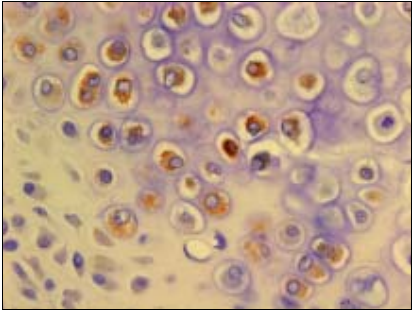
Group 2; Day 14; 35-day old rats Condyle		
Magnification	FGF8 Control	FGF8 Experimental
10X		
20X		
60X		

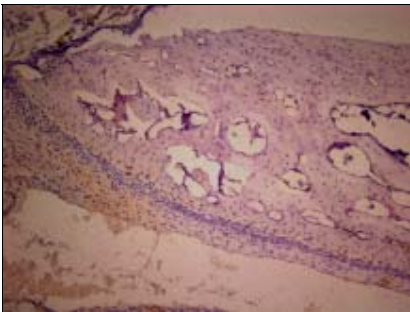
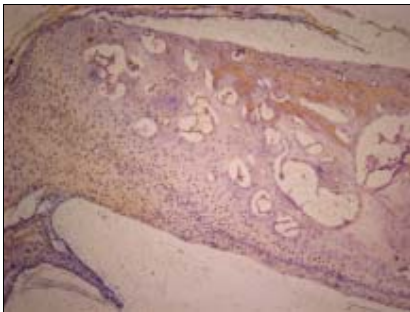
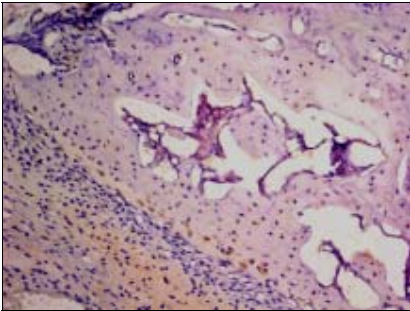
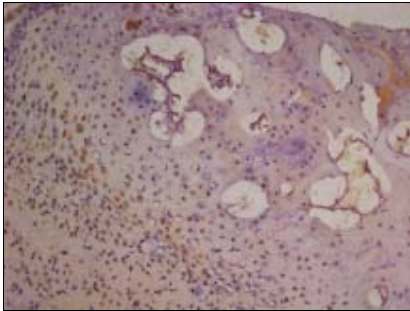
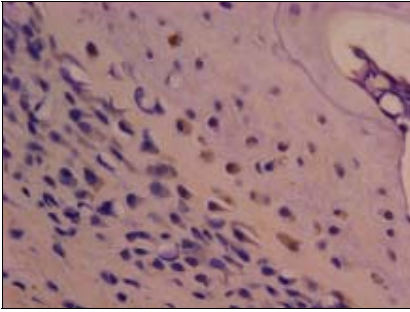
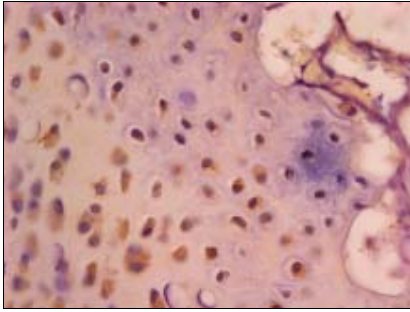
Group 3; Day 21; 45-day old rats Condyle		
Magnification	FGF8 Control	FGF8 Experimental
10X		
20X		
60X		

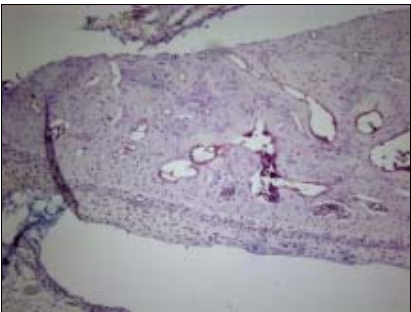
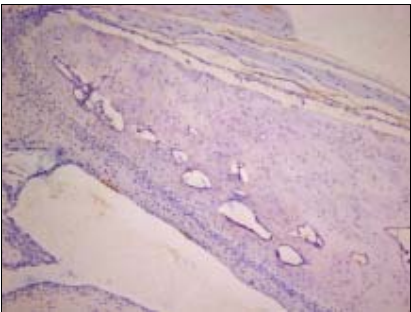
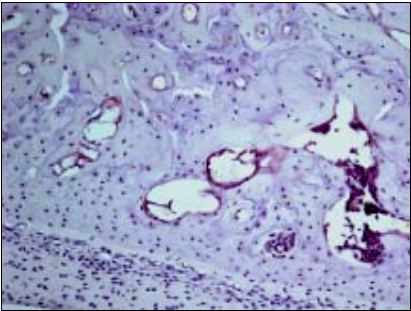
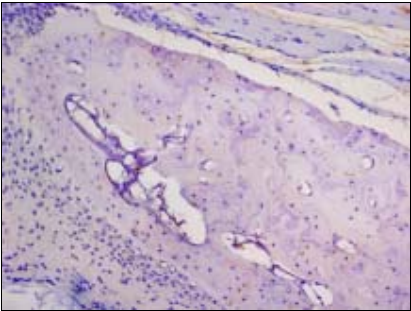
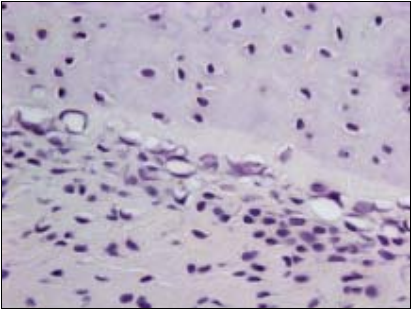
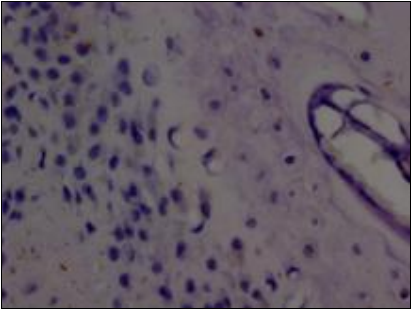
Group 4; Day 30; 53-day old rats Condyle		
Magnification	FGF8 CONTROL	FGF8 Experimental
10X		
20X		
60X		

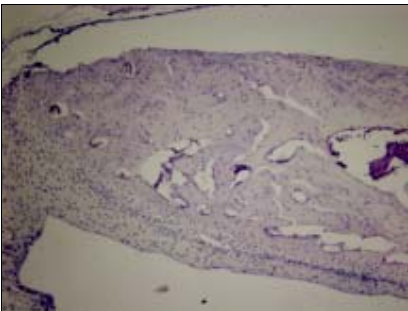
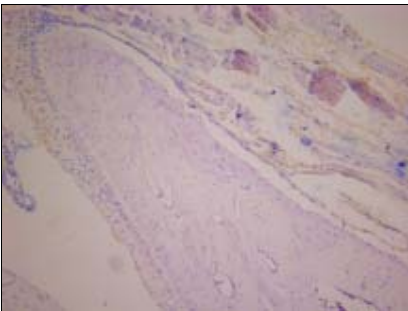
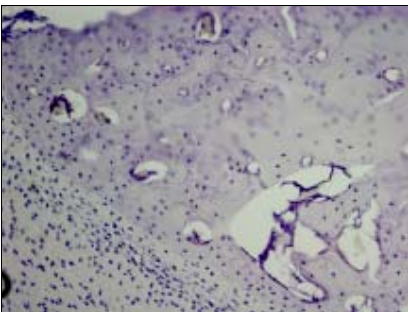
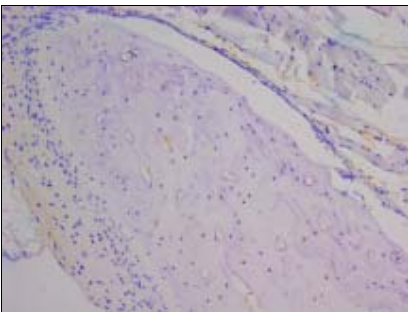
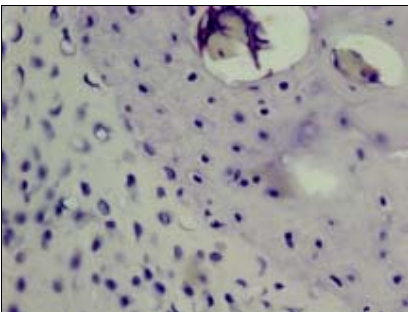
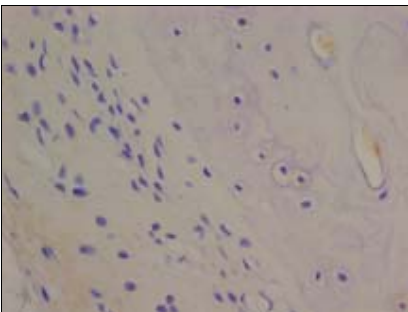
FGF8gf

- Electro-microscope images from immunohistochemically stained sections for Fibroblast Growth Factor 8 in the glenoid fossa:

Group 1; Day 3; 27-day old rats Glenoid Fossa		
Magnification	FGF8 Control	FGF8 Experimental
10X		
20X		
60X		

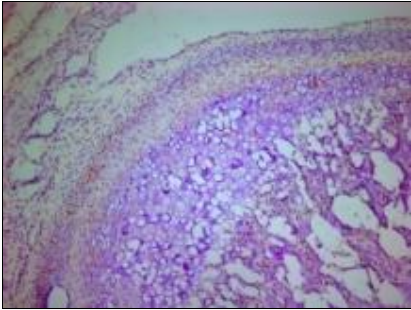
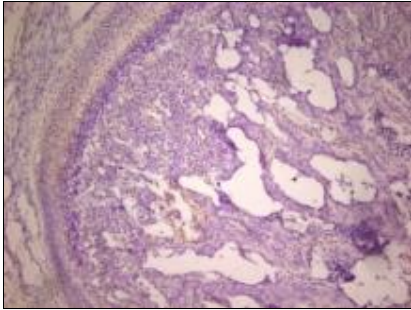
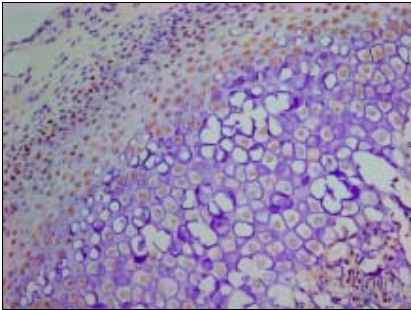
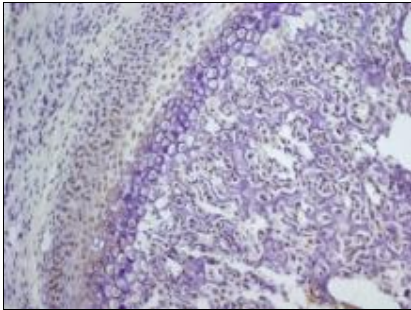
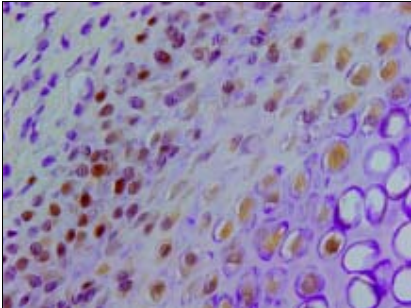
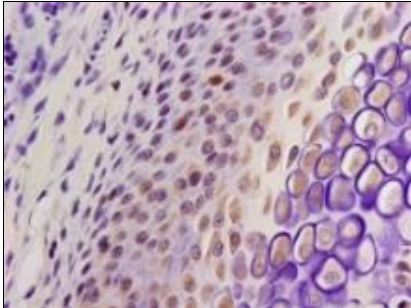
Group 2; Day 14; 38-day old rats Glenoid Fossa		
Magnification	FGF8 Control	FGF8 Experimental
10X		
20X		
60X		

Group 3; Day 21; 45-day old rats Glenoid Fossa		
Magnification	FGF8 Control	FGF8 Experimental
10X		
		
		

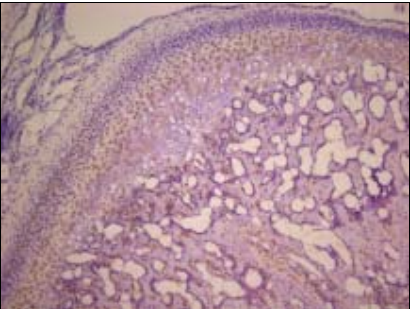
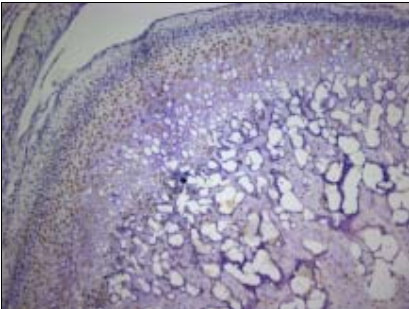
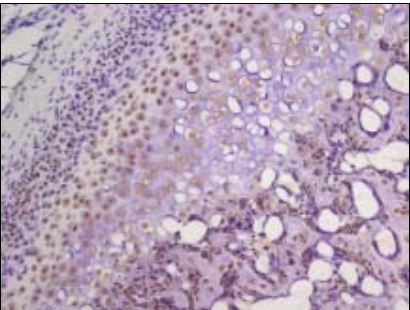
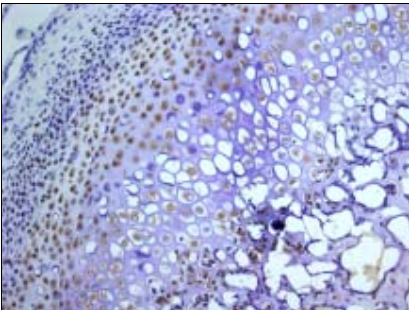
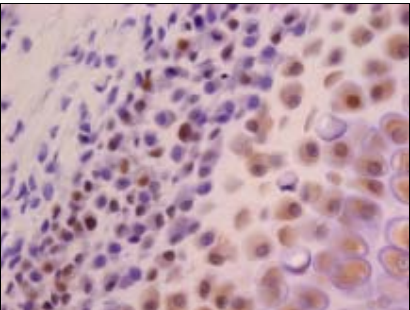
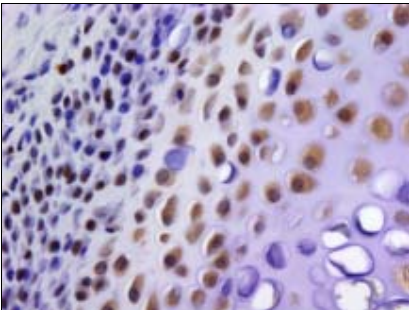
Group 4; Day 30; 53-day old rats Glenoid Fossa		
Magnification	FGF8 Control	FGF8 Experimental
10X		
20X		
60X		

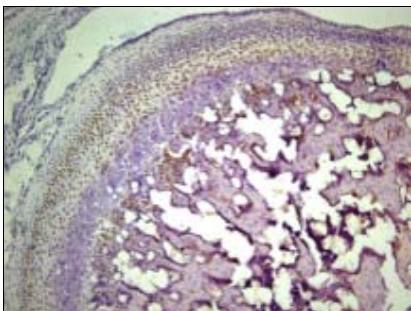
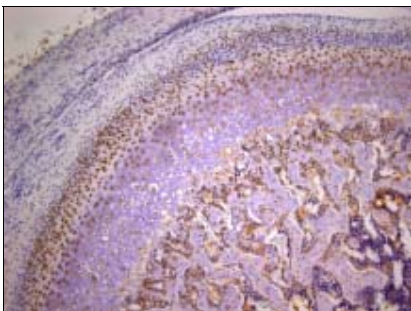
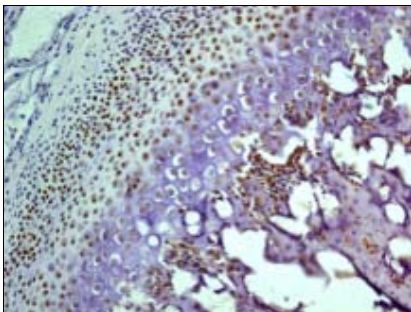
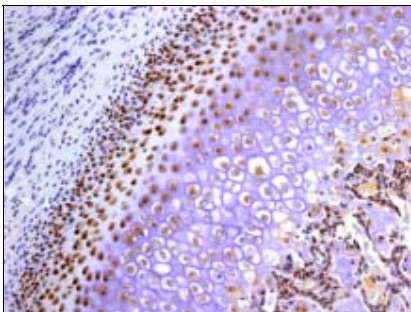
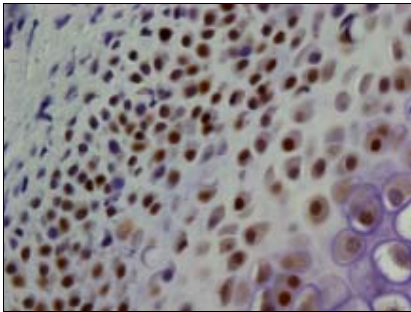
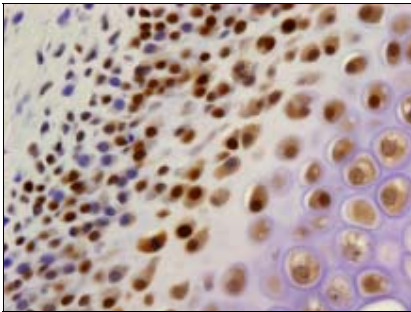
PCNAc⁶

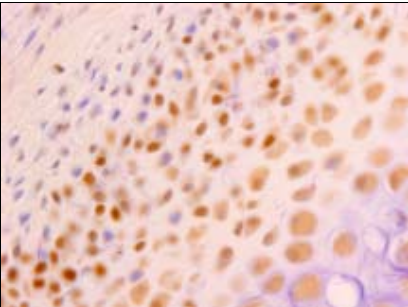
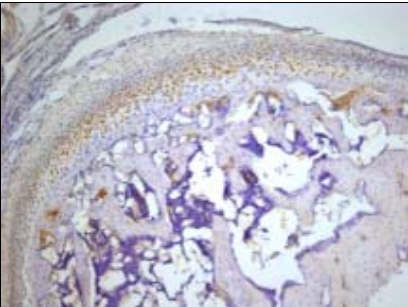
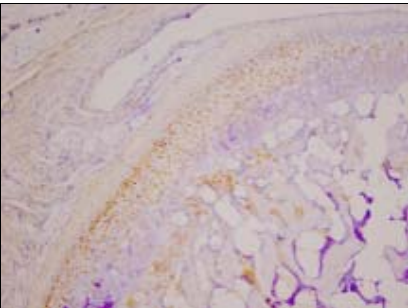
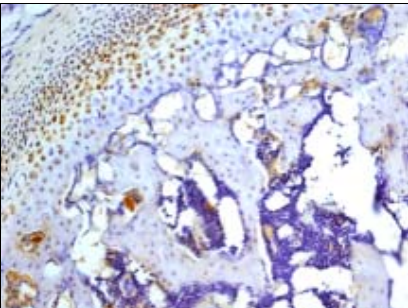
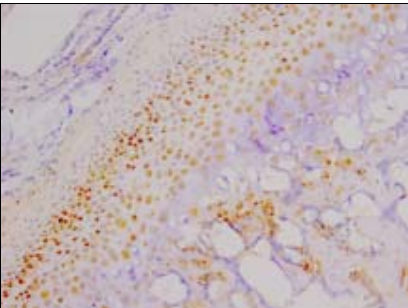
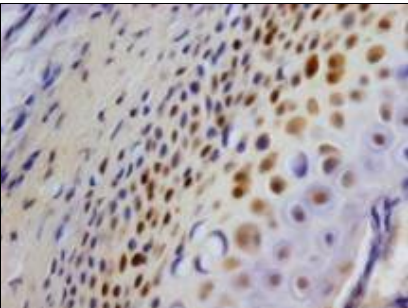
- Electro-microscope images from immunohistochemically stained sections for Proliferating Cell Nuclear Antigen in the mandibular condylar cartilage.

Group 1; Day 3; 27-day old rats Condyle		
Magnification	PCNA Control	PCNA Experimental
10X		
20X		
60X		

⁶ More details about PCNA_g are available in Dr. Zoe Potres's MPhil thesis on same project at the Department of Orthodontics, School of Dentistry, The University of Sydney, NSW- Australia 2009.

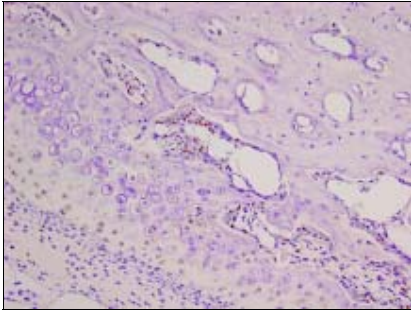
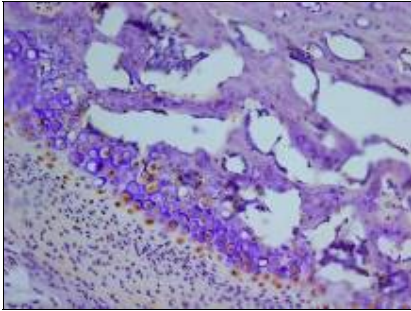
Group 2; Day 14; 38-day old rats Condyle		
Magnification	PCNA Control	PCNA Experimental
10X		
		
		

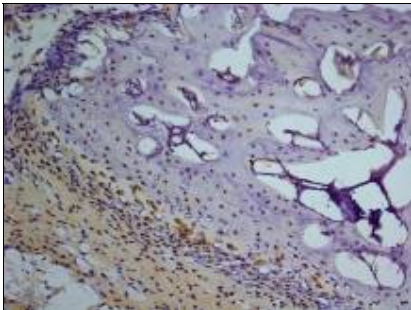
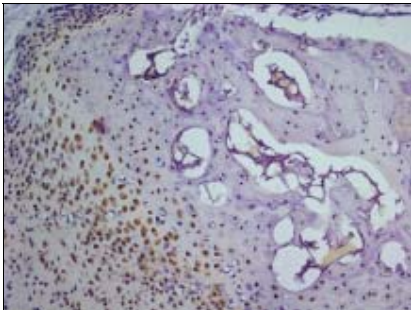
Group 3; Day 21; 45-day old rats Condyle		
Magnification	PCNA Control	PCNA Experimental
10X		
20X		
60X		

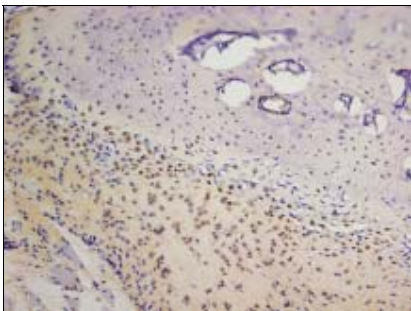
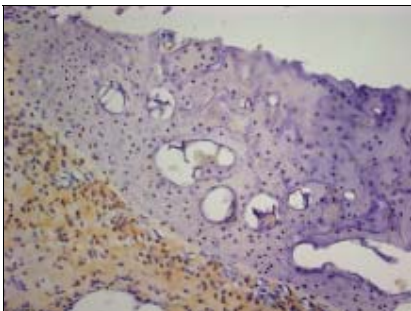
Group 4; Day 30; 53-day old rats Condyle		
Magnification	PCNA Control	PCNA Experimental
10X		
20X		
60X		

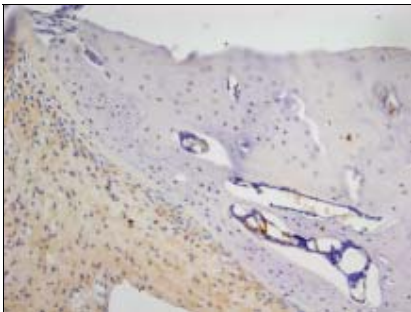
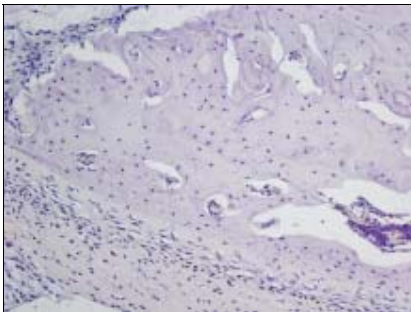
PCNA_gf

- Electro-microscope images from immunohistochemically stained sections for Proliferating Cell Nuclear Antigen in the glenoid fossa.

Group 1; Day 3; 27-day old rats Glenoid Fossa		
Magnification	PCNA Control	PCNA Experimental
20X		

Group 2; Day 14; 38-day old rats Glenoid Fossa		
Magnification	PCNA Control	PCNA Experimental
20X		

Group 3; Day 21; 45-day old rats Glenoid Fossa		
Magnification	PCNA Control	PCNA Experimental
20X		

Group 4; Day 30; 53-day old rats Glenoid Fossa		
Magnification	PCNA Control	PCNA Experimental
20X		

Appendix 2: Statistical Analysis (SPSS output)

FGF8c

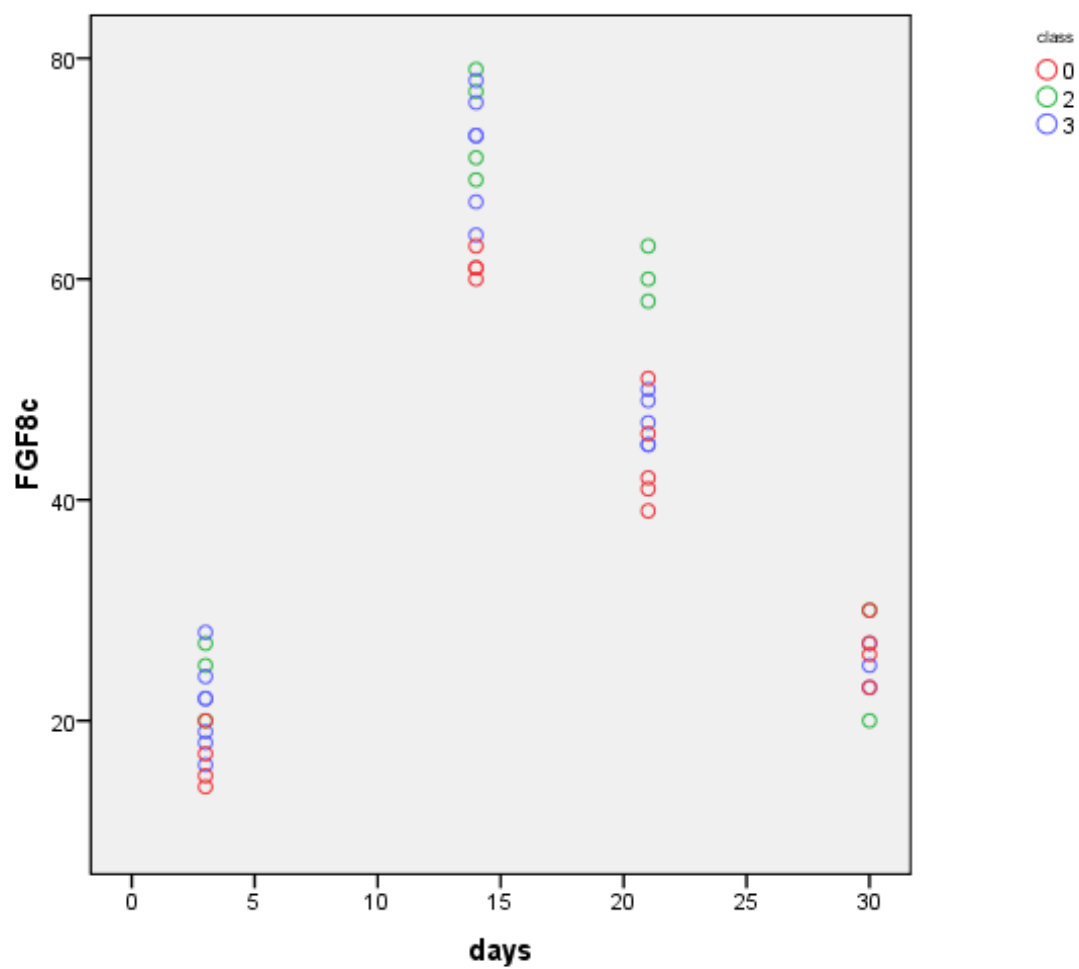
- Expression of Fibroblast Growth Factor 8 in the mandibular condylar cartilage:

Graph

Notes

Output Created	2008-11-24T14:27:43.500
Comments	
Input	Data
	D:\Documents and Settings\ppetocz\My Documents\Data\SPSSdata\Consult\Zoe1.sav
	Active Dataset
	\$DataSet
	Filter
	<none>
	Weight
	<none>
	Split File
	<none>
	N of Rows in Working Data File
	55
Syntax	GRAPH /SCATTERPLOT(BIVAR)=days WITH FGF8c BY class /MISSING=LISTWISE.
Resources	Processor Time
	0:00:00.328
	Elapsed Time
	0:00:00.219

[\$DataSet] D:\Documents and Settings\ppetocz\My Documents\Data\SPSSdata\Consult\Zoe1.sav



Univariate Analysis of Variance

Notes (class-days)

Output Created	2008-11-24T14:34:41.578	
Comments		
Input	Data	D:\Documents and Settings\ppetocz\My Documents\Data\SPSSdata\Consult\Zoe1.sav
	Active Dataset	\$DataSet
	Filter	<none>
	Weight	<none>
	Split File	<none>
	N of Rows in Working Data File	55
Missing Value Handling	Definition of Missing	User-defined missing values are treated as missing.
	Cases Used	Statistics are based on all cases with valid data for all variables in the model.
Syntax	UNIANOVA FGF8c BY days class WITH wts /METHOD=SSTYPE(3) /INTERCEPT=INCLUDE /EMMEANS=TABLES(days) WITH(wts=MEAN) COMPARE ADJ(BONFERRONI) /EMMEANS=TABLES(class) WITH(wts=MEAN) COMPARE ADJ(BONFERRONI) /EMMEANS=TABLES(class*days) WITH(wts=MEAN) /CRITERIA=ALPHA(.05) /DESIGN=days class class*days wts.	
Resources	Processor Time	0:00:00.031
	Elapsed Time	0:00:00.016

[\$DataSet] D:\Documents and Settings\ppetocz\My Documents\Data\SPSSdata\Consult\Zoe1.sav

Notes (appliance-days)

Output Created		2008-11-24T14:43:28.313
Comments		
Input	Data	D:\Documents and Settings\ppetocz\My Documents\Data\SPSSdata\Consult\Zoe1.sav
	Active Dataset	\$DataSet
	Filter	<none>
	Weight	<none>
	Split File	<none>
	N of Rows in Working Data File	55
Missing Value Handling	Definition of Missing	User-defined missing values are treated as missing.
	Cases Used	Statistics are based on all cases with valid data for all variables in the model.
Syntax		UNIANOVA FGF8c BY days appl WITH wts /METHOD=SSTYPE(3) /INTERCEPT=INCLUDE /EMMEANS=TABLES(days) WITH(wts=MEAN) /EMMEANS=TABLES(appl) WITH(wts=MEAN) /EMMEANS=TABLES(appl*days) WITH(wts=MEAN) /CRITERIA=ALPHA(.05) /DESIGN=days appl appl*days wts.
Resources	Processor Time	0:00:00.000
	Elapsed Time	0:00:00.000

[\$DataSet] D:\Documents and Settings\ppetocz\My Documents\Data\SPSSdata\Consult\Zoe1.sav

Between-Subjects Factors (class-days)

		N
Days	3	14
	14	14
	21	13
	30	9
Class	0	17
	2	12
	3	21

Tests of Between-Subjects Effects (class-days)

Dependent Variable: FGF8c

Source	Type III Sum of Squares	df	Mean Square	F	Sig.
Corrected Model	21056.756 ^a	12	1754.730	116.411	.000
Intercept	460.206	1	460.206	30.531	.000
Days	15945.871	3	5315.290	352.622	.000
Class	369.622	2	184.811	12.261	.000
days * class	405.643	6	67.607	4.485	.002
Wts	9.555	1	9.555	.634	.431
Error	557.724	37	15.074		
Total	112012.000	50			
Corrected Total	21614.480	49			

a. R Squared = .974 (Adjusted R Squared = .966)

0Between-Subjects Factors (appliance-days)

		N
days	3	14
	14	14
	21	15
	30	9
appl	0	17
	1	35

Tests of Between-Subjects Effects (appliance-days)

Dependent Variable:FGF8c

Source	Type III Sum of Squares	df	Mean Square	F	Sig.
Corrected Model	20870.182 ^a	8	2608.773	118.190	.000
Intercept	352.940	1	352.940	15.990	.000
days	13901.216	3	4633.739	209.931	.000
appl	236.500	1	236.500	10.715	.002
days * appl	205.175	3	68.392	3.098	.037
wt	.324	1	.324	.015	.904
Error	949.126	43	22.073		
Total	117452.000	52			
Corrected Total	21819.308	51			

a. R Squared = .957 (Adjusted R Squared = .948)

Estimated Marginal Means

1. Days

Estimates

Dependent Variable:FGF8c

Days	Mean	Std. Error	95% Confidence Interval	
			Lower Bound	Upper Bound
3	18.402 ^a	2.968	12.389	24.415
14	69.271 ^a	1.100	67.042	71.500
21	51.329 ^a	1.569	48.150	54.508
30	27.176 ^a	2.499	22.113	32.238

a. Covariates appearing in the model are evaluated at the following values: wt = 147.660.

Pairwise Comparisons

Dependent Variable:FGF8c

(I) days (J) days	Mean Difference (I-J)	Std. Error	Sig. ^a	95% Confidence Interval for Difference ^a	
				Lower Bound	Upper Bound
3 14	-50.869*	3.421	.000	-60.404	-41.334
3 21	-32.927*	4.170	.000	-44.551	-21.303
3 30	-8.774	5.162	.585	-23.163	5.616
14 3	50.869*	3.421	.000	41.334	60.404
14 21	17.942*	1.730	.000	13.120	22.765
14 30	42.095*	2.483	.000	35.173	49.018
21 3	32.927*	4.170	.000	21.303	44.551
21 14	-17.942*	1.730	.000	-22.765	-13.120
21 30	24.153*	2.008	.000	18.557	29.750
30 3	8.774	5.162	.585	-5.616	23.163
30 14	-42.095*	2.483	.000	-49.018	-35.173
30 21	-24.153*	2.008	.000	-29.750	-18.557

Based on estimated marginal means

*. The mean difference is significant at the .05 level

a. Adjustment for multiple comparisons: Bonferroni.

Univariate Tests

Dependent Variable:FGF8c

	Sum of Squares	df	Mean Square	F	Sig.
Contrast	15945.871	3	5315.290	352.622	.000
Error	557.724	37	15.074		

The F tests the effect of days. This test is based on the linearly independent pairwise comparisons among the estimated marginal means.

2. Class

Estimates

Dependent Variable:FGF8c

class	Mean	Std. Error	95% Confidence Interval	
			Lower Bound	Upper Bound
0	37.643 ^a	1.234	35.143	40.144
2	45.833 ^a	1.155	43.492	48.173
3	41.157 ^a	.917	39.298	43.015

a. Covariates appearing in the model are evaluated at the following values: wts = 147.660.

Pairwise Comparisons

Dependent Variable:FGF8c

(I) class	(J) class	Mean Difference (I-J)	Std. Error	Sig. ^a	95% Confidence Interval for Difference ^a	
					Lower Bound	Upper Bound
0	2	-8.189 [*]	1.691	.000	-12.429	-3.949
	3	-3.513	1.646	.118	-7.640	.613
2	0	8.189 [*]	1.691	.000	3.949	12.429
	3	4.676 [*]	1.475	.009	.977	8.375
3	0	3.513	1.646	.118	-.613	7.640
	2	-4.676 [*]	1.475	.009	-8.375	-.977

Based on estimated marginal means

*. The mean difference is significant at the .05 level.

a. Adjustment for multiple comparisons: Bonferroni.

Univariate Tests

Dependent Variable:FGF8c

	Sum of Squares	df	Mean Square	F	Sig.
Contrast	369.622	2	184.811	12.261	.000
Error	557.724	37	15.074		

The F tests the effect of class. This test is based on the linearly independent pairwise comparisons among the estimated marginal means.

3. Class * days

Dependent Variable:FGF8c

class	days	Mean	Std. Error	95% Confidence Interval	
				Lower Bound	Upper Bound
0	3	14.720 ^a	2.961	8.721	20.719
	14	61.761 ^a	2.044	57.618	65.903
	21	45.022 ^a	2.317	40.327	49.717
	30	29.071 ^a	3.768	21.437	36.705
2	3	21.545 ^a	3.812	13.821	29.269
	14	74.027 ^a	1.942	70.093	77.961
	21	61.224 ^a	2.505	56.148	66.299
	30	26.535 ^a	3.355	19.738	33.332
3	3	18.940 ^a	3.291	12.272	25.609
	14	72.025 ^a	1.603	68.777	75.274
	21	47.740 ^a	1.864	43.963	51.518
	30	25.921 ^a	2.522	20.810	31.032

a. Covariates appearing in the model are evaluated at the following values: wts = 147.660.

4. Appl

Dependent Variable:FGF8c

appl	Mean	Std. Error	95% Confidence Interval	
			Lower Bound	Upper Bound
0	37.121 ^a	1.451	34.194	40.047
1	42.952 ^a	.852	41.233	44.671

a. Covariates appearing in the model are evaluated at the following values: wts = 148.077.

5. Appl * days

Dependent Variable:FGF8c

appl	days	Mean	Std. Error	95% Confidence Interval	
				Lower Bound	Upper Bound
0	3	16.182 ^a	3.521	9.081	23.283
	14	61.337 ^a	2.456	56.384	66.290
	21	44.012 ^a	2.737	38.494	49.531
	30	26.951 ^a	4.400	18.078	35.823
1	3	21.676 ^a	3.798	14.017	29.336
	14	72.719 ^a	1.494	69.706	75.732
	21	52.209 ^a	1.738	48.705	55.713
	30	25.203 ^a	2.686	19.786	30.619

a. Covariates appearing in the model are evaluated at the following values: wts = 148.077.

FGF8gf

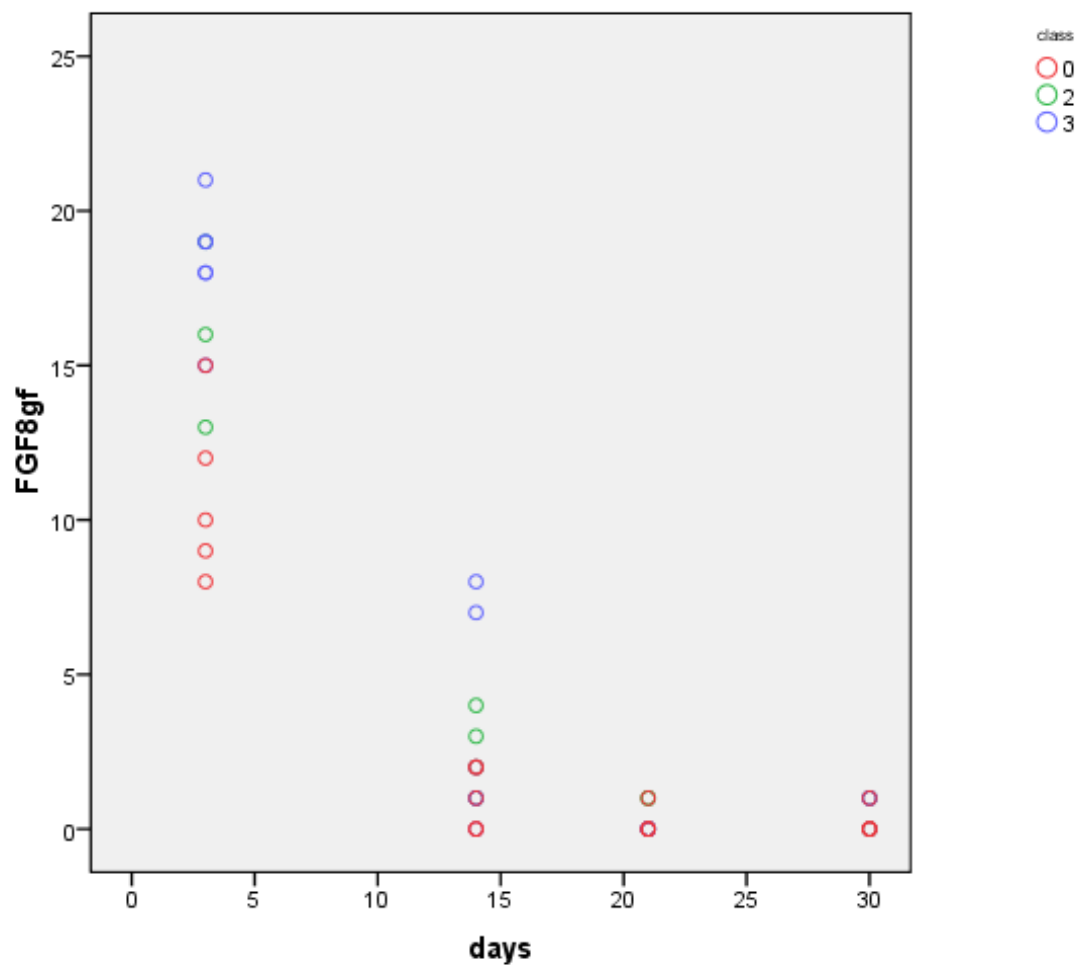
- Expression of Fibroblast Growth Factor 8 in the glenoid fossa:

Graph

Notes

Output Created	2008-11-24T14:28:06.969
Comments	
Input Data	D:\Documents and Settings\ppetocz\My Documents\Data\SPSSdata\Consult\Zoe1.sav
Active Dataset	\$DataSet
Filter	<none>
Weight	<none>
Split File	<none>
N of Rows in Working Data File	55
Syntax	GRAPH /SCATTERPLOT(BIVAR)=days WITH FGF8gf BY class /MISSING=LISTWISE.
Resources Processor Time	0:00:00.344
Elapsed Time	0:00:00.234

[\$DataSet] D:\Documents and Settings\ppetocz\My Documents\Data\SPSSdata\Consult\Zoe1.sav



Univariate Analysis of Variance

Notes (class-days)

Output Created		2008-11-24T14:35:24.219
Comments		
Input	Data	D:\Documents and Settings\ppetocz\My Documents\Data\SPSSdata\Consult\Zoe1.sav
	Active Dataset	\$DataSet
	Filter	<none>
	Weight	<none>
	Split File	<none>
	N of Rows in Working Data File	55
Missing Value Handling	Definition of Missing	User-defined missing values are treated as missing.
	Cases Used	Statistics are based on all cases with valid data for all variables in the model.
Syntax		UNIANOVA FGF8gf BY days class WITH wts /METHOD=SSTYPE(3) /INTERCEPT=INCLUDE /EMMEANS=TABLES(days) WITH(wts=MEAN) COMPARE ADJ(BONFERRONI) /EMMEANS=TABLES(class) WITH(wts=MEAN) COMPARE ADJ(BONFERRONI) /EMMEANS=TABLES(class*days) WITH(wts=MEAN) /CRITERIA=ALPHA(.05) /DESIGN=days class class*days wts.
Resources	Processor Time	0:00:00.031
	Elapsed Time	0:00:00.015

[\$DataSet] D:\Documents and Settings\ppetocz\My Documents\Data\SPSSdata\Consult\Zoe1.sav

Notes (appliance-days)

Output Created		2008-11-24T14:43:45.063
Comments		
Input	Data	D:\Documents and Settings\ppetocz\My Documents\Data\SPSSdata\Consult\Zoe1.sav
	Active Dataset	\$DataSet
	Filter	<none>
	Weight	<none>
	Split File	<none>
	N of Rows in Working Data File	55
Missing Value Handling	Definition of Missing	User-defined missing values are treated as missing.
	Cases Used	Statistics are based on all cases with valid data for all variables in the model.
Syntax		UNIANOVA FGF8gf BY days appl WITH wts /METHOD=SSTYPE(3) /INTERCEPT=INCLUDE /EMMEANS=TABLES(days) WITH(wts=MEAN) /EMMEANS=TABLES(appl) WITH(wts=MEAN) /EMMEANS=TABLES(appl*days) WITH(wts=MEAN) /CRITERIA=ALPHA(.05) /DESIGN=days appl appl*days wts.
Resources	Processor Time	0:00:00.031
	Elapsed Time	0:00:00.015

[\$DataSet] D:\Documents and Settings\ppetocz\My Documents\Data\SPSSdata\Consult\Zoe1.sav

Between-Subjects Factors (class-days)

		N
days	3	14
	14	15
	21	11
	30	9
class	0	18
	2	12
	3	19

Tests of Between-Subjects Effects (class-days)

Dependent Variable:FGF8gf

Source	Type III Sum of Squares	df	Mean Square	F	Sig.
Corrected Model	2155.694 ^a	12	179.641	46.526	.000
Intercept	6.387	1	6.387	1.654	.207
days	260.586	3	86.862	22.497	.000
class	32.819	2	16.409	4.250	.022
days * class	90.509	6	15.085	3.907	.004
wt	.300	1	.300	.078	.782
Error	139.000	36	3.861		
Total	3601.000	49			
Corrected Total	2294.694	48			

a. R Squared = .939 (Adjusted R Squared = .919)

Between-Subjects Factors (appliance-days)

		N
days	3	14
	14	15
	21	13
	30	9
appl	0	18
	1	33

Tests of Between-Subjects Effects (appliance-days)

Dependent Variable:FGF8gf

Source	Type III Sum of Squares	df	Mean Square	F	Sig.
Corrected Model	2184.363 ^a	8	273.045	75.142	.000
Intercept	3.899	1	3.899	1.073	.306
days	279.925	3	93.308	25.678	.000
appl	37.768	1	37.768	10.394	.002
wt	.005	1	.005	.001	.970
days * appl	83.884	3	27.961	7.695	.000
Error	152.617	42	3.634		
Total	3602.000	51			
Corrected Total	2336.980	50			

a. R Squared = .935 (Adjusted R Squared = .922)

Estimated Marginal Means

1. days

Estimates

Dependent Variable:FGF8gf

Days	Mean	Std. Error	95% Confidence Interval	
			Lower Bound	Upper Bound
3	14.655 ^a	1.501	11.610	17.700
14	2.263 ^a	.535	1.178	3.348
21	.471 ^a	.842	-1.236	2.177
30	.774 ^a	1.281	-1.823	3.372

a. Covariates appearing in the model are evaluated at the following values: wt = 147.388.

Pairwise Comparisons

Dependent Variable:FGF8gf

(I) days (J) days	Mean Difference (I-J)	Std. Error	Sig. ^a	95% Confidence Interval for Difference ^a	
				Lower Bound	Upper Bound
3 14	12.392*	1.718	.000	7.595	17.188
3 21	14.184*	2.149	.000	8.185	20.184
3 30	13.881*	2.632	.000	6.533	21.228
14 3	-12.392*	1.718	.000	-17.188	-7.595
14 21	1.793	.906	.333	-.736	4.321
14 30	1.489	1.268	1.000	-2.051	5.029
21 3	-14.184*	2.149	.000	-20.184	-8.185
21 14	-1.793	.906	.333	-4.321	.736
21 30	-.304	1.032	1.000	-3.184	2.577
30 3	-13.881*	2.632	.000	-21.228	-6.533
30 14	-1.489	1.268	1.000	-5.029	2.051
30 21	.304	1.032	1.000	-2.577	3.184

Based on estimated marginal means

*. The mean difference is significant at the .05 level.

a. Adjustment for multiple comparisons: Bonferroni.

Univariate Tests

Dependent Variable:FGF8gf

	Sum of Squares	df	Mean Square	F	Sig.
Contrast	260.586	3	86.862	22.497	.000
Error	139.000	36	3.861		

The F tests the effect of days. This test is based on the linearly independent pairwise comparisons among the estimated marginal means.

2. class

Estimates

Dependent Variable:FGF8gf

class	Mean	Std. Error	95% Confidence Interval	
			Lower Bound	Upper Bound
0	3.184 ^a	.608	1.950	4.418
2	4.919 ^a	.585	3.733	6.105
3	5.520 ^a	.477	4.552	6.487

a. Covariates appearing in the model are evaluated at the following values: wts = 147.388.

Pairwise Comparisons

Dependent Variable:FGF8gf

(I) class (J) class	Mean Difference (I-J)	Std. Error	Sig. ^a	95% Confidence Interval for Difference ^a	
				Lower Bound	Upper Bound
0 2	-1.735	.840	.139	-3.845	.375
0 3	-2.336 [*]	.812	.020	-4.375	-.296
2 0	1.735	.840	.139	-.375	3.845
2 3	-.601	.755	1.000	-2.498	1.296
3 0	2.336 [*]	.812	.020	.296	4.375
3 2	.601	.755	1.000	-1.296	2.498

Based on estimated marginal means

a. Adjustment for multiple comparisons: Bonferroni.

*. The mean difference is significant at the .05 level.

Univariate Tests

Dependent Variable:FGF8gf

	Sum of Squares	Df	Mean Square	F	Sig.
Contrast	32.819	2	16.409	4.250	.022
Error	139.000	36	3.861		

The F tests the effect of class. This test is based on the linearly independent pairwise comparisons among the estimated marginal means.

3. class * days

Dependent Variable:FGF8gf

class	days	Mean	Std. Error	95% Confidence Interval	
				Lower Bound	Upper Bound
0	3	10.469 ^a	1.478	7.471	13.466
	14	1.079 ^a	.924	-.794	2.952
	21	.475 ^a	1.273	-2.106	3.057
	30	.712 ^a	1.928	-3.199	4.623
2	3	15.563 ^a	1.936	11.636	19.489
	14	2.507 ^a	.983	.514	4.500
	21	.828 ^a	1.274	-1.756	3.412
	30	.777 ^a	1.708	-2.688	4.242
3	3	17.933 ^a	1.645	14.598	21.269
	14	3.203 ^a	.813	1.555	4.852
	21	.108 ^a	1.056	-2.034	2.250
	30	.834 ^a	1.283	-1.769	3.436

a. Covariates appearing in the model are evaluated at the following values: wts = 147.388.

4. appl

Dependent Variable:FGF8gf

appl	Mean	Std. Error	95% Confidence Interval	
			Lower Bound	Upper Bound
0	3.088 ^a	.573	1.933	4.244
1	5.345 ^a	.349	4.641	6.050

a. Covariates appearing in the model are evaluated at the following values: wts = 147.824.

5. appl * days

Dependent Variable:FGF8gf

appl	days	Mean	Std. Error	95% Confidence Interval	
				Lower Bound	Upper Bound
0	3	10.758 ^a	1.405	7.923	13.592
	14	1.010 ^a	.889	-.785	2.804
	21	.278 ^a	1.207	-2.157	2.713
	30	.308 ^a	1.803	-3.330	3.945
1	3	17.503 ^a	1.526	14.424	20.583
	14	2.903 ^a	.607	1.678	4.128
	21	.348 ^a	.749	-1.162	1.859
	30	.626 ^a	1.098	-1.590	2.842

a. Covariates appearing in the model are evaluated at the following values: wts = 147.824.

PCNAc

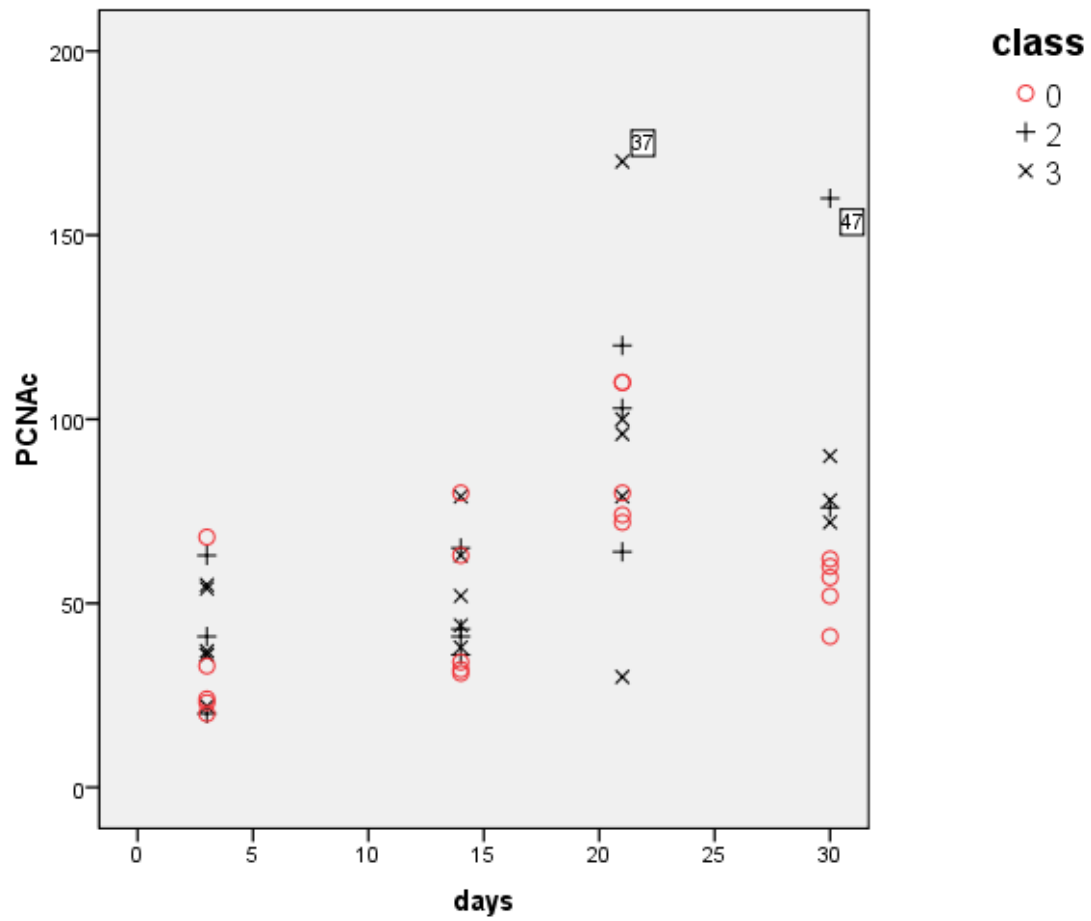
- PCNA expression in the mandibular condylar cartilage:

Graph

Notes (PCNAc by class)

Output Created	2008-11-24T14:19:02.328
Comments	
Input Data	D:\Documents and Settings\ppetocz\My Documents\Data\SPSSdata\Consult\Zoe1.sav
Active Dataset	\$DataSet
Filter	<none>
Weight	<none>
Split File	<none>
N of Rows in Working Data File	55
Syntax	GRAPH /SCATTERPLOT(BIVAR)=days WITH PCNAc BY class /MISSING=LISTWISE.
Resources Processor Time	0:00:00.297
Elapsed Time	0:00:00.297

[\$DataSet] D:\Documents and Settings\ppetocz\My Documents\Data\SPSSdata\Consult\Zoe1.sav



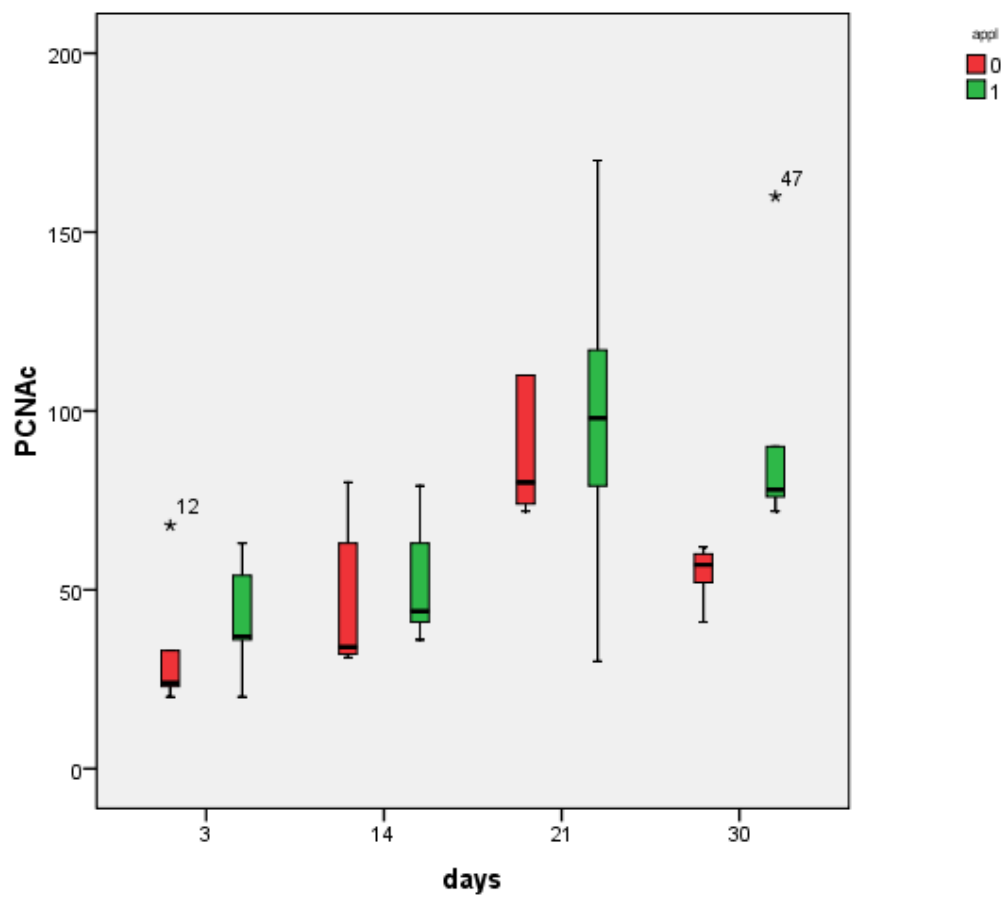
Explore

Notes (PCNAc by days by appliance)

Output Created	2008-09-23T13:35:58.570	
Comments		
Input	Data	D:\Documents and Settings\ppetocz\My Documents\Data\SPSSdata\Consult\Zoe1.sav
	Active Dataset	DataSet1
	Filter	<none>
	Weight	<none>
	Split File	<none>
	N of Rows in Working Data File	55
Missing Value Handling	Definition of Missing Cases Used	User-defined missing values for dependent variables are treated as missing. Statistics are based on cases with no missing values for any dependent variable or factor used.
Syntax	EXAMINE VARIABLES=PCNAc BY days BY appl /PLOT=BOXPLOT /STATISTICS=NONE /NOTOTAL.	
Resources	Processor Time	0:00:00.219
	Elapsed Time	0:00:00.219

[DataSet1] D:\Documents and Settings\ppetocz\My Documents\Data\SPSSdata\Consult\Zoe1.sav

Days*appl
PCNAc

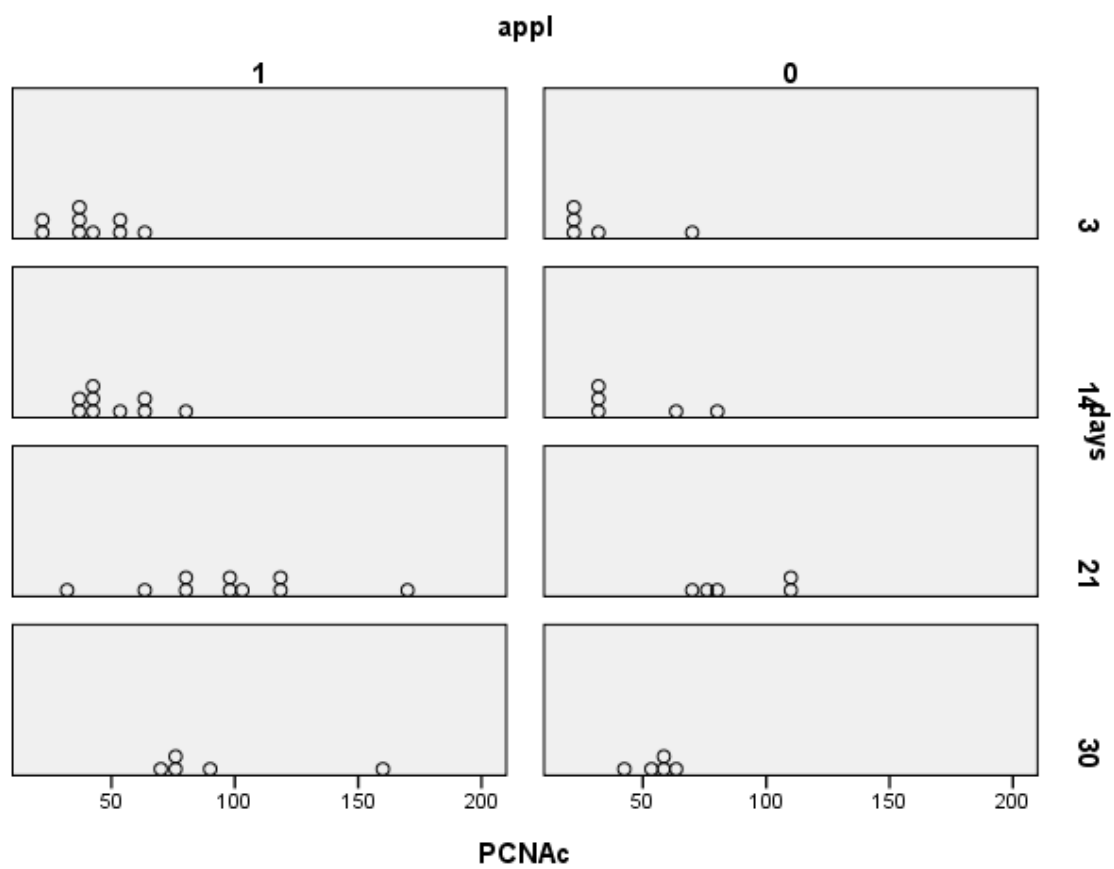


XGraph

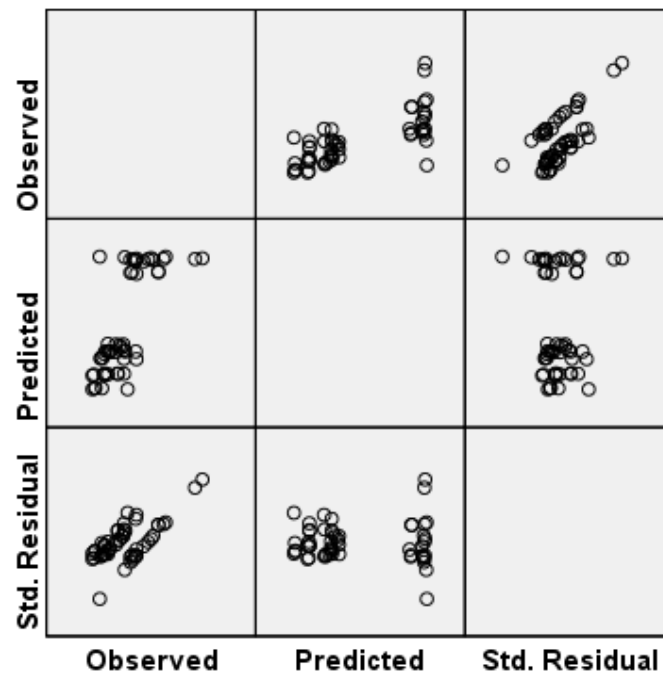
Notes (PCNAc by days by appliance)

Output Created	2008-09-23T13:36:52.913	
Comments		
Input	Data	D:\Documents and Settings\ppetocz\My Documents\Data\SPSSdata\Consult\Zoe1.sav
	Active Dataset	DataSet1
	Filter	<none>
	Weight	<none>
	Split File	<none>
	N of Rows in Working Data File	55
Syntax	XGRAPH CHART=[POINT] BY PCNAc[s] /DISPLAY DOT=ASYMMETRIC /PANEL COLVAR=appl COLOP=CROSS ROWVAR=days ROWOP=CROSS.	
Resources	Processor Time	0:00:00.172
	Elapsed Time	0:00:00.156

[DataSet1] D:\Documents and Settings\ppetocz\My Documents\Data\SPSSdata\Consult\Zoe1.sav



Dependent Variable: PCNAc



Model: Intercept + days + appl + days * appl + wts

Univariate Analysis of Variance

Notes (class-days)

Output Created	2008-11-24T14:29:29.484	
Comments		
Input	Data	D:\Documents and Settings\ppetocz\My Documents\Data\SPSSdata\Consult\Zoe1.sav
	Active Dataset	\$DataSet
	Filter	<none>
	Weight	<none>
	Split File	<none>
	N of Rows in Working Data File	55
Missing Value Handling	Definition of Missing	User-defined missing values are treated as missing.
	Cases Used	Statistics are based on all cases with valid data for all variables in the model.
Syntax	UNIANOVA PCNAc BY days class WITH wts /METHOD=SSTYPE(3) /INTERCEPT=INCLUDE /EMMEANS=TABLES(days) WITH(wts=MEAN) COMPARE ADJ(BONFERRONI) /EMMEANS=TABLES(class) WITH(wts=MEAN) COMPARE ADJ(BONFERRONI) /EMMEANS=TABLES(class*days) WITH(wts=MEAN) /CRITERIA=ALPHA(.05) /DESIGN=days class class*days wts.	
Resources	Processor Time	0:00:00.015
	Elapsed Time	0:00:00.032

[\$DataSet] D:\Documents and Settings\ppetocz\My Documents\Data\SPSSdata\Consult\Zoe1.sav

Notes (appliance-days)

Output Created		2008-11-24T14:41:51.266
Comments		
Input	Data	D:\Documents and Settings\ppetocz\My Documents\Data\SPSSdata\Consult\Zoe1.sav
	Active Dataset	\$DataSet
	Filter	<none>
	Weight	<none>
	Split File	<none>
	N of Rows in Working Data File	55
Missing Value Handling	Definition of Missing	User-defined missing values are treated as missing.
	Cases Used	Statistics are based on all cases with valid data for all variables in the model.
Syntax		UNIANOVA PCNAc BY days appl WITH wts /METHOD=SSTYPE(3) /INTERCEPT=INCLUDE /EMMEANS=TABLES(days) WITH(wts=MEAN) /EMMEANS=TABLES(appl) WITH(wts=MEAN) /EMMEANS=TABLES(appl*days) WITH(wts=MEAN) /CRITERIA=ALPHA(.05) /DESIGN=days appl appl*days wts.
Resources	Processor Time	0:00:00.031
	Elapsed Time	0:00:00.015

[\$DataSet] D:\Documents and Settings\ppetocz\My Documents\Data\SPSSdata\Consult\Zoe1.sav

Between-Subjects Factors (class-days)

		N
days	3	14
	14	14
	21	13
	30	10
class	0	20
	2	12
	3	19

Tests of Between-Subjects Effects (class-days)

Dependent Variable: PCNAc

Source	Type III Sum of Squares	df	Mean Square	F	Sig.
Corrected Model	30519.090 ^a	12	2543.257	4.022	.000
Intercept	1251.399	1	1251.399	1.979	.168
days	10177.782	3	3392.594	5.365	.004
class	1776.271	2	888.135	1.405	.258
days * class	3990.721	6	665.120	1.052	.408
wt	34.467	1	34.467	.055	.817
Error	24027.616	38	632.306		
Total	253953.000	51			
Corrected Total	54546.706	50			

a. R Squared = .560 (Adjusted R Squared = .420)

Between-Subjects Factors (appliance-days)

		N
days	3	14
	14	14
	21	15
	30	10
appl	0	20
	1	33

Tests of Between-Subjects Effects (appliance-days)

Dependent Variable: PCNAc

Source	Type III Sum of Squares	df	Mean Square	F	Sig.
Corrected Model	31053.936 ^a	8	3881.742	6.405	.000
Intercept	665.863	1	665.863	1.099	.300
wt	11.293	1	11.293	.019	.892
days	10434.587	3	3478.196	5.739	.002
appl	1752.509	1	1752.509	2.892	.096
days * appl	2152.748	3	717.583	1.184	.327
Error	26667.385	44	606.077		
Total	274042.000	53			
Corrected Total	57721.321	52			

a. R Squared = .538 (Adjusted R Squared = .454)

Estimated Marginal Means

1. days

Estimates

Dependent Variable: PCNAc

days	Mean	Std. Error	95% Confidence Interval	
			Lower Bound	Upper Bound
3	34.011 ^a	19.706	-5.882	73.905
14	50.114 ^a	6.877	36.193	64.035
21	94.805 ^a	9.678	75.212	114.397
30	87.231 ^a	15.768	55.311	119.151

a. Covariates appearing in the model are evaluated at the following values: wt = 149.471.

Pairwise Comparisons

Dependent Variable:PCNAc

(I) days (J) days	Mean Difference (I-J)	Std. Error	Sig. ^a	95% Confidence Interval for Difference ^a	
				Lower Bound	Upper Bound
3 14	-16.103	21.967	1.000	-77.247	45.041
21	-60.793	26.854	.176	-135.540	13.954
30	-53.220	33.551	.726	-146.607	40.168
14 3	16.103	21.967	1.000	-45.041	77.247
21	-44.691*	11.154	.002	-75.738	-13.643
30	-37.117	16.190	.165	-82.182	7.948
21 3	60.793	26.854	.176	-13.954	135.540
14	44.691*	11.154	.002	13.643	75.738
30	7.574	13.039	1.000	-28.721	43.869
30 3	53.220	33.551	.726	-40.168	146.607
14	37.117	16.190	.165	-7.948	82.182
21	-7.574	13.039	1.000	-43.869	28.721

Based on estimated marginal means

a. Adjustment for multiple comparisons: Bonferroni.

*. The mean difference is significant at the .05 level.

Univariate Tests

Dependent Variable:PCNAc

	Sum of Squares	df	Mean Square	F	Sig.
Contrast	10177.782	3	3392.594	5.365	.004
Error	24027.616	38	632.306		

The F tests the effect of days. This test is based on the linearly independent pairwise comparisons among the estimated marginal means.

2. class**Estimates**

Dependent Variable:PCNAc

class	Mean	Std. Error	95% Confidence Interval	
			Lower Bound	Upper Bound
0	57.322 ^a	7.126	42.897	71.747
2	75.154 ^a	7.513	59.944	90.363
3	67.145 ^a	6.211	54.572	79.718

a. Covariates appearing in the model are evaluated at the following values: wts = 149.471.

Pairwise Comparisons

Dependent Variable:PCNAc

(I) class (J) class		Mean Difference (I-J)	Std. Error	Sig. ^a	95% Confidence Interval for Difference ^a	
					Lower Bound	Upper Bound
0	2	-17.832	10.639	.306	-44.478	8.815
	3	-9.823	10.224	1.000	-35.430	15.784
2	0	17.832	10.639	.306	-8.815	44.478
	3	8.008	9.626	1.000	-16.101	32.118
3	0	9.823	10.224	1.000	-15.784	35.430
	2	-8.008	9.626	1.000	-32.118	16.101

Based on estimated marginal means

a. Adjustment for multiple comparisons: Bonferroni.

Univariate Tests

Dependent Variable:PCNAc

	Sum of Squares	df	Mean Square	F	Sig.
Contrast	1776.271	2	888.135	1.405	.258
Error	24027.616	38	632.306		

The F tests the effect of class. This test is based on the linearly independent pairwise comparisons among the estimated marginal means.

3. class * days

Dependent Variable:PCNAc

class	days	Mean	Std. Error	95% Confidence Interval	
				Lower Bound	Upper Bound
0	3	29.917 ^a	19.373	-9.302	69.135
	14	48.656 ^a	11.591	25.191	72.121
	21	91.355 ^a	14.548	61.905	120.805
	30	59.360 ^a	24.038	10.698	108.023
2	3	36.529 ^a	25.183	-14.451	87.509
	14	46.144 ^a	12.581	20.675	71.613
	21	97.194 ^a	15.924	64.958	129.430
	30	1.207E2	21.321	77.584	163.910
3	3	35.588 ^a	21.506	-7.948	79.124
	14	55.542 ^a	11.341	32.584	78.500
	21	95.865 ^a	11.840	71.896	119.835
	30	81.585 ^a	16.027	49.139	114.031

a. Covariates appearing in the model are evaluated at the following values: wts = 149.471.

4. appl

Dependent Variable:PCNAc

appl	Mean	Std. Error	95% Confidence Interval	
			Lower Bound	Upper Bound
0	55.758 ^a	6.787	42.080	69.436
1	70.886 ^a	4.669	61.476	80.295

a. Covariates appearing in the model are evaluated at the following values: wts = 149.811.

5. appl * days

Dependent Variable:PCNAc

appl	days	Mean	Std. Error	95% Confidence Interval	
				Lower Bound	Upper Bound
0	3	35.628 ^a	18.489	-1.634	72.889
	14	47.658 ^a	11.291	24.902	70.414
	21	88.040 ^a	13.910	60.006	116.073
	30	51.707 ^a	22.590	6.181	97.234
1	3	42.941 ^a	20.049	2.536	83.347
	14	51.160 ^a	8.219	34.597	67.724
	21	95.344 ^a	8.787	77.635	113.052
	30	94.097 ^a	13.658	66.570	121.623

a. Covariates appearing in the model are evaluated at the following values: wts = 149.811.

NPar Tests**Notes**

Output Created		2008-09-23T13:47:05.413	
Comments			
Input	Data	D:\Documents and Settings\ppetocz\My Documents\Data\SPSSdata\Consult\Zoe1.sav	
	Active Dataset	DataSet1	
	Filter	days=3 (FILTER)	
	Weight	<none>	
	Split File	<none>	
	N of Rows in Working Data File	15	
Missing Value Handling	Definition of Missing	User-defined missing values are treated as missing.	
	Cases Used	Statistics for each test are based on all cases with valid data for the variable(s) used in that test.	
Syntax	NPAR TESTS /M-W= PCNAc BY appl(0 1) /MISSING ANALYSIS.		
Resources	Processor Time	0:00:00.000	
	Elapsed Time	0:00:00.016	
	Number of Cases Allowed ^a	112347	

a. Based on availability of workspace memory.

[DataSet1] D:\Documents and Settings\ppetocz\My Documents\Data\SPSSdata\Consult\Zoe1.sav

Mann-Whitney Test day 3**Ranks**

	appl	N	Mean Rank	Sum of Ranks
PCNAc	0	5	6.10	30.50
	1	9	8.28	74.50
	Total	14		

Test Statistics^b

	PCNAc
Mann-Whitney U	15.500
Wilcoxon W	30.500
Z	-.935
Asymp. Sig. (2-tailed)	.350
Exact Sig. [2*(1-tailed Sig.)]	.364 ^a

a. Not corrected for ties.

b. Grouping Variable: appl

NPar Tests**Notes**

Output Created	2008-09-23T13:47:34.273	
Comments		
Input	Data	D:\Documents and Settings\ppetocz\My Documents\Data\SPSSdata\Consult\Zoe1.sav
	Active Dataset	DataSet1
	Filter	days=14 (FILTER)
	Weight	<none>
	Split File	<none>
	N of Rows in Working Data File	15
Missing Value Handling	Definition of Missing	User-defined missing values are treated as missing.
	Cases Used	Statistics for each test are based on all cases with valid data for the variable(s) used in that test.
Syntax	NPAR TESTS /M-W= PCNAc BY appl(0 1) /MISSING ANALYSIS.	
Resources	Processor Time	0:00:00.031
	Elapsed Time	0:00:00.015
	Number of Cases Allowed ^a	112347

a. Based on availability of workspace memory.

[DataSet1] D:\Documents and Settings\ppetocz\My Documents\Data\SPSSdata\Consult\Zoe1.sav

Mann-Whitney Test day 14**Ranks**

appl		N	Mean Rank	Sum of Ranks
PCNAc	0	5	6.10	30.50
	1	9	8.28	74.50
	Total	14		

Test Statistics^b

	PCNAc
Mann-Whitney U	15.500
Wilcoxon W	30.500
Z	-.934
Asymp. Sig. (2-tailed)	.350
Exact Sig. [2*(1-tailed Sig.)]	.364 ^a

a. Not corrected for ties.

b. Grouping Variable: appl

NPar Tests**Notes**

Output Created		2008-09-23T13:48:10.038	
Comments			
Input	Data	D:\Documents and Settings\ppetocz\My Documents\Data\SPSSdata\Consult\Zoe1.sav	
	Active Dataset	DataSet1	
	Filter	days=21 (FILTER)	
	Weight	<none>	
	Split File	<none>	
	N of Rows in Working Data File	15	
Missing Value Handling	Definition of Missing	User-defined missing values are treated as missing.	
	Cases Used	Statistics for each test are based on all cases with valid data for the variable(s) used in that test.	
Syntax	NPAR TESTS /M-W= PCNAc BY appl(0 1) /MISSING ANALYSIS.		
Resources	Processor Time	0:00:00.000	
	Elapsed Time	0:00:00.000	
	Number of Cases Allowed ^a	112347	

a. Based on availability of workspace memory.

[DataSet1] D:\Documents and Settings\ppetocz\My Documents\Data\SPSSdata\Consult\Zoe1.sav

Mann-Whitney Test day 21**Ranks**

	appl	N	Mean Rank	Sum of Ranks
PCNAc	0	5	7.30	36.50
	1	10	8.35	83.50
	Total	15		

Test Statistics^b

	PCNAc
Mann-Whitney U	21.500
Wilcoxon W	36.500
Z	-.429
Asymp. Sig. (2-tailed)	.668
Exact Sig. [2*(1-tailed Sig.)]	.679 ^a

a. Not corrected for ties.

b. Grouping Variable: appl

NPar Tests**Notes**

Output Created	2008-09-23T13:48:30.179	
Comments		
Input	Data	D:\Documents and Settings\ppetocz\My Documents\Data\SPSSdata\Consult\Zoe1.sav
	Active Dataset	DataSet1
	Filter	days=30 (FILTER)
	Weight	<none>
	Split File	<none>
	N of Rows in Working Data File	10
Missing Value Handling	Definition of Missing	User-defined missing values are treated as missing.
	Cases Used	Statistics for each test are based on all cases with valid data for the variable(s) used in that test.
Syntax	NPAR TESTS /M-W= PCNAc BY appl(0 1) /MISSING ANALYSIS.	
Resources	Processor Time	0:00:00.016
	Elapsed Time	0:00:00.015
	Number of Cases Allowed ^a	112347

a. Based on availability of workspace memory.

[DataSet1] D:\Documents and Settings\ppetocz\My Documents\Data\SPSSdata\Consult\Zoe1.sav

Mann-Whitney Test day 30**Ranks**

appl	N	Mean Rank	Sum of Ranks
PCNAc 0	5	3.00	15.00
1	5	8.00	40.00
Total	10		

Test Statistics^b

	PCNAc
Mann-Whitney U	.000
Wilcoxon W	15.000
Z	-2.611
Asymp. Sig. (2-tailed)	.009
Exact Sig. [2*(1-tailed Sig.)]	.008 ^a

a. Not corrected for ties.

b. Grouping Variable: appl

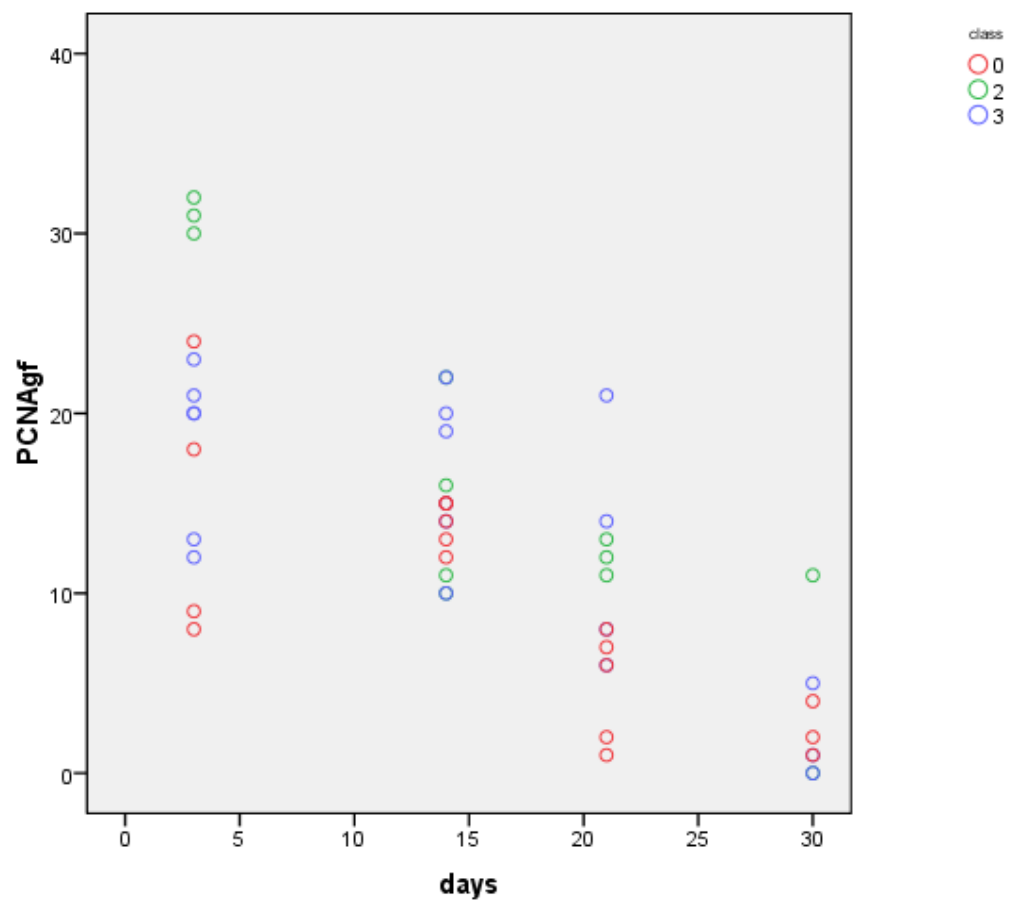
PCNAgf

- PCNA expression in the glenoid fossa:

Graph**Notes**

Output Created	2008-11-24T14:26:13.125
Comments	
Input Data	D:\Documents and Settings\ppetocz\My Documents\Data\SPSSdata\Consult\Zoe1.sav
Active Dataset	\$DataSet
Filter	<none>
Weight	<none>
Split File	<none>
N of Rows in Working Data File	55
Syntax	GRAPH /SCATTERPLOT(BIVAR)=days WITH PCNAgf BY class /MISSING=LISTWISE.
Resources Processor Time	0:00:00.250
Elapsed Time	0:00:00.234

[\$DataSet] D:\Documents and Settings\ppetocz\My Documents\Data\SPSSdata\Consult\Zoe1.sav



Univariate Analysis of Variance

Notes (class-days)

Output Created	2008-11-24T14:31:35.547	
Comments		
Input	Data	D:\Documents and Settings\ppetocz\My Documents\Data\SPSSdata\Consult\Zoe1.sav
	Active Dataset	\$DataSet
	Filter	<none>
	Weight	<none>
	Split File	<none>
	N of Rows in Working Data File	55
Missing Value Handling	Definition of Missing	User-defined missing values are treated as missing.
	Cases Used	Statistics are based on all cases with valid data for all variables in the model.
Syntax	UNIANOVA PCNAgf BY days class WITH wts /METHOD=SSTYPE(3) /INTERCEPT=INCLUDE /EMMEANS=TABLES(days) WITH(wts=MEAN) COMPARE ADJ(BONFERRONI) /EMMEANS=TABLES(class) WITH(wts=MEAN) COMPARE ADJ(BONFERRONI) /EMMEANS=TABLES(class*days) WITH(wts=MEAN) /CRITERIA=ALPHA(.05) /DESIGN=days class class*days wts.	
Resources	Processor Time	0:00:00.032
	Elapsed Time	0:00:00.015

[\$DataSet] D:\Documents and Settings\ppetocz\My Documents\Data\SPSSdata\Consult\Zoe1.sav

Notes (appliance-days)

Output Created		2008-11-24T14:42:19.578
Comments		
Input	Data	D:\Documents and Settings\ppetocz\My Documents\Data\SPSSdata\Consult\Zoe1.sav
	Active Dataset	\$DataSet
	Filter	<none>
	Weight	<none>
	Split File	<none>
	N of Rows in Working Data File	55
Missing Value Handling	Definition of Missing	User-defined missing values are treated as missing.
	Cases Used	Statistics are based on all cases with valid data for all variables in the model.
Syntax		UNIANOVA PCNAgf BY days appl WITH wts /METHOD=SSTYPE(3) /INTERCEPT=INCLUDE /EMMEANS=TABLES(days) WITH(wts=MEAN) /EMMEANS=TABLES(appl) WITH(wts=MEAN) /EMMEANS=TABLES(appl*days) WITH(wts=MEAN) /CRITERIA=ALPHA(.05) /DESIGN=days appl appl*days wts.
Resources	Processor Time	0:00:00.032
	Elapsed Time	0:00:00.016

[\$DataSet] D:\Documents and Settings\ppetocz\My Documents\Data\SPSSdata\Consult\Zoe1.sav

Between-Subjects Factors (class-days)

		N
Days	3	13
	14	15
	21	12
	30	8
Class	0	17
	2	12
	3	19

Tests of Between-Subjects Effects (class-days)

Dependent Variable: PCNAgf

Source	Type III Sum of Squares	df	Mean Square	F	Sig.
Corrected Model	2411.362 ^a	12	200.947	9.761	.000
Intercept	66.785	1	66.785	3.244	.080
days	224.572	3	74.857	3.636	.022
class	198.530	2	99.265	4.822	.014
days * class	373.161	6	62.194	3.021	.017
wt	12.629	1	12.629	.613	.439
Error	720.555	35	20.587		
Total	11192.000	48			
Corrected Total	3131.917	47			

a. R Squared = .770 (Adjusted R Squared = .691)

Between-Subjects Factors (appliance-days)

		N
Days	3	13
	14	15
	21	14
	30	8
Appl	0	17
	1	33

Tests of Between-Subjects Effects (appliance-days)

Dependent Variable: PCNAgf

Source	Type III Sum of Squares	df	Mean Square	F	Sig.
Corrected Model	2058.550 ^a	8	257.319	9.719	.000
Intercept	45.694	1	45.694	1.726	.196
days	286.055	3	95.352	3.602	.021
appl	79.750	1	79.750	3.012	.090
days * appl	94.082	3	31.361	1.185	.327
wt	5.425	1	5.425	.205	.653
Error	1085.470	41	26.475		
Total	11413.000	50			
Corrected Total	3144.020	49			

a. R Squared = .655 (Adjusted R Squared = .587)

Estimated Marginal Means

1. days

Estimates

Dependent Variable: PCNAgf

days	Mean	Std. Error	95% Confidence Interval	
			Lower Bound	Upper Bound
3	18.260 ^a	4.103	9.930	26.590
14	15.412 ^a	1.264	12.845	17.978
21	10.826 ^a	1.980	6.806	14.846
30	5.772 ^a	3.579	-1.494	13.038

a. Covariates appearing in the model are evaluated at the following values: wt = 146.958.

Pairwise Comparisons

Dependent Variable: PCNAgf

(I) days (J) days	Mean Difference (I-J)	Std. Error	Sig. ^a	95% Confidence Interval for Difference ^a	
				Lower Bound	Upper Bound
3 14	2.848	4.670	1.000	-10.211	15.907
21	7.434	5.666	1.000	-8.412	23.280
30	12.488	7.377	.596	-8.142	33.117
14 3	-2.848	4.670	1.000	-15.907	10.211
21	4.586	2.063	.197	-1.183	10.354
30	9.640*	3.413	.047	.095	19.185
21 3	-7.434	5.666	1.000	-23.280	8.412
14	-4.586	2.063	.197	-10.354	1.183
30	5.054	2.727	.434	-2.573	12.681
30 3	-12.488	7.377	.596	-33.117	8.142
14	-9.640*	3.413	.047	-19.185	-.095
21	-5.054	2.727	.434	-12.681	2.573

Based on estimated marginal means

a. Adjustment for multiple comparisons: Bonferroni.

*. The mean difference is significant at the .05 level.

Univariate Tests

Dependent Variable: PCNAgf

	Sum of Squares	Df	Mean Square	F	Sig.
Contrast	224.572	3	74.857	3.636	.022
Error	720.555	35	20.587		

The F tests the effect of days. This test is based on the linearly independent pairwise comparisons among the estimated marginal means

2. class

Estimates

Dependent Variable: PCNAgf

class	Mean	Std. Error	95% Confidence Interval	
			Lower Bound	Upper Bound
0	9.878 ^a	1.661	6.506	13.250
2	15.856 ^a	1.351	13.113	18.599
3	11.969 ^a	1.153	9.629	14.308

a. Covariates appearing in the model are evaluated at the following values: wts = 146.958.

Pairwise Comparisons

Dependent Variable: PCNAgf

(I) class	(J) class	Mean Difference (I-J)	Std. Error	Sig. ^a	95% Confidence Interval for Difference ^a	
					Lower Bound	Upper Bound
0	2	-5.978 [*]	2.109	.023	-11.282	-.673
	3	-2.091	2.243	1.000	-7.730	3.549
2	0	5.978 [*]	2.109	.023	.673	11.282
	3	3.887	1.788	.110	-.609	8.383
3	0	2.091	2.243	1.000	-3.549	7.730
	2	-3.887	1.788	.110	-8.383	.609

Based on estimated marginal means

*. The mean difference is significant at the .05 level.

a. Adjustment for multiple comparisons: Bonferroni.

Univariate Tests

Dependent Variable: PCNAgf

	Sum of Squares	df	Mean Square	F	Sig.
Contrast	198.530	2	99.265	4.822	.014
Error	720.555	35	20.587		

The F tests the effect of class. This test is based on the linearly independent pairwise comparisons among the estimated marginal means.

3. **class * days**Dependent Variable: PCNA_{gf}

class	days	Mean	Std. Error	95% Confidence Interval	
				Lower Bound	Upper Bound
0	3	12.193 ^a	3.976	4.122	20.264
	14	14.431 ^a	2.183	9.999	18.863
	21	6.511 ^a	2.982	.458	12.564
	30	6.377 ^a	5.789	-5.376	18.130
2	3	27.694 ^a	4.967	17.610	37.779
	14	14.831 ^a	2.271	10.221	19.442
	21	13.259 ^a	3.073	7.019	19.498
	30	7.638 ^a	4.213	-.914	16.191
3	3	14.892 ^a	4.572	5.610	24.175
	14	16.973 ^a	1.893	13.130	20.816
	21	12.708 ^a	2.343	7.952	17.464
	30	3.301 ^a	3.102	-2.996	9.598

a. Covariates appearing in the model are evaluated at the following values: wts = 146.958.

4. **appl**

Dependent Variable: PCNA_{gf}

appl	Mean	Std. Error	95% Confidence Interval	
			Lower Bound	Upper Bound
0	9.484 ^a	1.782	5.885	13.084
1	13.265 ^a	.964	11.317	15.212

a. Covariates appearing in the model are evaluated at the following values: wts = 147.420.

5. **appl * days**

Dependent Variable: PCNA_{gf}

appl	days	Mean	Std. Error	95% Confidence Interval	
				Lower Bound	Upper Bound
0	3	13.180 ^a	4.318	4.459	21.901
	14	14.165 ^a	2.438	9.241	19.090
	21	5.821 ^a	3.222	-.687	12.329
	30	4.770 ^a	6.149	-7.648	17.189
1	3	20.433 ^a	4.763	10.813	30.053
	14	16.014 ^a	1.646	12.689	19.339
	21	12.236 ^a	1.992	8.214	16.259
	30	4.375 ^a	3.153	-1.991	10.742

a. Covariates appearing in the model are evaluated at the following values: wts = 147.420.

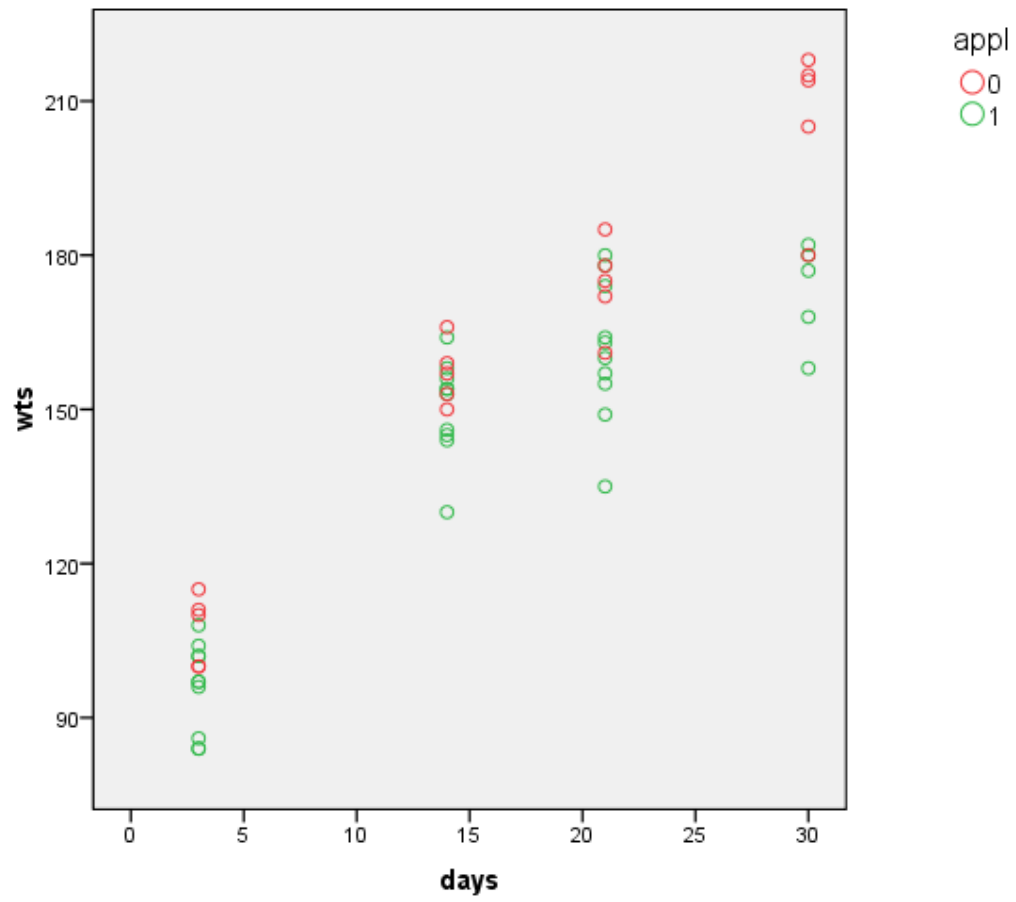
Weight

- Rats weight at four weeks of age (wt4, beginning of the study) and at the day of sacrifice (wts):

Graph**Notes**

Output Created	2008-09-10T11:04:59.453
Comments	
Input Data	D:\Documents and Settings\ppetocz\My Documents\Data\SPSSdata\Consult\Zoe1.sav
Active Dataset	DataSet0
Filter	<none>
Weight	<none>
Split File	<none>
N of Rows in Working Data File	55
Syntax	GRAPH /SCATTERPLOT(BIVAR)=days WITH <u>wts BY appl</u> /MISSING=LISTWISE.
Resources Processor Time	0:00:00.234
Elapsed Time	0:00:00.235

[DataSet0] D:\Documents and Settings\ppetocz\My Documents\Data\SPSSdata\Consult\Zoe1.sav



Univariate Analysis of Variance

Notes (class-days)

Output Created		2008-09-10T11:16:32.968
Comments		
Input	Data	D:\Documents and Settings\ppetocz\My Documents\Data\SPSSdata\Consult\Zoe1.sav
	Active Dataset	DataSet0
	Filter	<none>
	Weight	<none>
	Split File	<none>
	N of Rows in Working Data File	55
Missing Value Handling	Definition of Missing	User-defined missing values are treated as missing.
	Cases Used	Statistics are based on all cases with valid data for all variables in the model.
Syntax		UNIANOVA wts BY days class WITH wt4 /METHOD=SSTYPE(3) /INTERCEPT=INCLUDE /EMMEANS=TABLES(days) WITH(wt4=MEAN) /EMMEANS=TABLES(class) WITH(wt4=MEAN) /EMMEANS=TABLES(days*class) WITH(wt4=MEAN) /PLOT=RESIDUALS /CRITERIA=ALPHA(.05) /DESIGN=wt4 days class days*class.
Resources	Processor Time	0:00:00.235
	Elapsed Time	0:00:00.202

[DataSet0] D:\Documents and Settings\ppetocz\My Documents\Data\SPSSdata\Consult\Zoe1.sav

Notes (appliance-days)

Output Created	2008-09-10T11:08:07.734	
Comments		
Input	Data	D:\Documents and Settings\ppetocz\My Documents\Data\SPSSdata\Consult\Zoe1.sav
	Active Dataset	DataSet0
	Filter	<none>
	Weight	<none>
	Split File	<none>
	N of Rows in Working Data File	55
Missing Value Handling	Definition of Missing	User-defined missing values are treated as missing.
	Cases Used	Statistics are based on all cases with valid data for all variables in the model.
Syntax	UNIANOVA wts BY days appl WITH wt4 /METHOD=SSTYPE(3) /INTERCEPT=INCLUDE /EMMEANS=TABLES(days) WITH(wt4=MEAN) /EMMEANS=TABLES(appl) WITH(wt4=MEAN) /EMMEANS=TABLES(days*appl) WITH(wt4=MEAN) /PLOT=RESIDUALS /CRITERIA=ALPHA(.05) /DESIGN=wt4 days appl days*appl.	
Resources	Processor Time	0:00:00.265
	Elapsed Time	0:00:00.219

[DataSet0] D:\Documents and Settings\ppetocz\My Documents\Data\SPSSdata\Consult\Zoe1.sav

Between-Subjects Factors (class-days)

		N
Days	3	15
	14	14
	21	12
	30	10
Class	0	18
	2	12
	3	21

Tests of Between-Subjects Effects (class-days)

Dependent Variable: wts

Source	Type III Sum of Squares	df	Mean Square	F	Sig.
Corrected Model	61309.520 ^a	12	5109.127	45.711	.000
Intercept	968.288	1	968.288	8.663	.006
wt4	549.070	1	549.070	4.913	.033
days	36150.597	3	12050.199	107.813	.000
class	3319.610	2	1659.805	14.850	.000
days * class	1588.671	6	264.778	2.369	.048
Error	4247.225	38	111.769		
Total	1174978.000	51			
Corrected Total	65556.745	50			

a. R Squared = .935 (Adjusted R Squared = .915)

Between-Subjects Factors (appliance-days)

		N
Days	3	15
	14	14
	21	14
	30	10
Appl	0	18
	1	35

Tests of Between-Subjects Effects (appliance-days)

Dependent Variable: wts

Source	Type III Sum of Squares	df	Mean Square	F	Sig.
Corrected Model	61077.961 ^a	8	7634.745	71.223	.000
Intercept	1331.025	1	1331.025	12.417	.001
wt4	471.082	1	471.082	4.395	.042
days	40292.009	3	13430.670	125.292	.000
appl	3196.598	1	3196.598	29.820	.000
days * appl	1216.944	3	405.648	3.784	.017
Error	4716.568	44	107.195		
Total	1225227.000	53			
Corrected Total	65794.528	52			

a. R Squared = .928 (Adjusted R Squared = .915)

Estimated Marginal Means

1. days

Dependent Variable: wts

days	Mean	Std. Error	95% Confidence Interval	
			Lower Bound	Upper Bound
3	102.16 ^a	3.151	95.779	108.536
14	150.76 ^a	2.967	144.753	156.765
21	166.80 ^a	3.121	160.479	173.115
30	183.64 ^a	3.636	176.282	191.003

a. Covariates appearing in the model are evaluated at the following values: wt4 = 91.473.

2. class

Dependent Variable: wts

class	Mean	Std. Error	95% Confidence Interval	
			Lower Bound	Upper Bound
0	161.70 ^a	2.513	156.612	166.786
2	148.01 ^a	3.150	141.630	154.383
3	142.81 ^a	2.476	137.799	147.824

a. Covariates appearing in the model are evaluated at the following values: wt4 = 91.473.

Pairwise Comparisons

Dependent Variable: wts

(I) class	(J) class	Mean Difference (I-J)	Std. Error	Sig. ^a	95% Confidence Interval for Difference ^a	
					Lower Bound	Upper Bound
0	2	13.693*	4.023	.005	3.617	23.768
	3	18.888*	3.550	.000	9.996	27.780
2	0	-13.693*	4.023	.005	-23.768	-3.617
	3	5.195	4.027	.614	-4.890	15.281
3	0	-18.888*	3.550	.000	-27.780	-9.996
	2	-5.195	4.027	.614	-15.281	4.890

Based on estimated marginal means

*. The mean difference is significant at the .05 level.

a. Adjustment for multiple comparisons: Bonferroni.

3. days * class

Dependent Variable: wts

days	class	Mean	Std. Error	95% Confidence Interval	
				Lower Bound	Upper Bound
3	0	110.09 ^a	4.905	100.164	120.023
	2	96.48 ^a	6.180	83.971	108.993
	3	99.90 ^a	4.246	91.301	108.492
14	0	154.72 ^a	5.385	143.816	165.620
	2	148.76 ^a	5.291	138.050	159.472
	3	148.80 ^a	4.528	139.631	157.964
21	0	176.06 ^a	5.319	165.289	186.824
	2	167.64 ^a	6.111	155.270	180.011
	3	156.69 ^a	4.883	146.809	166.579
30	0	205.93 ^a	4.733	196.347	215.509
	2	179.14 ^a	7.522	163.914	194.371
	3	165.86 ^a	6.158	153.390	178.323

a. Covariates appearing in the model are evaluated at the following values: wt4 = 91.473.

4. **appl**

Dependent Variable: wts

appl	Mean	Std. Error	95% Confidence Interval	
			Lower Bound	Upper Bound
0	161.67 ^a	2.46	156.71	166.63
1	144.84 ^a	1.84	141.13	148.55

a. Covariates appearing in the model are evaluated at the following values: wt4 = 91.489.

5. **days * appl**

Dependent Variable: wts

days	appl	Mean	Std. Error	95% Confidence Interval	
				Lower Bound	Upper Bound
3	0	109.76 ^a	4.79	100.11	119.42
	1	98.55 ^a	3.49	91.51	105.58
14	0	155.00 ^a	5.26	144.39	165.61
	1	148.98 ^a	3.34	142.25	155.72
21	0	175.91 ^a	5.21	165.42	186.41
	1	160.43 ^a	3.31	153.75	167.11
30	0	205.99 ^a	4.63	196.65	215.33
	1	171.40 ^a	4.69	161.94	180.85

a. Covariates appearing in the model are evaluated at the following values: wt4 = 91.489.

Appendix 3: Progressive report

A summarised progressive report of the project;

2007 February-April	<ul style="list-style-type: none"> • Enrollment • Initial Settlements • Initial Research Topic Determination and Literature Review
2007 May-August	<ul style="list-style-type: none"> • Student Visa Procedure • Pilot Study <ul style="list-style-type: none"> – Key Points: <ul style="list-style-type: none"> Rat – Mice – Spheno Occipital Synchondrosis – Intermaxillary Suture – Micro Surgical Techniques - Tensile Force – Tissue Culture Media - Bone Remodeling
2007 September- 2008 April	<ul style="list-style-type: none"> • Study Design: <ul style="list-style-type: none"> – Condylar Cartilage and Glenoid Fossa during Mandibular Advancement (A Histological and Biochemical Study) • Animal Ethics Approval and Animal Welfare Course • 55 Rats arrival and Animal Laboratory Arrangements, Westmead • Animals and Experimental Design: <ul style="list-style-type: none"> – Providing Materials – Bite-Jumping Appliance – Euthanizing • Tissue Preparation: <ul style="list-style-type: none"> – Tissue Fixation in 4% Paraformaldehyde – Tissue Decalcification in 20% EDTA – TMJ Paraffin Embedding – Microtome Serial Sectioning
2008 May-July	<ul style="list-style-type: none"> • Immunohistochemical examinations: <ul style="list-style-type: none"> – Providing Materials and Facilities, and Immunostaining Method Design at IDR, Westmead – Immunohistochemical Staining of the TMJ for Fibroblast Growth Factor 8 (FGF8) and Proliferating Cell Nuclear Antigen (PCNA) – Digital Microscopic Imaging – Stained Cells Counting in the Condylar Cartilage and the Glenoid Fossa for FGF8 and PCNA
2008 August-September	<ul style="list-style-type: none"> • Initial Quantitative Statistical Analysis • Writing the Initial Draft of the Manuscript
2008 October-December	<ul style="list-style-type: none"> • Final Quantitative Statistical Analysis • Writing the Literature Review • Completion of the Manuscript and the Thesis • Accepted for Oral Presentation at AAO Annual Meeting in Boston-USA May 2009
2009 January	<ul style="list-style-type: none"> • Submitting the Manuscript to the American Journal of Orthodontics and Dentofacial Orthopedics (AJO-DO) • Submitting the Thesis to the University of Sydney.
2009 May	<ul style="list-style-type: none"> • Presented as an oral research abstract presentation at the American Association of Orthodontists (AAO) 109th Annual Session in Boston, Massachusetts - USA

American Association of
Orthodontists



401 North Lindbergh Boulevard • St. Louis, Missouri 63141-7816 • 314.993.1700 phone • 314.997.1745 fax

Raymond George, Sr., DMD
President

27 Du Carl Drive
Lincoln, RI 02865
401.334.3772 phone
401.333.4592 fax
rgeorgesr@earthlink.net

Robert James Bray, DDS, MS
President-Elect

620 Shore Road
PO Box 446
Somers Point, NJ 08244
609.601.0045 phone
609.653.0189 fax
rjbray@earthlink.net

Lee W. Graber, DDS, MS, MS, PhD
Secretary-Treasurer

830 West End Ct #175
Vernon Hills, IL 60061-4920
847.367.4920 phone
847.949.6396 fax
leegraber@earthlink.net

Chris P. Vranas, CAE
Executive Director

401 North Lindbergh Boulevard
St. Louis, MO 63141-7816
314.993.1700 phone
314.993.0142 fax
cvranas@aaortho.org

May 4, 2009

Dr. Payam Owtad
Z. Potres, G. Shen, A. Darendeliler
Tucson, AZ, USA

Presentation: Condylar Cartilage and Glenoid Fossa during Mandibular
Advancement, a Histological and Biochemical Study

Dear Dr. Owtad:

Thank you for participating as an Oral Research Presenter at the American
Association of Orthodontists (AAO) 109th Annual Session in Boston,
Massachusetts.

The Planning Committee recognizes that the real success of the Annual
Session is active involvement by individuals in programs such as this.
Your Oral Research presentation was an important contribution. We
appreciate the time spent in preparing your scientific information and trust
other attendees benefited from your presentation.

Again, thank you for your participation in this momentous event. The
AAO looks forward to your continued participation at the 110th AAO
Annual Session in Washington, DC.

Sincerely,

Dr. Bhavna Shroff
Chair, Council on Scientific Affairs

REFERENCES

References

1. Visnapuu V, Peltomaki T, Saamanen AM, Ronning O. Collagen I and II mRNA distribution in the rat temporomandibular joint region during growth. *J Craniofac Genet Dev Biol.* 2000 Jul-Sep;20(3):144-9.
2. Birkebaek L, Melsen B, Terp S. A laminagraphic study of the alterations in the temporo-mandibular joint following activator treatment. *Eur J Orthod.* 1984 Nov;6(4):257-66.
3. Pancherz H. The Herbst appliance--its biologic effects and clinical use. *Am J Orthod.* 1985 Jan;87(1):1-20.
4. Ingber D. Integrins as mechanochemical transducers. *Curr Opin Cell Biol.* 1991 Oct;3(5):841-8.
5. Ruoslahti E. Stretching is good for a cell. *Science.* 1997 May 30;276(5317):1345-6.
6. Rabie AB, She TT, Hagg U, Rabie ABM, Hagg U. Functional appliance therapy accelerates and enhances condylar growth. *Am J Orthod Dentofacial Orthop.* 2003 Jan;123(1):40-8.
7. Rabie AB, Xiong H, Hagg U, Rabie ABM. Forward mandibular positioning enhances condylar adaptation in adult rats. *Eur J Orthod.* [Comparative Study Research Support, Non-U.S. Gov't]. 2004 Aug;26(4):353-8.
8. Shen G, Rabie AB, Zhao ZH, Kaluarachchi K, Shen G, Rabie AB, *et al.* Forward deviation of the mandibular condyle enhances endochondral ossification of condylar cartilage indicated by increased expression of type X collagen. *Arch Oral Biol.* [Research Support, Non-U.S. Gov't]. 2006 Apr;51(4):315-24.
9. Fuentes MA, Opperman LA, Buschang P, Bellinger LL, Carlson DS, Hinton RJ. Lateral functional shift of the mandible: Part II. Effects on gene expression in condylar cartilage. *Am J Orthod Dentofacial Orthop.* 2003 Feb;123(2):160-6.
10. Woodside DG, Metaxas A, Altuna G. The influence of functional appliance therapy on glenoid fossa remodeling. *Am J Orthod Dentofacial Orthop.* 1987 Sep;92(3):181-98.
11. Hinton RJ, McNamara JA, Jr. Temporal bone adaptations in response to protrusive function in juvenile and young adult rhesus monkeys (*Macaca mulatta*). *Eur J Orthod.* 1984 Aug;6(3):155-74.
12. Rabie AB, Zhao Z, Shen G, Hagg EU, Dr O, Robinson W. Osteogenesis in the glenoid fossa in response to mandibular advancement. *Am J Orthod Dentofacial Orthop.* [Comparative Study Research Support, Non-U.S. Gov't]. 2001 Apr;119(4):390-400.
13. Altuna G, Niegel S. Bionators in Class II treatment. *J Clin Orthod.* 1985 Mar;19(3):185-91.
14. Caplan AI. Mesenchymal stem cells. *J Orthop Res.* 1991 Sep;9(5):641-50.
15. Bruder SP, Fink DJ, Caplan AI. Mesenchymal stem cells in bone development, bone repair, and skeletal regeneration therapy. *J Cell Biochem.* 1994 Nov;56(3):283-94.
16. Hinton RJ, Carlson DS. Histological changes in the articular eminence and mandibular fossa during growth of the rhesus monkey (*Macaca mulatta*). *Am J Anat.* 1983 Jan;166(1):99-116.
17. Shen G, Darendeliler MA. The adaptive remodeling of condylar cartilage---a transition from chondrogenesis to osteogenesis. *J Dent Res.* [Review]. 2005 Aug;84(8):691-9.
18. Bosshardt-Luehrs CPB, Luder HU. Cartilage matrix production and chondrocyte enlargement as contributors to mandibular condylar growth in monkeys (*Macaca fascicularis*). *American Journal of Orthodontics and Dentofacial Orthopedics.* 1991;100(4):362-9.

19. Chu FT, Tang GH, Hu Z, Qian YF, Shen G. Mandibular functional positioning only in vertical dimension contributes to condylar adaptation evidenced by concomitant expressions of L-Sox5 and type II collagen. *Arch Oral Biol.* 2008 Jun;53(6):567-74.
20. Dai J, Rabie AB, Rabie ABM. VEGF: an essential mediator of both angiogenesis and endochondral ossification. *J Dent Res.* [Research Support, Non-U.S. Gov't Review]. 2007 Oct;86(10):937-50.
21. Jukes JM, Both SK, Leusink A, Sterk LM, van Blitterswijk CA, de Boer J, *et al.* Endochondral bone tissue engineering using embryonic stem cells. *Proc Natl Acad Sci U S A.* [Research Support, Non-U.S. Gov't]. 2008 May 13;105(19):6840-5.
22. Hajjar D, Santos MF, Kimura ET. Propulsive appliance stimulates the synthesis of insulin-like growth factors I and II in the MCCof young rats. *Arch Oral Biol.* 2003;48(9):635-42.
23. Leung FY, Rabie AB, Hagg U, Leung FYC, Rabie ABM. Neovascularization and bone formation in the condyle during stepwise mandibular advancement. *Eur J Orthod.* [Research Support, Non-U.S. Gov't]. 2004 Apr;26(2):137-41.
24. Ross M RL, Kaye G. *Histology - A text and Atlas.* Maryland: Williams and Wilkins; 1995.
25. Bergman RA KA, M HP. *Histology.* Philadelphia: W.B. Saunders Company; 1996.
26. Cowan R, Morris VB. Cell population dynamics during the differentiative phase of tissue development. *J Theor Biol.* 1986 Sep 21;122(2):205-24.
27. Nemes Z. Differentiation markers in hemangiopericytoma. *Cancer.* 1992 Jan 1;69(1):133-40.
28. Xiong H, Rabie AB, Hagg U, Xiong H, Rabie ABM, Hagg U. Neovascularization and mandibular condylar bone remodeling in adult rats under mechanical strain. *Front Biosci.* [Research Support, Non-U.S. Gov't]. 2005 Jan 1;10:74-82.
29. Kaback LA, Soung do Y, Naik A, Smith N, Schwarz EM, O'Keefe RJ, *et al.* Osterix/Sp7 regulates mesenchymal stem cell mediated endochondral ossification. *J Cell Physiol.* [Research Support, N.I.H., Extramural]. 2008 Jan;214(1):173-82.
30. Havens BA, Velonis D, Kronenberg MS, Lichtler AC, Oliver B, Mina M, *et al.* Roles of FGFR3 during morphogenesis of Meckel's cartilage and mandibular bones. *Dev Biol.* [Research Support, N.I.H., Extramural]. 2008 Apr 15;316(2):336-49.
31. Mizoguchi I, Takahashi I, Sasano Y, Kagayama M, Kuboki Y, Mitani H. Localization of types I, II and X collagen and osteocalcin in intramembranous, endochondral and chondroid bone of rats. *Anat Embryol (Berl).* 1997 Oct;196(4):291-7.
32. Rabie AB, Dan Z, Samman N. Ultrastructural identification of cells involved in the healing of intramembranous and endochondral bones. *Int J Oral Maxillofac Surg.* [Research Support, Non-U.S. Gov't]. 1996 Oct;25(5):383-8.
33. Basilico C, Moscatelli D. The FGF family of growth factors and oncogenes. *Adv Cancer Res.* 1992;59:115-65.
34. Mansukhani A, Dell'Era P, Moscatelli D, Kornbluth S, Hanafusa H, Basilico C. Characterization of the murine BEK fibroblast growth factor (FGF) receptor: activation by three members of the FGF family and requirement for heparin. *Proc Natl Acad Sci U S A.* 1992 Apr 15;89(8):3305-9.
35. Tanaka A, Miyamoto K, Minamino N, Takeda M, Sato B, Matsuo H, *et al.* Cloning and characterization of an androgen-induced growth factor essential for the androgen-dependent growth of mouse mammary carcinoma cells. *Proc Natl Acad Sci U S A.* 1992 Oct 1;89(19):8928-32.
36. Hu MC, Qiu WR, Wang YP, Hill D, Ring BD, Scully S, *et al.* FGF-18, a novel member of the fibroblast growth factor family, stimulates hepatic and intestinal proliferation. *Mol Cell Biol.* 1998 Oct;18(10):6063-74.

37. LaVallee TM, Prudovsky IA, McMahon GA, Hu X, Maciag T. Activation of the MAP kinase pathway by FGF-1 correlates with cell proliferation induction while activation of the Src pathway correlates with migration. *J Cell Biol.* 1998 Jun 29;141(7):1647-58.
38. Pincus DW, Keyoung HM, Harrison-Restelli C, Goodman RR, Fraser RA, Edgar M, *et al.* Fibroblast growth factor-2/brain-derived neurotrophic factor-associated maturation of new neurons generated from adult human subependymal cells. *Ann Neurol.* 1998 May;43(5):576-85.
39. Rabie AB, Deng YM, Jin LJ. Adjunctive orthodontic treatment of periodontally involved teeth: case reports. *Quintessence Int.* [Case Reports]. 1998 Jan;29(1):13-9.
40. Powers CJ, McLeskey SW, Wellstein A. Fibroblast growth factors, their receptors and signaling. *Endocr Relat Cancer.* 2000 Sep;7(3):165-97.
41. Zammit C, Coope R, Gomm JJ, Shousha S, Johnston CL, Coombes RC. Fibroblast growth factor 8 is expressed at higher levels in lactating human breast and in breast cancer. *Br J Cancer.* 2002 Apr 8;86(7):1097-103.
42. Minina E, Schneider S, Rosowski M, Lauster R, Vortkamp A. Expression of Fgf and Tgfbeta signaling related genes during embryonic endochondral ossification. *Gene Expr Patterns.* 2005 Dec;6(1):102-9.
43. Tsurimoto T. PCNA binding proteins. *Front Biosci.* 1999 Dec 1;4:D849-58.
44. Bruck I, O'Donnell M. The ring-type polymerase sliding clamp family. *Genome Biol.* 2001;2(1):REVIEWS3001.
45. Kohler T, Prols F, Brand-Saberi B. PCNA in situ hybridization: a novel and reliable tool for detection of dynamic changes in proliferative activity. *Histochem Cell Biol.* 2005 Mar;123(3):315-27.
46. Tanno M, Taguchi T. Proliferating Cell Nuclear Antigen in Normal and Regenerating Rat Livers. *Experimental and Molecular Pathology.* 1999;67(3):192-200.
47. Narinobou M, Takatsuka S, Nakagawa K, Kubota Y, Terai K, Yamamoto E. Histological changes in the rabbit condyle following posterolateral disc perforation. *Journal of Cranio-Maxillofacial Surgery.* 2000;28(6):345-51.
48. Houston WTB, WJ. . A textbook of orthodontics. England: Wright & Sons; 1986.
49. Proffit WR. Contemporary Orthodontics. 4th Edition ed.: Mosby; 2006.
50. Graber TM, Vanarsdall, R.L., Vig, K.W.L. Orthodontics: Current Principles and Techniques. 4th edition ed. St. Louis: Elsevier Mosby, Inc.; 2005.
51. Proffit WR, Fields HW, Jr., Moray LJ. Prevalence of malocclusion and orthodontic treatment need in the United States: estimates from the NHANES III survey. *Int J Adult Orthodon Orthognath Surg.* 1998;13(2):97-106.
52. Bishara SE. Textbook of Orthodontics. Philadelphia: WB Saunders, A Harcourt. Health Sciences; 2001.
53. Bishara SE. Class II Malocclusions: Diagnostic and Clinical Considerations With and Without Treatment. *Seminars in Orthodontics.* 2006;12(1):11-24.
54. Keeling SD, Wheeler TT, King GJ, Garvan CW, Cohen DA, Cabassa S, *et al.* Anteroposterior skeletal and dental changes after early Class II treatment with bionators and headgear. *Am J Orthod Dentofacial Orthop.* 1998 Jan;113(1):40-50.
55. Bishara SE, Ziaja RR. Functional appliances: A review. *American Journal of Orthodontics and Dentofacial Orthopedics.* 1989;95(3):250-8.
56. Wahl N. Orthodontics in 3 millennia. Chapter 9: Functional appliances to midcentury. *American Journal of Orthodontics and Dentofacial Orthopedics.* 2006;129(6):829-33.
57. Shen G, Hagg U, Darendeliler MA. Skeletal effects of bite jumping therapy on the mandible - removable vs. fixed functional appliances. *Orthod Craniofac Res.* [Review]. 2005 Feb;8(1):2-10.

58. Hagg U, Du X, Rabie AB, Hagg U, Du X, Rabie ABM. Initial and late treatment effects of headgear-Herbst appliance with mandibular step-by-step advancement. *Am J Orthod Dentofacial Orthop.* [Research Support, Non-U.S. Gov't]. 2002 Nov;122(5):477-85.
59. Phan KL, Bendeus M, Hagg U, Hansen K, Rabie AB, Phan KLD, *et al.* Comparison of the headgear activator and Herbst appliance--effects and post-treatment changes. *Eur J Orthod.* [Comparative Study Evaluation Studies]. 2006 Dec;28(6):594-604.
60. Pancherz H, Anehus-Pancherz M. The effect of continuous bite jumping with the Herbst appliance on the masticatory system: a functional analysis of treated class II malocclusions. *Eur J Orthod.* 1982 Feb;4(1):37-44.
61. Arici S, Akan H, Yakubov K, Arici N, Arici S, Akan H, *et al.* Effects of fixed functional appliance treatment on the temporomandibular joint. *Am J Orthod Dentofacial Orthop.* [Randomized Controlled Trial]. 2008 Jun;133(6):809-14.
62. Cozza P, Baccetti T, Franchi L, De Toffol L, McNamara JJA. Mandibular changes produced by functional appliances in Class II malocclusion: A systematic review. *American Journal of Orthodontics and Dentofacial Orthopedics.* 2006;129(5):599.e1-e12.
63. Hiniker JJ, Ramfjord SP. Anterior displacement of the mandible in adult rhesus monkeys. *The Journal of Prosthetic Dentistry.* 1966;16(3):503-12.
64. McNamara JJA, Peterson JJE, Pancherz H. Histologic changes associated with the Herbst appliance in adult rhesus monkeys (*Macaca mulatta*). *Seminars in Orthodontics.* 2003;9(1):26-40.
65. McNamara JA, Carlson DS. Quantitative analysis of temporomandibular joint adaptations to protrusive function. *American Journal of Orthodontics.* 1979;76(6):593-611.
66. Shen G, Darendeliler MA. Cephalometric evaluation of condylar and mandibular growth modification: a review. *Orthod Craniofac Res.* [Review]. 2006 Feb;9(1):2-9.
67. Hagg U, Pancherz H. Dentofacial orthopaedics in relation to chronological age, growth period and skeletal development. An analysis of 72 male patients with Class II division 1 malocclusion treated with the Herbst appliance. *Eur J Orthod.* 1988 Aug;10(3):169-76.
68. Malmgren O, Omblus J, Hagg U, Pancherz H. Treatment with an orthopedic appliance system in relation to treatment intensity and growth periods. A study of initial effects. *Am J Orthod Dentofacial Orthop.* 1987 Feb;91(2):143-51.
69. Wey MC, Bendeus M, Peng L, Hagg U, Rabie AB, Robinson W, *et al.* Stepwise advancement versus maximum jumping with headgear activator. *Eur J Orthod.* [Comparative Study]. 2007 Jun;29(3):283-93.
70. Ulusoy Ç, Darendeliler N. Effects of Class II activator and Class II activator high-pull headgear combination on the mandible: A 3-dimensional finite element stress analysis study. *American Journal of Orthodontics and Dentofacial Orthopedics.* 2008;133(4):490.e9-e15.
71. Roberts WE, Hartsfield JK. Bone development and function: genetic and environmental mechanisms. *Seminars in Orthodontics.* 2004;10(2):100-22.
72. Ingervall B, Carlsson GE, Thilander B. Postnatal development of the human temporomandibular joint. II. A microradiographic study. *Acta Odontol Scand.* 1976;34(3):133-9.
73. Lubsen CC, Hansson TL, Nordström BB, Solberg WK. Histomorphometric analysis of cartilage and subchondral bone in mandibular condyles of young human adults at autopsy. *Arch Oral Biol.* 1985;30(2):129-36.
74. Wright DM, Moffett BC, Jr. The postnatal development of the human temporomandibular joint. *Am J Anat.* 1974 Oct;141(2):235-49.
75. Pullinger AG, Baldioceda F, Bibb CA. Relationship of TMJ articular soft tissue to underlying bone in young adult condyles. *J Dent Res.* 1990 Aug;69(8):1512-8.

76. Thilander B, Carlsson GE, Ingervall B. Postnatal development of the human temporomandibular joint. I. A histological study. *Acta Odontol Scand*. 1976;34(2):117-26.
77. Copray JCVM, Jansen HWB, Duterloo HS. Growth and growth pressure of mandibular condylar and some primary cartilages of the rat in vitro. *American Journal of Orthodontics and Dentofacial Orthopedics*. 1986;90(1):19-28.
78. Voudouris JC, Woodside DG, Altuna G, Kuftinec MM, Angelopoulos G, Bourque PJ. Condyle-fossa modifications and muscle interactions during herbst treatment, part 1. New technological methods. *Am J Orthod Dentofacial Orthop*. 2003 Jun;123(6):604-13.
79. Petrovic AG. Mechanisms and regulation of mandibular condylar growth. *Acta Morphol Neerl Scand*. 1972 Oct;10(1):25-34.
80. Voudouris JC, Kuftinec MM. Improved clinical use of Twin-block and Herbst as a result of radiating viscoelastic tissue forces on the condyle and fossa in treatment and long-term retention: growth relativity. *Am J Orthod Dentofacial Orthop*. 2000 Mar;117(3):247-66.
81. Moss ML. The functional matrix hypothesis revisited. 1. The role of mechanotransduction. *Am J Orthod Dentofacial Orthop*. 1997 Jul;112(1):8-11.
82. Moss ML. The functional matrix hypothesis revisited. 2. The role of an osseous connected cellular network. *American Journal of Orthodontics and Dentofacial Orthopedics*. 1997;112(2):221-6.
83. Moss ML. The functional matrix hypothesis revisited. 3. The genomic thesis. *American Journal of Orthodontics and Dentofacial Orthopedics*. 1997;112(3):338-42.
84. Moss ML. The functional matrix hypothesis revisited. 4. The epigenetic antithesis and the resolving synthesis. *American Journal of Orthodontics and Dentofacial Orthopedics*. 1997;112(4):410-7.
85. Moss ML, Salentijn L. The primary role of functional matrices in facial growth. *American Journal of Orthodontics*. 1969;55(6):566-77.
86. Frost HM. Mechanical determinants of bone modeling. *Metab Bone Dis Relat Res*. 1982;4(4):217-29.
87. Nanci A WS, Bianco P. Bone. Ten cate's oral histology: development, structure, and function. 6th ed ed.: St. Louis: Mosby Inc.; 2003.
88. Lei WY, Wong RW, Rabie AB, Lei WY, Wong RWK, Rabie ABM. Factors regulating endochondral ossification in the spheno-occipital synchondrosis. *Angle Orthod*. [Research Support, Non-U.S. Gov't]. 2008 Mar;78(2):215-20.
89. Blair HC, Zaidi M, Schlesinger PH. Mechanisms balancing skeletal matrix synthesis and degradation. *Biochem J*. 2002 Jun 1;364(Pt 2):329-41.
90. Shibata S, Baba O, Oda T, Yokohama-Tamaki T, Qin C, Butler WT, *et al*. An immunohistochemical and ultrastructural study of the pericellular matrix of uneroded hypertrophic chondrocytes in the mandibular condyle of aged c-src-deficient mice. *Arch Oral Biol*. 2008;53(3):220-30.
91. Bellus GA, McIntosh I, Smith EA, Aylsworth AS, Kaitila I, Horton WA, *et al*. A recurrent mutation in the tyrosine kinase domain of fibroblast growth factor receptor 3 causes hypochondroplasia. *Nat Genet*. 1995 Jul;10(3):357-9.
92. Rousseau F, Bonaventure J, Legeai-Mallet L, Pelet A, Rozet JM, Maroteaux P, *et al*. Mutations in the gene encoding fibroblast growth factor receptor-3 in achondroplasia. *Nature*. 1994 Sep 15;371(6494):252-4.
93. Tavormina PL, Shiang R, Thompson LM, Zhu YZ, Wilkin DJ, Lachman RS, *et al*. Thanatophoric dysplasia (types I and II) caused by distinct mutations in fibroblast growth factor receptor 3. *Nat Genet*. 1995 Mar;9(3):321-8.
94. Ueno T, Kagawa T, Kanou M, Fujii T, Fukunaga J, Mizukawa N, *et al*. Immunohistochemical observations of cellular differentiation and proliferation in endochondral bone formation from grafted periosteum:: expression and localization of BMP-

- 2 and -4 in the grafted periosteum. *Journal of Cranio-Maxillofacial Surgery*. 2003;31(6):356-61.
95. Day TF, Yang Y, Day TF, Yang Y. Wnt and hedgehog signaling pathways in bone development. *J Bone Joint Surg Am*. [Review]. 2008 Feb;90 Suppl 1:19-24.
96. Yu K, Ornitz DM. FGF signaling regulates mesenchymal differentiation and skeletal patterning along the limb bud proximodistal axis. *Development*. 2008 Feb;135(3):483-91.
97. Tsiairis CD, McMahon AP. *Displ* regulates growth of mammalian long bones through the control of *Ihh* distribution. *Dev Biol*. 2008;317(2):480-5.
98. Suda N, Shibata S, Yamazaki K, Kuroda T, Senior PV, Beck F, *et al*. Parathyroid hormone-related protein regulates proliferation of condylar hypertrophic chondrocytes. *J Bone Miner Res*. 1999 Nov;14(11):1838-47.
99. Kronenberg HM. Developmental regulation of the growth plate. *Nature*. 2003 May 15;423(6937):332-6.
100. TAYLOR RT. A Discussion of Wolff's Law. *Journal of Bone and Joint Surgery American volume*. 1902;s1(5):221-31.
101. KUSHNER A. Evaluation of Wolff's Law of Bone Formation. *Journal of Bone and Joint Surgery American volume*. 1940;22:589 - 96.
102. Enlow, DH. The condyle and facial growth. Sarnat BG LD, editor. Philadelphia: WB Saunders; 1992.
103. Rabie AB, Hagg U, Rabie ABM. Factors regulating mandibular condylar growth. *Am J Orthod Dentofacial Orthop*. [Research Support, Non-U.S. Gov't]. 2002 Oct;122(4):401-9.
104. Lefebvre V, de Crombrughe B. Toward understanding SOX9 function in chondrocyte differentiation. *Matrix Biol*. 1998 Mar;16(9):529-40.
105. Akiyama H, Lyons JP, Mori-Akiyama Y, Yang X, Zhang R, Zhang Z, *et al*. Interactions between Sox9 and beta-catenin control chondrocyte differentiation. *Genes Dev*. 2004 May 1;18(9):1072-87.
106. Rabie AB, Tang GH, Xiong H, Hagg U, Rabie ABM. PTHrP regulates chondrocyte maturation in condylar cartilage. *J Dent Res*. [Comparative Study Research Support, Non-U.S. Gov't]. 2003 Aug;82(8):627-31.
107. Ohkubo K, Shimokawa H, Ogawa T, Suzuki S, Fukada K, Ohya K, *et al*. Immunohistochemical localization of matrix metalloproteinase 13 (MMP-13) in mouse mandibular condylar cartilage. *J Med Dent Sci*. 2003 Sep;50(3):203-11.
108. Rabie AB, Tang GH, Hagg U, Rabie ABM, Tang GH, Hagg U. *Cbfa1* couples chondrocytes maturation and endochondral ossification in rat mandibular condylar cartilage. *Arch Oral Biol*. [Research Support, Non-U.S. Gov't]. 2004 Feb;49(2):109-18.
109. Shen G, Hagg U, Rabie AB, Kaluarachchi K. Identification of temporal pattern of mandibular condylar growth: a molecular and biochemical experiment. *Orthod Craniofac Res*. [Research Support, Non-U.S. Gov't]. 2005 May;8(2):114-22.
110. Wang L, Detamore MS. Tissue engineering the mandibular condyle. *Tissue Eng*. 2007 Aug;13(8):1955-71.
111. Tsutsui TW, Riminucci M, Holmbeck K, Bianco P, Robey PG. Development of craniofacial structures in transgenic mice with constitutively active PTH/PTHrP receptor. *Bone*. 2008;42(2):321-31.
112. Luder HU, Leblond CP, von der Mark K. Cellular stages in cartilage formation as revealed by morphometry, radioautography and type II collagen immunostaining of the mandibular condyle from weanling rats. *Am J Anat*. 1988 Jul;182(3):197-214.
113. Silbermann M, Reddi AH, Hand AR, Leapman RD, Von der Mark K, Franzen A. Further characterisation of the extracellular matrix in the mandibular condyle in neonatal mice. *J Anat*. 1987 Apr;151:169-88.

114. Mizoguchi I, Nakamura M, Takahashi I, Kagayama M, Mitani H. An immunohistochemical study of localization of type I and type II collagens in MCC compared with tibial growth plate. *Histochemistry*. 1990;93(6):593-9.
115. Mizoguchi I, Takahashi I, Nakamura M, Sasano Y, Sato S, Kagayama M, *et al*. An immunohistochemical study of regional differences in the distribution of type I and type II collagens in rat mandibular condylar cartilage. *Arch Oral Biol*. 1996;41(8-9):863-9.
116. Takano T, Takigawa M, Shirai E, Nakagawa K, Sakuda M, Suzuki F. The effect of parathyroid hormone (1-34) on cyclic AMP level, ornithine decarboxylase activity, and glycosaminoglycan synthesis of chondrocytes from mandibular condylar cartilage, nasal septal cartilage, and spheno-occipital synchondrosis in culture. *J Dent Res*. 1987 Jan;66(1):84-7.
117. Chayanupatkul A, Rabie AB, Hagg U. Temporomandibular response to early and late removal of bite-jumping devices. *Eur J Orthod*. 2003 Oct;25(5):465-70.
118. Rabie ABM, She TT, Hägg U. Functional appliance therapy accelerates and enhances condylar growth. *American Journal of Orthodontics and Dentofacial Orthopedics*. 2003;123(1):40-8.
119. Wieslander L. Intensive treatment of severe Class II malocclusions with a headgear-Herbst appliance in the early mixed dentition. *Am J Orthod*. 1984 Jul;86(1):1-13.
120. McNamara JA, Jr., Bookstein FL, Shaughnessy TG. Skeletal and dental changes following functional regulator therapy on class II patients. *Am J Orthod*. 1985 Aug;88(2):91-110.
121. Johnston LE, Jr. Functional appliances: a mortgage on mandibular position. *Aust Orthod J*. 1996 Oct;14(3):154-7.
122. Tonge EA, Heath JK, Meikle MC. Anterior mandibular displacement and condylar growth , : An experimental study in the rat. *American Journal of Orthodontics*. 1982;82(4):277-87.
123. Tang GH, Rabie AB, Hagg U, Rabie ABM. Indian hedgehog: a mechanotransduction mediator in condylar cartilage. *J Dent Res*. [Research Support, Non-U.S. Gov't]. 2004 May;83(5):434-8.
124. Ramfjord SP, Enlow RD. Anterior displacement of the mandible in adult rhesus monkeys: long-term observations. *J Prosthet Dent*. 1971 Nov;26(5):517-31.
125. De Luca F, Barnes KM, Uyeda JA, De-Levi S, Abad V, Palese T, *et al*. Regulation of growth plate chondrogenesis by bone morphogenetic protein-2. *Endocrinology*. 2001 Jan;142(1):430-6.
126. Rabie AB, Leung FY, Chayanupatkul A, Hagg U, Rabie ABM, Leung FYC. The correlation between neovascularization and bone formation in the condyle during forward mandibular positioning. *Angle Orthod*. [Comparative Study Research Support, Non-U.S. Gov't]. 2002 Oct;72(5):431-8.
127. Xiong H, Hagg U, Tang GH, Rabie AB, Robinson W, Xiong H, *et al*. The effect of continuous bite-jumping in adult rats: a morphological study. *Angle Orthod*. [Research Support, Non-U.S. Gov't]. 2004 Feb;74(1):86-92.
128. McNamara JA, Allen Bryan F. Long-term mandibular adaptations to protrusive function: An experimental study in *Macaca mulatta*. *American Journal of Orthodontics and Dentofacial Orthopedics*. 1987;92(2):98-108.
129. Rabie AB, Tsai MJ, Hagg U, Du X, Chou BW, Rabie ABM, *et al*. The correlation of replicating cells and osteogenesis in the condyle during stepwise advancement. *Angle Orthod*. [Comparative Study Research Support, Non-U.S. Gov't]. 2003 Aug;73(4):457-65.
130. Shum L, Rabie AB, Hagg U, Shum L, Rabie ABM, Hagg U. Vascular endothelial growth factor expression and bone formation in posterior glenoid fossa during stepwise

- mandibular advancement. *Am J Orthod Dentofacial Orthop.* [Comparative Study]. 2004 Feb;125(2):185-90.
131. Rabie AB, She TT, Harley VR, Rabie ABM. Forward mandibular positioning up-regulates SOX9 and type II collagen expression in the glenoid fossa. *J Dent Res.* [Comparative Study Research Support, Non-U.S. Gov't]. 2003 Sep;82(9):725-30.
 132. Rabie AB, Wong L, Tsai M. Replicating mesenchymal cells in the condyle and the glenoid fossa during mandibular forward positioning. *Am J Orthod Dentofacial Orthop.* 2003 Jan;123(1):49-57.
 133. Rabie AB, Shum L, Chayanupatkul A, Rabie ABM, Shum L, Chayanupatkul A. VEGF and bone formation in the glenoid fossa during forward mandibular positioning. *Am J Orthod Dentofacial Orthop.* 2002 Aug;122(2):202-9.
 134. Peterson JJE, McNamara JJA. Temporomandibular joint adaptations associated with Herbst appliance treatment in juvenile rhesus monkeys (*Macaca mulatta*). *Seminars in Orthodontics.* 2003;9(1):12-25.
 135. Ruf S, Pancherz H. Temporomandibular joint remodeling in adolescents and young adults during Herbst treatment: A prospective longitudinal magnetic resonance imaging and cephalometric radiographic investigation. *Am J Orthod Dentofacial Orthop.* 1999 Jun;115(6):607-18.
 136. Serbesis-Tsarudis C, Pancherz H. Effective TMJ and chin position changes in Class II treatment. *Angle Orthod.* 2008 Sep;78(5):813-8.
 137. Vargervik K, Harvold EP. Response to activator treatment in Class II malocclusions. *Am J Orthod.* 1985 Sep;88(3):242-51.
 138. Cascone P, Spallaccia F, Fatone FM, Rivaroli A, Saltarel A, Iannetti G. Rigid versus semirigid fixation for condylar fracture: experience with the external fixation system. *J Oral Maxillofac Surg.* 2008 Feb;66(2):265-71.
 139. Rabie AB, Wong L, Hagg U. Correlation of replicating cells and osteogenesis in the glenoid fossa during stepwise advancement. *Am J Orthod Dentofacial Orthop.* 2003 May;123(5):521-6.
 140. Shum L, Rabie AB, Hagg U. Vascular endothelial growth factor expression and bone formation in posterior glenoid fossa during stepwise mandibular advancement. *Am J Orthod Dentofacial Orthop.* 2004 Feb;125(2):185-90.
 141. Diaz-Flores L, Gutierrez R, Lopez-Alonso A, Gonzalez R, Varela H. Pericytes as a supplementary source of osteoblasts in periosteal osteogenesis. *Clin Orthop Relat Res.* 1992 Feb(275):280-6.
 142. Lakes R. Negative Poisson's ratio. Wisconsin Department of Engineering Physics, University of Wisconsin; 2008 [updated 2008; cited DEC.2008]; Available from: <http://silver.neep.wisc.edu/~lakes/Poisson.html>.
 143. Gercek H. Poisson's ratio values for rocks. *International Journal of Rock Mechanics and Mining Sciences.* 2007;44(1):1-13.
 144. Keaveny TM, Borchers RE, Gibson LJ, Hayes WC. Theoretical analysis of the experimental artifact in trabecular bone compressive modulus. *J Biomech.* 1993;26(4-5):599-607.
 145. Harris AK, Stopak D, Wild P. Fibroblast traction as a mechanism for collagen morphogenesis. *Nature.* 1981 Mar 19;290(5803):249-51.
 146. Sato K, Adachi T, Matsuo M, Tomita Y. Quantitative evaluation of threshold fiber strain that induces reorganization of cytoskeletal actin fiber structure in osteoblastic cells. *J Biomech.* 2005;38(9):1895-901.
 147. Vanderploeg EJ, Imler SM, Brodtkin KR, García AJ, Levenston ME. Oscillatory tension differentially modulates matrix metabolism and cytoskeletal organization in chondrocytes and fibrochondrocytes. *J Biomech.* 2004;37(12):1941-52.

148. Rabie AB, Wong L, Tsai M, Rabie ABM, Wong L, Tsai M. Replicating mesenchymal cells in the condyle and the glenoid fossa during mandibular forward positioning. *Am J Orthod Dentofacial Orthop*. 2003 Jan;123(1):49-57.
149. Wang N, Butler JP, Ingber DE. Mechanotransduction across the cell surface and through the cytoskeleton. *Science*. 1993 May 21;260(5111):1124-7.
150. Ruf S, Pancherz H. Long-term TMJ effects of Herbst treatment: a clinical and MRI study. *Am J Orthod Dentofacial Orthop*. 1998 Nov;114(5):475-83.
151. Pancherz H, Ruf S, Thomalske-Faubert C. Mandibular articular disc position changes during Herbst treatment: a prospective longitudinal MRI study. *Am J Orthod Dentofacial Orthop*. 1999 Aug;116(2):207-14.
152. Ruf S, Pancherz H. Temporomandibular joint growth adaptation in Herbst treatment: a prospective magnetic resonance imaging and cephalometric roentgenographic study. *Eur J Orthod*. 1998 Aug;20(4):375-88.
153. Witzany G. Life: The Communicative Structure; Taking the semiotic turn, or how significant philosophy of biology should be done. *Life: The Communicative Structure*. Hamburg Norderstedt, Libri Books on Demand; 2000. p. 155-61.
154. Safran A, Avivi A, Orr-Urtreger A, Neufeld G, Lonai P, Givol D, *et al*. The murine flg gene encodes a receptor for fibroblast growth factor. *Oncogene*. 1990 May;5(5):635-43.
155. McNeil PL, Muthukrishnan L, Warder E, D'Amore PA. Growth factors are released by mechanically wounded endothelial cells. *J Cell Biol*. 1989 Aug;109(2):811-22.
156. Werner S, Roth WK, Bates B, Goldfarb M, Hofschneider PH. Fibroblast growth factor 5 proto-oncogene is expressed in normal human fibroblasts and induced by serum growth factors. *Oncogene*. 1991 Nov;6(11):2137-44.
157. Olsen SK, Li JY, Bromleigh C, Eliseenkova AV, Ibrahimi OA, Lao Z, *et al*. Structural basis by which alternative splicing modulates the organizer activity of FGF8 in the brain. *Genes & Development*. [Research Support, N.I.H., Extramural Research Support, Non-U.S. Gov't]. 2006 Jan 15;20(2):185-98.
158. Nie X, Luukko K, Kettunen P. FGF signalling in craniofacial development and developmental disorders. *Oral Dis*. 2006 Mar;12(2):102-11.
159. Naski MC, Ornitz DM. FGF signaling in skeletal development. *Front Biosci*. 1998;3:d781-94.
160. Wang Q, Green RP, Zhao G, Ornitz DM. Differential regulation of endochondral bone growth and joint development by FGFR1 and FGFR3 tyrosine kinase domains. *Development*. 2001 Oct;128(19):3867-76.
161. Ornitz DM, Marie PJ. FGF signaling pathways in endochondral and intramembranous bone development and human genetic disease. *Genes Dev*. 2002 Jun 15;16(12):1446-65.
162. Minina E, Kreschel C, Naski MC, Ornitz DM, Vortkamp A. Interaction of FGF, Ihh/Pthlh, and BMP Signaling Integrates Chondrocyte Proliferation and Hypertrophic Differentiation. *Developmental Cell*. 2002;3(3):439-49.
163. Payson RA, Wu J, Liu Y, Chiu IM. The human FGF-8 gene localizes on chromosome 10q24 and is subjected to induction by androgen in breast cancer cells. *Oncogene*. 1996 Jul 4;13(1):47-53.
164. Sato B, Kouhara H, Koga M, Kasayama S, Saito H, Sumitani S, *et al*. Androgen-induced growth factor and its receptor: demonstration of the androgen-induced autocrine loop in mouse mammary carcinoma cells. *J Steroid Biochem Mol Biol*. 1993 Dec;47(1-6):91-8.
165. Valta MP, Hentunen T, Qu Q, Valve EM, Harjula A, Seppanen JA, *et al*. Regulation of osteoblast differentiation: a novel function for fibroblast growth factor 8. *Endocrinology*. 2006 May;147(5):2171-82.

166. Cholfin JA, Rubenstein JL, Cholfin JA, Rubenstein JLR. Frontal cortex subdivision patterning is coordinately regulated by Fgf8, Fgf17, and Emx2.[see comment]. J Comp Neurol. [Comparative Study Research Support, N.I.H., Extramural Research Support, Non-U.S. Gov't]. 2008 Jul 10;509(2):144-55.
167. Brito JM, Teillet MA, Le Douarin NM, Brito JM, Teillet M-A, Le Douarin NM. Induction of mirror-image supernumerary jaws in chicken mandibular mesenchyme by Sonic Hedgehog-producing cells. Development. [Research Support, N.I.H., Extramural Research Support, Non-U.S. Gov't]. 2008 Jul;135(13):2311-9.
168. Thomason HA, Dixon MJ, Dixon J, Thomason HA, Dixon MJ, Dixon J. Facial clefting in Tp63 deficient mice results from altered Bmp4, Fgf8 and Shh signaling. Dev Biol. [Research Support, N.I.H., Extramural Research Support, Non-U.S. Gov't]. 2008 Sep 1;321(1):273-82.
169. Jiang HB, Tian WD, Liu LK, Xu Y, Jiang H-B, Tian W-D, *et al.* In vitro odontoblast-like cell differentiation of cranial neural crest cells induced by fibroblast growth factor 8 and dentin non-collagen proteins. Cell Biol Int. [Research Support, Non-U.S. Gov't]. 2008 Jun;32(6):671-8.
170. Maruyama-Takahashi K, Shimada N, Imada T, Maekawa-Tokuda Y, Ishii T, Ouchi J, *et al.* A neutralizing anti-fibroblast growth factor (FGF) 8 monoclonal antibody shows anti-tumor activity against FGF8b-expressing LNCaP xenografts in androgen-dependent and -independent conditions. Prostate. 2008 May 1;68(6):640-50.
171. Valta MP, Tuomela J, Bjartell A, Valve E, Vaananen HK, Harkonen P, *et al.* FGF-8 is involved in bone metastasis of prostate cancer. Int J Cancer. [Research Support, Non-U.S. Gov't]. 2008 Jul 1;123(1):22-31.
172. Carev D, Saraga M, Saraga-Babic M, Carev D, Saraga M, Saraga-Babic M. Involvement of FGF and BMP family proteins and VEGF in early human kidney development. Histol Histopathol. [Research Support, Non-U.S. Gov't]. 2008 Jul;23(7):853-62.
173. Okada T, Okumura Y, Motoyama J, Ogawa M. FGF8 signaling patterns the telencephalic midline by regulating putative key factors of midline development. Dev Biol. 2008;320(1):92-101.
174. Wittkopf M, Goudy SL. Fgf8 is Necessary for Normal Frontonasal Development. Otolaryngology - Head and Neck Surgery. 2008;139(2, Supplement 1):P105-P.
175. Boulet AM, Capecchi MR. The role of FGF4 and FGF8 in posterior development of the mouse embryo. Dev Biol. 2008;319(2):509-.
176. Jensen P, Pedersen EG, Zimmer J, Widmer HR, Meyer M. Functional effect of FGF2- and FGF8-expanded ventral mesencephalic precursor cells in a rat model of Parkinson's disease. Brain Research. 2008;1218:13-20.
177. Kataoka A, Shimogori T, Kataoka A, Shimogori T. Fgf8 controls regional identity in the developing thalamus. Development. [Research Support, Non-U.S. Gov't]. 2008 Sep;135(17):2873-81.
178. Falardeau J, Chung WC, Beenken A, Raivio T, Plummer L, Sidis Y, *et al.* Decreased FGF8 signaling causes deficiency of gonadotropin-releasing hormone in humans and mice. J Clin Invest. [Case Reports Research Support, N.I.H., Extramural Research Support, Non-U.S. Gov't]. 2008 Aug;118(8):2822-31.
179. Okada T, Okumura Y, Motoyama J, Ogawa M, Okada T, Okumura Y, *et al.* FGF8 signaling patterns the telencephalic midline by regulating putative key factors of midline development. Dev Biol. 2008 Aug 1;320(1):92-101.
180. Delgado I, Dominguez-Frutos E, Schimmang T, Ros MA, Delgado I, Dominguez-Frutos E, *et al.* The incomplete inactivation of Fgf8 in the limb ectoderm affects the

- morphogenesis of the anterior autopod through BMP-mediated cell death. *Dev Dyn.* [Research Support, Non-U.S. Gov't]. 2008 Mar;237(3):649-58.
181. Ueda Y, Lewandoski M, Plisov S, Wilson C, Sharma N, Elder C, *et al.* Fgf8 is essential for development of the male reproductive tract. *Dev Biol.* 2007;306(1):306-7.
 182. Von Scheven G, Dietrich S. The role of Fgf8 in head myogenesis. *Dev Biol.* 2007;306(1):352-.
 183. Hernández-Martínez R, Castro-Obregon S, Covarrubias L. Fgf8 and retinoic acid control the initiation of interdigital cell death without the direct participation of Bmp7 in the mouse limb. *Dev Biol.* 2007;306(1):447-8.
 184. Jaskoll T, Witcher D, Toreno L, Bringas P, Moon AM, Melnick M. FGF8 dose-dependent regulation of embryonic submandibular salivary gland morphogenesis. *Dev Biol.* 2004;268(2):457-69.
 185. Walshe J, Maroon H, McGonnell IM, Dickson C, Mason I. Establishment of hindbrain segmental identity requires signaling by FGF3 and FGF8. *Curr Biol.* 2002 Jul 9;12(13):1117-23.
 186. St.Amand TR, Zhang Y, Semina EV, Zhao X, Hu Y, Nguyen L, *et al.* Antagonistic Signals between BMP4 and FGF8 Define the Expression of Pitx1 and Pitx2 in Mouse Tooth-Forming Anlage. *Dev Biol.* 2000;217(2):323-32.
 187. Crossley PH, Minowada G, MacArthur CA, Martin GR. Roles for FGF8 in the Induction, Initiation, and Maintenance of Chick Limb Development. *Cell.* 1996;84(1):127-36.
 188. Crossley PH, Martinez S, Martin GR. Midbrain development induced by FGF8 in the chick embryo. *Nature.* 1996 Mar 7;380(6569):66-8.
 189. Mariani FV, Ahn CP, Martin GR, Mariani FV, Ahn CP, Martin GR. Genetic evidence that FGFs have an instructive role in limb proximal-distal patterning. *Nature.* [Research Support, N.I.H., Extramural Research Support, Non-U.S. Gov't]. 2008 May 15;453(7193):401-5.
 190. Sun X, Meyers EN, Lewandoski M, Martin GR. Targeted disruption of Fgf8 causes failure of cell migration in the gastrulating mouse embryo. *Genes Dev.* 1999 Jul 15;13(14):1834-46.
 191. Ye W, Shimamura K, Rubenstein JL, Hynes MA, Rosenthal A. FGF and Shh signals control dopaminergic and serotonergic cell fate in the anterior neural plate. *Cell.* 1998 May 29;93(5):755-66.
 192. Geduspan JS, Solursh M. A growth-promoting influence from the mesonephros during limb outgrowth. *Dev Biol.* 1992 May;151(1):242-50.
 193. Walshe J, Mason I. Fgf signalling is required for formation of cartilage in the head. *Dev Biol.* 2003 Dec 15;264(2):522-36.
 194. Huang R, Stolte D, Kurz H, Ehehalt F, Cann GM, Stockdale FE, *et al.* Ventral axial organs regulate expression of myotomal Fgf-8 that influences rib development. *Dev Biol.* 2003 Mar 1;255(1):30-47.
 195. Praul CA, Ford BC, Leach RM. Effect of fibroblast growth factors 1, 2, 4, 5, 6, 7, 8, 9, and 10 on avian chondrocyte proliferation. *J Cell Biochem.* 2002;84(2):359-66.
 196. Kettunen P, Karavanova I, Thesleff I. Responsiveness of developing dental tissues to fibroblast growth factors: expression of splicing alternatives of FGFR1, -2, -3, and of FGFR4; and stimulation of cell proliferation by FGF-2, -4, -8, and -9. *Dev Genet.* 1998;22(4):374-85.
 197. Zhou YX, Xu X, Chen L, Li C, Brodie SG, Deng CX. A Pro250Arg substitution in mouse Fgfr1 causes increased expression of Cbfa1 and premature fusion of calvarial sutures. *Hum Mol Genet.* 2000 Aug 12;9(13):2001-8.
 198. Abzhanov A, Tabin CJ. Shh and Fgf8 act synergistically to drive cartilage outgrowth during cranial development. *Dev Biol.* 2004 Sep 1;273(1):134-48.

199. Zhou J, Meng J, Guo S, Gao B, Ma G, Zhu X, *et al.* IHH and FGF8 coregulate elongation of digit primordia. *Biochemical and Biophysical Research Communications*. 2007;363(3):513-8.
200. Tucker AS, Yamada G, Grigoriou M, Pachnis V, Sharpe PT. Fgf-8 determines rostral-caudal polarity in the first branchial arch. *Development*. 1999 Jan;126(1):51-61.
201. Fischer A, Viebahn C, Blum M. FGF8 Acts as a Right Determinant during Establishment of the Left-Right Axis in the Rabbit. *Current Biology*. 2002;12(21):1807-16.
202. Cobourne MT, Sharpe PT. Tooth and jaw: molecular mechanisms of patterning in the first branchial arch. *Arch Oral Biol*. 2003 Jan;48(1):1-14.
203. Zhang X, Ibrahimi OA, Olsen SK, Umemori H, Mohammadi M, Ornitz DM, *et al.* Receptor specificity of the fibroblast growth factor family. The complete mammalian FGF family. *J Biol Chem*. [Research Support, N.I.H., Extramural Research Support, Non-U.S. Gov't]. 2006 Jun 9;281(23):15694-700.
204. Miyachi K, Fritzler MJ, Tan EM. Autoantibody to a nuclear antigen in proliferating cells. *J Immunol*. 1978 Dec;121(6):2228-34.
205. Bravo R, Frank R, Blundell PA, Macdonald-Bravo H. Cyclin/PCNA is the auxiliary protein of DNA polymerase-delta. *Nature*. 1987 Apr 2-8;326(6112):515-7.
206. Bravo R, Macdonald-Bravo H. Existence of two populations of cyclin/proliferating cell nuclear antigen during the cell cycle: association with DNA replication sites. *J Cell Biol*. 1987 Oct;105(4):1549-54.
207. Prelich G, Kostura M, Marshak DR, Mathews MB, Stillman B. The cell-cycle regulated proliferating cell nuclear antigen is required for SV40 DNA replication in vitro. *Nature*. 1987 Apr 2-8;326(6112):471-5.
208. Bauer GA, Burgers PM. Molecular cloning, structure and expression of the yeast proliferating cell nuclear antigen gene. *Nucleic Acids Res*. 1990 Jan 25;18(2):261-5.
209. McAlear MA, Howell EA, Espenshade KK, Holm C. Proliferating cell nuclear antigen (p130) mutations suppress cdc44 mutations and identify potential regions of interaction between the two encoded proteins. *Mol Cell Biol*. 1994 Jul;14(7):4390-7.
210. Ayyagari R, Impellizzeri KJ, Yoder BL, Gary SL, Burgers PM. A mutational analysis of the yeast proliferating cell nuclear antigen indicates distinct roles in DNA replication and DNA repair. *Mol Cell Biol*. 1995 Aug;15(8):4420-9.
211. Stukenberg PT, Studwell-Vaughan PS, O'Donnell M. Mechanism of the sliding beta-clamp of DNA polymerase III holoenzyme. *J Biol Chem*. 1991 Jun 15;266(17):11328-34.
212. Li X, Li J, Harrington J, Lieber MR, Burgers PM. Lagging strand DNA synthesis at the eukaryotic replication fork involves binding and stimulation of FEN-1 by proliferating cell nuclear antigen. *J Biol Chem*. 1995 Sep 22;270(38):22109-12.
213. Paunesku T, Mittal S, Protic M, Oryhon J, Korolev SV, Joachimiak A, *et al.* Proliferating cell nuclear antigen (PCNA): ringmaster of the genome. *Int J Radiat Biol*. 2001 Oct;77(10):1007-21.
214. Hall PA, Woods AL. Immunohistochemical markers of cellular proliferation: achievements, problems and prospects. *Cell Tissue Kinet*. 1990 Nov;23(6):505-22.
215. Sanders EJ, Varedi M, French AS. Cell proliferation in the gastrulating chick embryo: a study using BrdU incorporation and PCNA localization. *Development*. 1993 Jun;118(2):389-99.
216. Shirvan A, Ziv I, Machlin T, Zilkha-Falb R, Melamed E, Barzilai A. Two waves of cyclin B and proliferating cell nuclear antigen expression during dopamine-triggered neuronal apoptosis. *J Neurochem*. 1997 Aug;69(2):539-49.
217. Lin MI, Das I, Schwartz GM, Tsoulfas P, Mikawa T, Hempstead BL. Trk C Receptor Signaling Regulates Cardiac Myocyte Proliferation during Early Heart Development in Vivo. *Dev Biol*. 2000;226(2):180-91.

218. Castaño FJ, Troulis MJ, Glowacki J, Kaban LB, Yates KE. Proliferation of masseter myocytes after distraction osteogenesis of the porcine mandible. *Journal of Oral and Maxillofacial Surgery*. 2001;59(3):302-7.
219. Wadhwa S, Embree MC, Kilts T, Young MF, Ameye LG. Accelerated osteoarthritis in the temporomandibular joint of biglycan/fibromodulin double-deficient mice. *Osteoarthritis Cartilage*. 2005 Sep;13(9):817-27.
220. Wolf DC, Gross EA, Lyght O, Bermudez E, Recio L, Morgan KT. Immunohistochemical Localization of p53, PCNA, and TGF-[alpha] Proteins in Formaldehyde-Induced Rat Nasal Squamous Cell Carcinomas. *Toxicology and Applied Pharmacology*. 1995;132(1):27-35.
221. Funaoka K, Arisue M, Kobayashi I, Iizuka T, Kohgo T, Amemiya A, *et al.* Immunohistochemical detection of Proliferating cell nuclear antigen (PCNA) in 23 cases of ameloblastoma. *European Journal of Cancer Part B: Oral Oncology*. 1996;32(5):328-32.
222. Ingervall B, Fredén H, Heyden G. Histochemical study of mandibular joint adaptation in experimental posterior mandibular displacement in the rat. *Arch Oral Biol*. 1972;17(4):661-70.
223. Bai Y, Luo S. [A study on the changes of the estrogen level in the condylar cartilages in young growing rats after functional mandibular protrusion]. *Zhonghua Kou Qiang Yi Xue Za Zhi*. 1997 May;32(3):161-3.
224. Chayanupatkul A, Rabie AB, Hagg U, Chayanupatkul A, Rabie ABM, Hagg U. Temporomandibular response to early and late removal of bite-jumping devices. *Eur J Orthod*. 2003 Oct;25(5):465-70.
225. Fuentes MA, Opperman LA, Buschang P, Bellinger LL, Carlson DS, Hinton RJ. Lateral functional shift of the mandible: Part I. Effects on condylar cartilage thickness and proliferation. *Am J Orthod Dentofacial Orthop*. 2003 Feb;123(2):153-9.
226. Ng TC, Chiu KW, Rabie AB, Hagg U, Ng TCS, Chiu KWK, *et al.* Repeated mechanical loading enhances the expression of Indian hedgehog in condylar cartilage. *Front Biosci*. 2006;11:943-8.
227. Rabie AB, Wong L, Hagg U, Rabie ABM, Wong L, Hagg U. Correlation of replicating cells and osteogenesis in the glenoid fossa during stepwise advancement. *Am J Orthod Dentofacial Orthop*. [Comparative Study]. 2003 May;123(5):521-6.
228. Shen G, Rabie AB, Hagg U, Chen RJ. [An immunohistochemical study on neovascularization in TMJ during mandibular advancement]. *Shanghai Kou Qiang Yi Xue*. 2003 Apr;12(2):115-9.
229. Shen G, Rabie AB, Hagg U, Zhao Z. [Expression of type X collagen in condylar cartilage during mandibular protrusion]. *Hua Xi Kou Qiang Yi Xue Za Zhi*. 2000 Apr;18(2):78-80, 4.
230. Shen G, Zhao Z, Kaluarachchi K, Bakr Rabie A. Expression of type X collagen and capillary endothelium in condylar cartilage during osteogenic transition--a comparison between adaptive remodelling and natural growth. *Eur J Orthod*. 2006 Jun;28(3):210-6.
231. Tang GH, Rabie AB, Rabie ABM. Runx2 regulates endochondral ossification in condyle during mandibular advancement. *J Dent Res*. [Comparative Study Research Support, Non-U.S. Gov't]. 2005 Feb;84(2):166-71.
232. Nakano H, Watahiki J, Kubota M, Maki K, Shibasaki Y, Hatcher D, *et al.* Micro X-ray computed tomography analysis for the evaluation of asymmetrical condylar growth in the rat. *Orthod Craniofac Res*. 2003;6 Suppl 1:168-72; discussion 79-82.
233. Malek S, Rapaport M, Darendeliler MA. Varying treatments of Class II malocclusions: two case reports. *Aust Orthod J*. [Case Reports]. 2001 Nov;17(2):103-14.
234. Ramfjord SP, Blankenship JR. Interarticular disc in wide mandibular opening in rhesus monkeys. *J Prosthet Dent*. 1971 Aug;26(2):189-99.

-
235. Ramfjord SP, Walden JM, Enlow RD. Unilateral function and the temporomandibular joint in rhesus monkeys. *Oral Surg Oral Med Oral Pathol*. 1971 Aug;32(2):236-47.
236. Xiong H, Rabie AB, Hagg U, Xiong H, Rabie ABM, Hagg U. Mechanical strain leads to condylar growth in adult rats. *Front Biosci*. [Research Support, Non-U.S. Gov't]. 2005 Jan 1;10:67-73.
237. Schmuth GPF. Milestones in the development and practical application of functional appliances. *American Journal of Orthodontics*. 1983;84(1):48-53.
238. Shen G, Rabie AB, Hagg U, Chen RJ, Shen G, Chen R-j. [An immunohistochemical study on neovascularization in TMJ during mandibular advancement]. *Shanghai Kou Qiang Yi Xue*. [English Abstract]. 2003 Apr;12(2):115-9.
239. Rabie ABM, Zhao Z, Shen G, Hägg EU, Robinson W. Osteogenesis in the glenoid fossa in response to mandibular advancement. *American Journal of Orthodontics and Dentofacial Orthopedics*. 2001;119(4):390-400.
240. Rabie AB, Dai J, Xu R, Rabie ABM. Recombinant AAV-mediated VEGF gene therapy induces mandibular condylar growth. *Gene Ther*. [Research Support, Non-U.S. Gov't]. 2007 Jun;14(12):972-80.
241. Shum L, Rabie ABM, Hägg U. Vascular endothelial growth factor expression and bone formation in posterior glenoid fossa during stepwise mandibular advancement. *American Journal of Orthodontics and Dentofacial Orthopedics*. 2004;125(2):185-90.